Printed, Flexible Electrochemical Sensors

Margaret Payne

Electrical Engineering and Computer Sciences
University of California, Berkeley

Technical Report No. UCB/EECS-2022-12
http://www2.eecs.berkeley.edu/Pubs/TechRpts/2022/EECS-2022-12.html

May 1, 2022

Printed, Flexible Electrochemical Sensors

by

Margaret Payne

A dissertation submitted in partial satisfaction of the

requirements for the degree of

Doctor of Philosophy

in

Engineering - Electrical Engineering and Computer Sciences

in the

Graduate Division

of the

University of California, Berkeley

Committee in charge:

Professor Ana Claudia Arias, Chair
Professor Kristofer Pister
Professor Lydia Sohn

Spring 2020

Printed, Flexible Electrochemical Sensors

Abstract

Printed, Flexible Electrochemical Sensors

by

Margaret Payne

Doctor of Philosophy in Engineering - Electrical Engineering and Computer Sciences

University of California, Berkeley

Professor Ana Claudia Arias, Chair

Chemicals are ubiquitous, from the food we eat to the composition of our own bodies. Different chemicals can give us information about ourselves or our surroundings. For example, chemicals in the body can give information about the state of a person's health, while chemicals in the atmosphere can give information about pollution. Chemical sensors are necessary to gain this information. Electrochemical sensors can use electrical signal output to indicate the presence and amount of chemicals. This is done two ways: amperometric sensors output current, and potentiometric sensors output potential. The magnitude of the signal indicates the amount of chemical present. Printing is useful for fabricating these sensors in flexible form factors and for disposable uses.

This thesis discusses the development of several different printed electrochemical sensors. An overview is first given of the developments in printed electrochemical sensors which enabled this work. Printed amperometric sensors for determination of lactate in sweat are optimized for sensing the transition from aerobic to anaerobic metabolism. These sensors are printed to accommodate form factors closely matching that of skin. These sensors have a sensitivity of 4.8 μA/mM and a linear range up to 25 mM lactate. However, an investigation into the selectivity of these sensors determines they are susceptible to interference from the salt present in sweat, making them less useful as sensors and more useful as indicators. Potentiometric sensors are proposed as an alternative for sensing metabolites in sweat, due to their selectivity in sweat. Potentiometric sensors cannot be made for sensing lactate, but ammonium sensors are demonstrated instead for determining levels of carbohydrates and metabolic condition. Potentiometric ammonium sensors show a near-Nernstian response of 57.5 mV/decade $\pm$ 0.3 mV/decade. Sweat is not the only application for printed sensors. Printed potentiometric sensors for nitrate in soil are also demonstrated, where printing enables the use of degradable materials. The nitrate sensors have near-Nernstian sensitivity of -53.3 mV/decade $\pm$ 1.1 mV/decade, and the printed reference developed shows relative insensitivity to nitrate in solution. The work discussed here indicates a step toward distributed networks of sensors.

Contents

List of Figures

List of Tables

Acknowledgments

First and foremost, my deepest gratitude goes to my advisor, Professor Ana Claudia Arias. Thank you for creating an environment where I could pursue research that is important to me. The resources she brings to the group provide incredible opportunities and she is the reason any of this work was possible.

For funding throughout my graduate education, I would like to thank many sources, especially the National Science Foundation Graduate Research Fellowship Program. I am also grateful for support and collaborations from Intel, the National Science Foundation Nanosystems Engineering Research Center for Nanomanufacturing Systems for Mobile Computing and Mobile Energy Technologies, and the Department of Energy's Advanced Research Projects Agency-Energy on the project Precision Agriculture using Networks of Degradable Analytical Sensors.

Many thanks to Professor Vivek Subramanian for access to lab space and equipment, and for serving as the chair of my qualifying exam committee. Many thanks to Professors Kristofer Pister and Lydia Sohn for serving on both my qualifying exam committee and dissertation committee. Many thanks to Professor Jim Evans for thoughtful discussions on every topic ranging from the proper use of the Nernst equation to The Great British Baking Show. Thanks to Professor Anant Sahai for support throughout my teaching experience. Thanks to Professor Oana Jurchescu for being the reason I got to graduate school in the first place.

I had the privilege of working with many amazing labmates throughout my research. Alla Zamarayeva and Veronika Pister worked on developing lactate sensors with me. Natasha Yamamoto first taught me about potentiometric sensors. Anju Toor has been an invaluable collaborator on continuing the goal of the sweat sensor work. All four contributed to the sweat sensor work cited here. Thank you all.

The soil sensing work was done as part of the PANDAS project, on which Derek Wong, Carol Baumbauer, Payton Goodrich, and Anju Toor are amazing collaborators. Our collaborators in Colorado have also been wonderfully supportive: Professor Greg Whiting and his students Madhur Atreya and Yongkun Sui, as well as Professor Rajiv Khosla and his students Subash Dahal and Evan Phillippi. This group makes this project so fascinating. Thank you all.

The Arias Research Group is full of incredible characters past and present which make labwork entertaining. In addition to those listed above, thank you (in no particular order) to: Adrien Pierre, Aminy Ostfeld, Claire Lochner, Joe Corea, Balthazar Lechene, Igal Deckman, Abhinav Gaikwad, Donggeon Han, Yasser Khan, Maruf Ahmed, Xiaodong Wu, Juan Zhu, Seiya Ono, Jasmine Jan, Karthik Gopalan, and Jonathan Ting. I am also incredibly grateful to the EECS16B teaching/lab staff for their support, encouragement, and commiseration. Thank you (again in no particular order): Zain Zaidi, Mia Mirkovic, Karina Chang, Titan Yuan, Ramsey Mardini, Jove Yuan, Justin Lu, Mikaela Frichtel, Raymond Gu, Victor Lee, Meera Lester, Steven Lu, Vin Ramamurti, Kaitlyn Chan, Kevin Zhang, Peter Schafhalter,

Ashley Lin, Dinesh Parimi, Julian Chan, Rohan Konnur, Alyssa Huang, Tiffany Cappellari, and Regina Eckert.

Outside of the lab and teaching, I owe gratitude to Joshua Achiam, who was instrumental in getting me to come to Berkeley in the first place, and Andreana Rosnik, who has been a constant source of beauty, art, sarcasm, and kindness in the world of grad school. Julie Fornaciari has been a constant companion spanning from an REU together into graduate school and I am grateful for her friendship. Thanks to Abdulmalik Obaid for making the trip to Berkeley to see me multiple times through the years.

My parents, Kermit and Ada Payne, have supported me through every endeavor and I would literally not be here without them. I would not be where I am today were they not the kind, caring engineers who raised me to think logically and always know how to calculate the tip. My brother, Reuben Payne, has been my biggest cheerleader, and has shaped who I am in ways I don't think he realizes. John and Karina Menke have also been wonderful voices of support and encouragement through graduate school. I thank you with everything I am. I can never thank my family enough.

Finally, my family in Berkeley. Thank you, Kevin Ryan, for making home more livable, for commiserating on bad days and celebrating the good, for cooking delicious food and encouraging a house full of music and fun. Christie Dierk and Joe Menke are the pillars without whom I would not be able to stand. They are both my best allies. My best friend and the Ukuladies founding member, Christie Dierk has kept me (relatively) sane throughout graduate school. My fiance, Joe Menke has kept me grounded and inspired me. Selina and Jovi have brought so much comfort. Thank you, Berkeley family.

Chapter 1

Introduction

1.1 Fundamental Characteristics of Chemical Sensors

A chemical sensor is defined as a device that responds to an analyte selectively through a chemical reaction to determine the amount of analyte present[20]. Various types of chemical sensors exist, including electrochemical, optical, mass sensitive, and heat sensitive. This work will focus on electrochemical sensors, which rely on electrical signals as a product of the chemical reaction which takes place. Optical chemical sensors rely on the use of spectroscopic measurements to distinguish the product of the chemical reaction which takes place. Mass sensitive chemical sensors rely on material adsorbing to the surface of an oscillating crystal. This adsorption results in a change in mass on the surface of the oscillating crystal which changes the frequency of oscillation. Heat sensitive chemical sensors monitor the heat of a chemical reaction through thermistors or thermometers.

For each of these types of sensors, there is a transducer of some sort, a layer containing the species recognition agent, and contact with the analyte of interest. The transducer is the method of detecting the chemical reaction, which for electrochemical sensors is typically a conductor of some sort for measuring electrical signals. For optical sensors, this transducer becomes photodiodes or microscopes. For mass sensitive sensors, the transducer is the oscillating crystal and the method of measuring the frequency shift of oscillation. For heat sensitive sensors, the transducer is simply the thermistor or thermometer.

1.2 Electrochemical Sensor Introduction

The two main types of electrochemical sensors are discussed in this work: amperometric and potentiometric, though there are other ways to sense chemicals, such as the organic electrochemical transistor[27, 39, 48, 129, 142], optical sensing methods[28, 82, 88, 122], and lab-scale sensing methods such as spectrophotometric measurements. In particular, amperometric sensors indicate the amount of analyte present through the magnitude of the current output of the sensor, while potentiometric sensors indicate the amount of analyte present

through the magnitude of the potential output of the sensor. With humble beginnings, both of these types of sensors have gained popularity and even commercial and diagnostic viability. Amperometric sensors were most enabled by the immobilization of enzymes[60], while potentiometric sensors began as liquid membrane ion-selective electrodes[116] and gained popularity after poly(vinyl chloride) (PVC) was introduced for making solid potentiometric sensor membranes[93]. Each of these breakthroughs was key to enabling the types of sensors we see today. Since the sensing membranes of each kind of sensor are solution-processable, much effort has been dedicated to developing printed electrochemical sensors.

1.3 Fabrication Techniques

Printing as a fabrication method enables flexible, comfortable, wearable sensors to be made. Furthermore, printing can be done on disposable substrates, enabling single-use sensors, which is beneficial specifically for amperometric sensors, which contend with the limited lifetimes of enzymes since those are often the sensing method. While screen printing is overwhelmingly the printing method of choice for most electrochemical sensors[1, 23, 55, 61, 63, 72, 120, 126, 135], some have opted for inkjet-printed sensors[12, 107, 141], and even gravure-printed[16] and 3D-printed[67] sensors have been demonstrated. 3D-printing often results in mechanically robust, rigid components, which can be used in a variety of applications, including water and food testing. For wearable applications, typically, a much more flexible form factor is desired, both for comfort and for better contact with the skin. For wearable sensing applications as well as direct food contact applications, printing methods such as screen printing, inkjet printing, and gravure printing are much more desirable. Within these, screen printing results in relatively thick films with rougher surfaces, whereas inkjet printing results in much thinner, smoother films, and gravure printing lies in between the two. Thicker films are desirable for conductivity, while thinner films are more mechanically flexible. For many temporary wearable applications, such as electrochemical sensing, screen printing is often the fabrication method of choice since it is quick and can be used in roll-to-roll processing. Screen printing is also easily prototyped using stencil printing as a precursor[61].

A visualization of various printing techniques is shown in Figure 1.1. Use of these additive techniques allows material to be deposited over large areas at high speed and low temperature[35, 79, 130].

1.4 Amperometric Sensors

The immobilization of enzymes enabled the development of enzymatic sensors and eventually printed amperometric sensors[60]. Amperometric sensors are typically composed of three electrodes: a working electrode (WE), a reference electrode (RE), and a counter electrode (CE), as indicated in Figure 1.2. The RE is designed to maintain consistent potential in

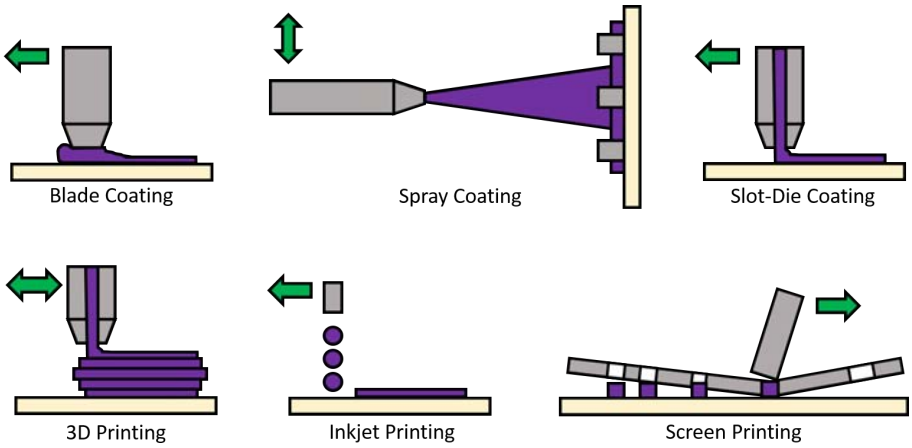

Figure 1.1: Depiction of 6 different printing techniques.

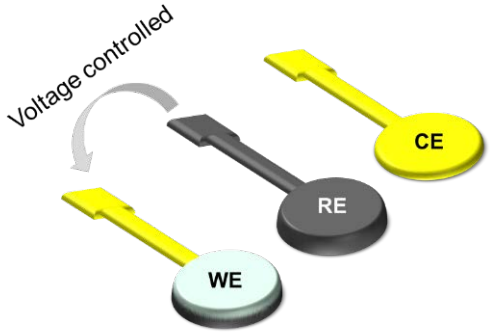

Figure 1.2: Depiction of the 3 electrodes typical of amperometric sensors.

varying ionic environments. The CE is designed to counter the reactions occurring at the surface of the WE. Potential is controlled between the WE and RE, and current is typically measured from the WE with respect to the CE. The surface of the WE is where chemical reactions occur when sensing a substance. In most cases, the chemical reactions at the WE surface are due to the immobilized enzyme.

In typical enzymatic amperometric sensors, the reactions occurring to allow the sensor to operate are as follows:

$$Substrate(2H) + FADoxidase \rightarrow Product + FADH_2oxidase \tag{1.1}$$

$$FADH_2oxidase + O_2 \rightarrow FADoxidase + H_2O_2 \tag{1.2}$$

$$H_2O_2 \rightarrow O_2 + 2H^+ + 2e^- \tag{1.3}$$

Where the substrate is the molecule of interest, FADoxidase refers to the Flavin adenine dinucleotide of the enzyme in use, and $FADH_2$oxidase is the reduced version of FADoxidase. These reactions were standard among enzymatic amperometric sensors until the introduction of mediating molecules. Mediators enable the same top reaction, Equation 1.1, while changing the bottom two Equations 1.2 and 1.3 such that they are not reliant on the presence of oxygen. Mediators can also reduce the operation voltage of enzymatic sensors, since the mediator often has a lower oxidation voltage than that of H_2O_2. One example of this is the use of tetrathiafulvalene (TTF) as a mediator for lactate[63], which changes Equations 1.1, 1.2, and 1.3 into Equations 1.4, 1.5 and 1.6:

$$Lactate + LactateOxidase(FAD) \rightarrow Pyruvate + LactateOxidase(FADH_2) \tag{1.4}$$

$$LactateOxidase(FADH_2) + 2TTF^+ \rightarrow LactateOxidase(FAD) + 2TTF + 2H^+ \tag{1.5}$$

$$2TTF \rightarrow 2TTF^+ + 2e^- \tag{1.6}$$

As evidenced by these reactions, the same number of electrons is produced by each set of reactions meaning the current is still being produced to allow the amperometric sensor to function; the only change is which molecule produces the electrons.

Michaelis-Menten kinetics are typically used to describe the rate of reaction and thus, the current in amperometric sensors. The current, i, in amperometric sensors is given by Equation 1.7

$$i = nFAv_a \tag{1.7}$$

Where n indicates the number of electrons transferred in reaction, F is Faraday's constant, A is the electrode area, and v_a is the rate of reaction. For enzyme-based sensors, the rate of reaction and thus the current achieved in a sensor has two main regimes, which are substrate diffusion-limited and enzyme activity-limited. When the concentration of substrate, or the molecule of interest, is low, sensors will operate in the substrate diffusion-limited regime, and the rate of reaction, and thus, the current will be linearly dependent upon the concentration of substrate in solution.

However, when the substrate diffuses to the sensor surface faster than the enzyme can react with it, the sensor will be limited by the enzyme's activity. To extend the linear, diffusion-limited region of sensor operation, some sensors will employ a diffusion-limiting membrane, which acts as a barrier with much lower internal diffusion than the surrounding solution, thus lowering the sensitivity of a sensor while extending its effective linear range[141]. The sensitivity of a sensor is typically reported as the rate of current increase per change in substrate concentration[1, 135, 23, 63, 126, 120, 12, 16, 67]. A summary of sensors, sensing methods, and printing methods can be found in Table 1.1.

Perhaps the most prevalent printed amperometric sensors throughout the years focus on the determination of glucose[1, 12, 16, 23, 67, 135]. All rely on the enzyme glucose oxidase as the sensing mechanism. The reaction between an enzyme and its substrate, in this case,

Printed Amperometric Sensor	Sensing Mechanism	Best Reported Sensitivity	Best Reported Detection Range	Applications	What Sensor Can Indicate	Printing Methods	Ref.
Glucose	Glucose Oxidase	105 μA mM^{-1} cm^{-2}	0-60 mM	Biosensing in blood and sweat	Management of diabetes	Screen, Inkjet, Gravure, 3D	[1, 12, 16, 23, 67, 135]
Lactate	Lactate Oxidase	68 μA mM^{-1} cm^{-2}	0-25 mM	Biosensing in sweat	Transition from aerobic to anaerobic metabolism	Screen, Inkjet	[37, 61, 63, 107]
Progesterone	Monoclonal Sheep Anit-Progesterone Antibodies	Not Specified	10^{-10}-10^{-5} M	Biosensing in plasma and milk	Fertility and pregnancy	Screen	[55]
Thiamine	Cobalt-mediated Thiolate Anion sensing in Basic Conditions	3.8 nA mL μg^{-1}	0.1-20 μg mL^{-1}	Sensing vitamin B1 in food	Vitamin B1 is part of a healthy diet	Screen	[126]
Amino Acids	Amino Acid Oxidase	345 nA mM^{-1}	0-1 mM	Bio- and food sensing	Fermentation and microbial contamination of dairy	Screen	[120]
Alcohols	Alcohol Dehydrogenase	0.362 μA mM^{-1}	0-36 mM	Biosensing in sweat	Sweat alcohol increases as blood alcohol increases	Screen	[72, 135]

Table 1.1: Review of amperometric sensors, their characteristics, and their uses.

glucose oxidase and glucose, is highly selective; thus, enzymes make a good choice for many sensors. Good sensitivities up to 105 μA mM^{-1} cm^{-2}[1], detection ranges up to 60 mM[12], and insensitivity to uric acid, ascorbic acid, and acetaminophen[135] have each been reported for glucose sensors for varying applications. Some glucose sensors are explicitly developed for the analysis of blood glucose[23], while many other sensors focus on sweat analysis[1, 16, 37]. However, it has been demonstrated that the levels of salt present in sweat can interfere with enzyme-based sensing methods[107], rendering enzymatic sweat sensors less useful than previously thought, unless studies can be done to mitigate the effects of salt on enzyme activity. However, enzymatic sensors are still useful in bodily fluids with lower salt concentrations, such as blood and saliva.

Similarly, printed lactate sensors[37, 61, 63, 107, 141] employ the enzyme lactate oxidase to sense lactate. Sensitivities up to 68 μA mM-1 cm-2[107], detection ranges up to 25 mM[37, 63, 107], and relative insensitivity to creatinine, glucose, uric acid, and ascorbic acid[63, 107] have been demonstrated. Also, Gao et al.[37] demonstrated relative insensitivity to glucose, sodium, and potassium. However, all lactate sensors cited here have been developed for the determination of lactate in sweat, since lactate in sweat can indicate the transition between aerobic metabolism and anaerobic metabolism[37, 61, 63, 107, 109]. The levels of salt in sweat affect lactate oxidase activity[107], which directly affects sensor current through the rate of reaction (see Equation 1.7), thus causing sensor interference. Unless the effects of salts can be accounted for through a multi-sensor patch[37, 141] or mitigated through the use of a membrane[141] lactate sweat sensors have limited reliability.

Other amperometric sensors may be less common but are highly promising. For example, printed biosensors for the determination of progesterone in plasma or milk have been developed using anti-progesterone antibodies as the sensing method[55]. These sensors exhibit sufficient performance for use in biological fluids. An amperometric sensor for thiamine, or vitamin B1, was developed using cobalt phthalocyanine-mediated carbon electrodes[126]. This sensor relies on the fact that at high pH, thiamine converts to an electrochemically active thiolate ion, which can then undergo redox reactions with cobalt. Amperometric sensors for L- and D-amino acids have been demonstrated using L- and D-amino acid oxidase[120]. These sensors showed sensitivity to a variety of amino acids. Finally, interest has been shown in sensing alcohol in sweat[72, 135]. These sensors operate using the enzyme alcohol dehydrogenase, which brings the same downfalls as other enzymatic sensors when it comes to salts[107]. However, these alcohol sensors are also applicable to food and sensing alcohol presence and concentrations in consumables.

Much of the focus of amperometric sensors has historically been for sensing chemicals in sweat[1, 16, 37, 61, 63, 107], though recently it has been shown that the enzymes used as the sensing mechanism for these amperometric sensors may react unpredictably in the presence of salt which is prevalent in sweat[107]. The enzymes present in these sensors may be studied carefully and incorporated with complementary sensors for more accurate determinations in sweat. However, this is not the only application these sensors may be used for. Sweat, while the most non-invasive bodily fluid, is by no means the only bodily fluid available for sensing. Tears are also salty, but saliva, blood, and urine may present alternatives for amperometric

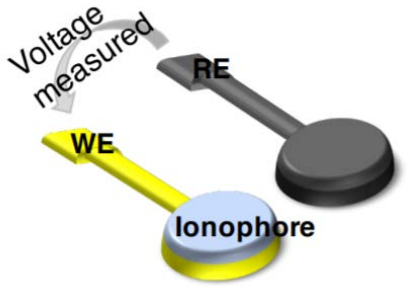

Figure 1.3: Depiction of the 2 electrodes used for potentiometric sensors.

biosensors. Furthermore, food is presented as a promising area for amperometric sensing methods.

1.5 Potentiometric Sensors

A potentiometric sensor measures the potential difference between a working and reference electrode under the conditions of no current flow (Figure 1.3). The potential of the working electrode undergoes significant changes as the concentration of the target analyte changes. Similar to the amperometry technique, the reference electrode is designed to maintain a constant potential in varying ionic environments. Typically, the working electrode is based on an ion-sensitive membrane of a polymeric type containing ionophore, a reagent which selectively binds with the ion of interest. PVC is the most commonly used membrane matrix.

The potential between the ion-selective electrode and the reference electrode, E, varies with the activity, a_{ion} (or concentration C_{ion}, for a dilute solution) of the ion of interest, according to the Nernst equation:

$$E = E_0 + 2.3026\frac{RT}{zF}log_{10}(a_{ion}) \tag{1.8}$$

where E_0 is the standard potential, R is the ideal gas constant and T is the temperature, z is the ion charge, and F is Faraday's constant. The sensitivity (V/dec) is evaluated by:

$$Sensitivity = \frac{dE}{dlog_{10}(a_{ion})} \tag{1.9}$$

The Nernstian response occurs when the response of an ion-selective electrode, according to local thermodynamic equilibrium is determined over a given range of the concentration of the target ion. According to the Nernst equation, at ambient temperature, the electrode will undergo a 59 mV step in potential per factor of ten change in the concentration of a monovalent ion (z=1).

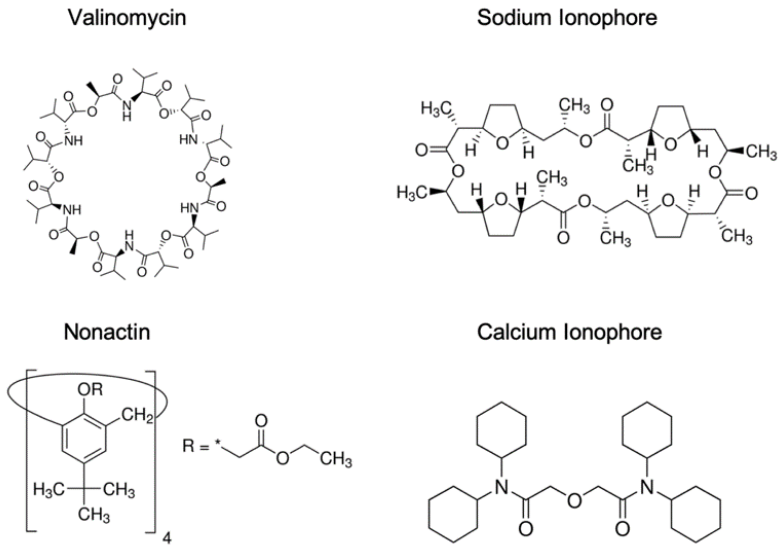

Figure 1.4: Examples of 4 different ionophores used in potentiometric sensors.

Printed potentiometric sensors involve fabrication of the electrodes using printing methods such as screen, inkjet, gravure printing etc. followed by the functionalization into sensors via drop-casting of the ion-selective membrane solution onto the sensing electrodes. A summary of sensors, sensing methods, and printing methods can be found in Table 1.2.

Potentiometric sensors based on polymer membranes have been developed to sense and detect ions such as sodium, potassium, ammonium, calcium, magnesium, pH, chloride, and nitrate, etc. For example, the potassium ion-selective membrane uses valinomycin as the ionophore. Valinomycin (Figure 1.4) in the membrane can selectively form a complex with potassium ion (K^+) from the solution. The other components of the membrane are bis(2-ethylehexyl) sebacate (plasticizer) and PVC. The potassium ions tend to fit in the cavity within the interior of the valinomycin and are held there due to their interactions with the ester carbonyl oxygen atoms of the valinomycin molecule. This gives rise to the selectivity of valinomycin for potassium and allows the reversible exchange of potassium ions with the analyte solution via complexation between potassium and valinomycin. Sensitivities in the 50-62 mV/dec range [24, 37] and a detection range of 0.4 mM - 1 M[24] have been reported in the literature. Potassium ion sensors have been developed for biomedical applications such as analysis of sweat[15, 24, 37, 125], blood[2], and urine[5] as well as in precision agriculture for soil analysis[10].

Similarly, for sodium ion-selective electrdes (ISEs) based on sodium ionophore (Figure 1.4), sensitivities around 64 mV/dec[14, 37] in the 0.1-100 mM[14] concentration range have been reported for sweat monitoring applications. Sodium ISEs have also been integrated with 3D printed platform for sweat-wicking through capillary action[123], and much effort

Printed Potentiometric Sensor	Sensing Mechanism	Reported Sensitivity Range	Best Reported Detection Range	Applications	What Sensor Can Indicate	Printing Methods	Ref.
K^+	Valinomycin	50-62 mV/dec	0.4 mM - 1 M	Biosensing, soil monitoring, water testing	Hypokalemia and kidney disease	Screen, Inkjet, Gravure	[16, 24, 57, 103, 117]
Na^+	Sodium Ionophore X	46-56 mV/dec	0.1-100 mM	Biosensing, water testing	Dehydration and heat cramps	Screen, Inkjet, Gravure	[16, 24, 117, 124, 127]
NH_4^+	Nonactin	54-59 mV/dec	0.1-100 mM	Biosensing in sweat, water testing	Carbohydrates and metabolic condition	Screen	[49]
Ca^{2+}	Calcium Ionophore II (ETH 129)	29-33 mV/dec	0.1-5 mM	Biosensing	Kidney stones	Screen	[110, 136]
pH	Polyaniline, Iridium Oxide, CNTs	-54 - -71 mV/pH	3-11 pH	Biosensing in sweat	Skin diseases	Screen, Gravure, Inkjet	[16, 65, 112, 102]
NO_3^-	Not Specified	-54 mV/dec	0.1-50 mM	Soil fertilizer	Nitrogen-rich fertilizer	Screen	[25]
Cl^-	Ag/AgCl	-51 mV/dec	0.5-50 mM	Soil monitoring, Corrosion	Corrosion of copper, damage to farmland	Screen	[22]

Table 1.2: Review of potentiometric sensors, their characteristics, and their uses.

has been put forth to integrate sweat sensing platforms with microfluidic systems to allow fluid flow over the sensing area[96, 124]. Sodium sensors developed for biosensing in sweat have been shown to be insensitive to potassium, ammonium, and magnesium ions[141], as well as chloride and pH[104].

Printed ammonium (NH_4^+) sensors employ nonactin as the ammonium-selective ionophore (Figure 1.4). Sensitivities for these sensors are near-Nernstian in the 54-59 mV/dec range[49, 51, 141] and can reach ranges from 0.1 mM to 100 mM[49, 141]. Ammonium sensors have been mostly developed for biosensing in sweat and have been shown to be insensitive to potassium, sodium, and magnesium ions[141].

Screen-printed calcium (Ca^{2+}) ion-selective sensors using calcium ionophore (ETH129) (Figure 1.4) have been reported with sensitivity of 29-33 mV/dec in the 0.1-5 mM ion concentration range[110, 136]. Since Ca^{2+} is a divalent ion, the ideal sensitivity of a Ca^{2+} ISE at standard temperature is 29.6 mV/dec of ion concentration. Calcium sensors have been demonstrated for biosensing in sweat, urine and blood.

Potentiometric pH sensors using polyaniline have also been demonstrated[16, 96] with sensitivities of -54 mV/pH to -71 mV/pH in pH ranging from 3-11. These sensors are proposed as useful in sweat pH monitoring, but could also apply to water testing and soil testing. Jovic et al.[65] reported an inkjet-printed potentiometric sensor based on the nano-assembly of iridium oxide (IrOx) nanoparticles and poly- diallyldimethylammonium (PDDA) polymer layers. The sensor was fabricated via layer by layer (LBL) inkjet printing methodology where the positively charged PDDA layer was first deposited on the negatively charged ITO/PET substrate followed by the deposition of the negatively charged IrOx ink. A near-Nernstian response was observed with a sensitivity of about 59 mV/pH in the pH range 3-11. Further, Qin et al.[112] reported an ink-jet printed potentiometric pH sensor using single-wall carbon nanotubes (CNTs) as the sensing mechanism.

While potentiometric sensors for sweat are most common, they are by no means the only interesting applications for potentiometric sensors. For example, printed potentiometric nitrate ion sensors have been developed for monitoring soil fertilizing[25]. These sensors exhibit near-Nernstian response of -54 mV/dec in a 0.1 mM to 50 mM concentration range and insensitivity to other anions commonly found in agricultural fertilizers. Nitrate ion sensors could also be useful for testing groundwater concentrations of nitrate for determining levels of nitrate that are safe for human consumption. Chloride ion sensors have also been developed for monitoring soil salt levels, cleverly using a common reference electrode material: Ag/AgCl[22]. These sensors have a sensitivity of -51 mV/dec in a concentration range of 0.05 mM to 50 mM and are stable over hundreds of days. They have also been proposed as useful in corrosion monitoring.

For printed potentiometric sensors, most effort has been put into developing sensors for sweat applications. This has been shown so far to be more promising than sweat sensors based on enzymatic sensing mechanisms. However, more applications await and show promising results, such as agriculture sensing and corrosion monitoring.

1.6 Conclusion

Printed, flexible sensors have a bright future. Many are currently developed for sweat sensing, which is important for determining a person's state of health non-invasively, though other bodily fluids are posited as also useful for measurement for determining the state of health. Many other potential applications include food sensing, soil sensing, water sensing, and even monitoring corrosion. The studies referenced here show two main types of electrochemical sensors: amperometric and potentiometric with a variety of applications, ranging from health and fitness monitoring to precision agriculture.

1.7 Thesis Outline

The work in this thesis focuses on the development of printed electrochemical sensors. The resulting sensors may be used for sweat sensing or precision agricultural sensing purposes. Two sensor types will be discussed here, as above.

The second chapter details the fabrication and optimization of printed lactate sensors for use in sweat. Inkjet printed and screen printed electrodes are utilized in combination with drop casted active membranes. The effect of changing each component of the working electrode on sensor performance is observed. Working electrode component parameters are chosen for optimizing sensor sensitivity and linear range. The resulting sensors have high sensitivity and physiologically relevant linear range for sensing lactate in a workout. Higher linear range is necessary to achieve sensors which can be useful for clinical applications.

The selectivity of these enzymatic lactate sensors is investigated in chapter three. Sensor current is evaluated in the presence of main components of sweat, resulting in interference. To fully understand this interference, enzyme activity assays are introduced as a method for quantifying interference to the enzyme. Sensors and enzyme activity are tested in multiple solutions moving closer to approximating sweat. Sensors and enzyme are also tested in multiple salts which are prevalent in sweat. Salts are found to affect enzyme activity and thus sensor performance, though each salt affects the sensor and enzyme in unique ways. From this study, it is concluded that until more sweat components are studied and characterized for their effect on enzymatic sensors, these sensors cannot be used *in vivo*. This is because the calibration curves obtained for these sensors *in vitro* in pH buffer no longer apply once the sensor is moved to a bodily, non-pH-buffered environment.

Chapter four proposes an alternative to enzymatic sensors for sweat sensing. Potentiometric sensors utilize a different sensing mechanism: ionophores. Ionophores have been developed for sensing many monovalent and divalent ions, and are less susceptible to salt interference. While lactate cannot be sensed using an ionophore, ammonium, sodium, and potassium can. A multi-sensor platform is proposed which combines all three sensors for a platform with more health information resulting from workouts.

Using the same type of sensor, a nitrate sensor for use in precision agriculture is discussed in chapter five. These nitrate sensors are developed for distribution across a field to show the

needs of a crop as they change across a field. Nitrate sensors are developed using commercially available, non-degradable materials using inkjet-printed and screen-printed electrodes with drop-casted membranes on top. A working electrode is first developed, followed by a reference electrode designed to maintain a relatively consistent potential in varying nitrate ion environments. The nitrate working electrode is characterized for selectivity using definitive screening and statistical analysis. Finally, nitrate working electrodes are characterized using various polymer matrices. Traditional working electrode membranes composed of poly(vinyl chloride) (PVC) are compared with electrode membranes made with degradable polymers poly(lactic acid) (PLA) and poly(caprolactone) (PCL). The results show that while PVC is not degradable, the performance of sensors is vastly improved compared to its degradable counterparts. The working electrode membrane is determined to be a small enough portion of the sensing node that it may be allowed to be non-degradable in comparison to the conductor, substrate, and insulator.

The sixth and final chapter details the main conclusions drawn from the work discussed in this thesis. Directions for future work in the area of printed electrochemical sensors are also addressed.

Chapter 2

Amperometric Lactate Sensors for Sweat Sensing Applications

2.1 Introduction

Since the 1940s, lactate has been a metabolite of interest in bodily fluids because it has been shown to indicate a transition from aerobic to anaerobic metabolism[37, 63, 109], and has been identified as a potential indicator for pressure ischemia[111], panic disorder[80], and cystic fibrosis[18, 31]. In recent years, personalized and mobile, wearable health monitoring have become increasingly popular[69, 70, 87, 101]. In particular, sweat promises to be a non-invasive way to monitor metabolites[31, 115]. Sweat sensors provide a unique platform for non-invasive, continuous, wearable health monitoring. The advent of immobilizing enzymes enabled the development of enzymatic lactate sensors[60, 73]. Since then, lactate sensors have been a popular area of study[33, 37, 61, 63, 68, 71], with some recent studies utilizing high-throughput fabrication methods, such as printing[61, 63].

An ideal lactate sensor will have high sensitivity and large linear range. In literature, the relevant range of lactate detection is up to 25 or 30 mM for sporting applications, especially in determining the transition between aerobic and anaerobic metabolism[6, 19, 29, 32, 34, 42, 43, 44, 45, 46, 77, 90, 91, 105, 106]. On the other hand, for clinical applications such as panic disorder, cystic fibrosis, and pressure ischemia, a linear range up to 50 mM is desired[31, 80, 121, 131].

Amperometric enzymatic sensors can be made at relatively low cost with a high sensitivity, making them ideal for commercial scale production, especially since the limited lifetime of enzymes dictates that enzymes are most appropriate for inexpensive disposable sensor applications. An amperometric lactate sensor is composed of 3 electrodes including a working electrode (WE), reference electrode (RE), and counter electrode (CE). A 2-electrode setup is occasionally chosen for ease of production, in which the counter and reference electrodes are combined into one electrode. Reference electrodes are typically composed of Ag/AgCl due to its ability to maintain a constant potential in varying ionic environments in addition

to its ease of processing[40]. Counter electrodes and working electrode transducers are most commonly made of carbon, but may also be composed of gold, platinum and other inert metals which can be used to counter redox reactions[52, 95]. The sensing layers on the working electrode transducer are fabricated using the enzyme lactate oxidase (LOX) immobilized in a polymer network, typically chitosan. LOX must be immobilized to prevent efflux of enzyme into the surrounding environment. Most sensors also employ a mediator in the composition of the working electrode, such as Prussian Blue[38, 85] or tetrathiafulvalene (TTF)[78, 86, 94]. Mediators function to lower the operation voltage of the sensor. LOX has an oxidation voltage arount 0.6 V[62, 113] when measured with an Ag/AgCl reference, at which other species in sweat such as uric acid and ascorbic acid also oxidize[8, 58]. Oxidation of multiple species at the sensor surface introduces interference in the sensor and reduces its selectivity. Thus, a mediator with a low oxidation voltage is vital to fabricating a selective lactate sensor.

Printing addresses many of the unique needs of enzymatic sensors. Components of all 3 electrodes are solution-processable. Printing can be done on a variety of disposable substrates. Printing is also a high-throughput additive process with the potential to reduce cost of production, leading to inexpensive products which are necessary in the case of disposable sensors such as enzymatic sensors. Sensors designed to wear during a workout must be able to reliably continuously monitor a metabolite while remaining comfortable. The close contact afforded by flexible substrates ensures that sensors come in close contact with sweat as it is formed, giving the potential for highly accurate measurements. Solution-printing is compatible with flexible substrates with form factors closely matching that of skin. Conventional electronic fabrication technology does not allow for this flexibility.

This work utilizes TTF as a mediator due to its low oxidation voltage, high sensitivity, and compatibility with dermal applications. TTF is a small molecule usually used in organic semiconductors and organic charge transfer complexes and is known for its crystalline nature[41, 74]. The sensors reported here are fabricated with ink-jet printed gold electrodes as the WE and CE and screen-printed Ag/AgCl as the RE to produce fully additively manufactured lactate sensors. By optimizing mediating and enzyme layer components of the working electrode, this work reports linear range up to 24 mM lactate and sensitivity up to 4.8 μA/mM which normalizes to 68 μA*cm^{-2}/mM when accounting for surface area, which is suitable for sporting applications in both sensitivity and linear range. Optimized sensors were characterized in both 3-electrode and 2-electrode setups, indicating that while 2-electrodes are easier to fabricate and integrate with external electronics, 3-electrode setups offer better performance in more physiologically relevant ranges. This work produced sensors which showed 97% current retention when operated continuously for an hour *in vitro* to mimic a typical workout.

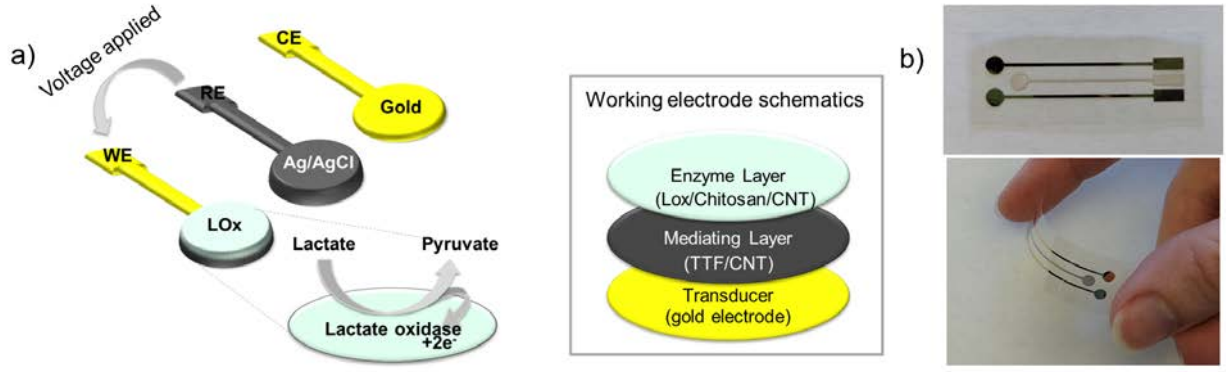

Figure 2.1: Lactate sensor electrodes: a) A schematic of a 3-electrode lactate sensor indicating chemical reactions occurring on the working electrode including a schematic of the working electrode sensing layers on the right of a); b) images of printed gold and Ag/AgCl electrodes prior to deposition of working electrode layers, with electrodes of 3 mm diameter, pictured straight and flexed.

2.2 Fundamental Operation Principles of Amperometric Lactate Sensors

Electrode Composition

An amperometric lactate sensor is composed of 3 electrodes including a working electrode (WE), reference electrode (RE), and counter electrode (CE), as shown in Figure 2.1a. Figure 2.1b shows these electrodes printed on plastic for a wearable form factor. Voltage is controlled between the RE and WE, and the surface of the WE is where reactions occur which release electrons that are read out as current. The RE is composed of printed Ag/AgCl, and the WE and CE are made of printed gold. The WE employs the enzyme lactate oxidase (LOX) as the sensing mechanism immobilized by the polymer chitosan with carbon nanotubes (CNTs). LOX has a high oxidation voltage around 0.6 V (vs. Ag/AgCl)[62, 113] at which other components in sweat oxidize and can introduce interference[8, 58], thus a mediator is used to lower the operation voltage. The mediator oxidizes at a lower voltage, spurring reactions between lactate and LOX. The mediating layer, composed of a mediator and CNTs, is placed below the enzyme layer. A mediator such as tetrathiafulvalene (TTF) has an oxidation voltage between 0-0.2 V when measured with an Ag/AgCl reference electrode, lower than that of LOX and other species found in sweat, preventing interference through oxidation. There are numerous mediators available for facilitating LOX reactions, though TTF has been shown to give high sensitivities and be compatible with dermal applications[63].

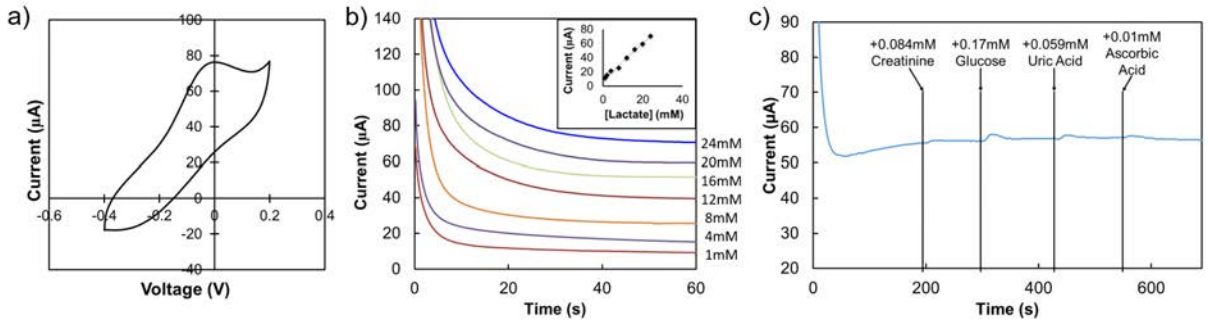

Figure 2.2: Graphs for determining the main figures of merit for lactate including: a) Cyclic voltammetry graph of a TTF-mediated lactate sensor vs. Ag/AgCl reference; b) Chronoamperometry of a lactate sensor with inset of steady-state points graphed to plot sensitivity; c) Standard interference plot of a lactate sensor.

Figures of Merit

There are 3 main figures of merit for lactate sensors: operating voltage, sensitivity, and selectivity. The operating voltage is measured using cyclic votammetry (CV) such as the CV plot in Figure 2.2a which was measured using an Ag/AgCl reference. The first oxidation peak indicates the oxidation of TTF to TTF+ which enables all of the reactions in the sensor. In Figure 2.2a, the first TTF oxidation peak occurs at 0V. Reduction peaks do not appear when performing CV on a lactate sensor in the presence of lactate due to the reversibility of the reactions within the sensor. Since oxidized TTF is reduced by LOX, it is not reduced by changing the voltage applied to the sensor and thus does not produce a reduction peak in the CV graph. For lactate sensors, lower magnitude operation voltages are ideal since high operation voltage can lead to interference with other species present in sweat.

The sensitivity of a lactate sensor is extracted from its chronoamperometry graph, such as that in Figure 2.2b. Chronoamperometry is the measure of current in the sensor over time in increasing concentrations of lactate. The steady state current for each lactate concentration is plotted against lactate concentration to extract a linear fit and thus a sensitivity, as shown in the inset of Figure 2.2b where the current recorded at 60s is plotted against the corresponding lactate concentration.

The selectivity of a sensor is determined from its interference plot, as illustrated in Figure 2.2c. In an interference plot, the current of a sensor in a single concentration of lactate is measured as other sweat metabolites are added. An ideal sensor shows minimal current change in the presence of each species introduced, as does the sensor in Figure 2.2c. Uric acid and ascorbic acid are included due to their low oxidation voltages[8, 58] and show that the sensor operation voltage is low enough to prevent interference, while glucose and creatinine both undergo enzymatic reactions[134, 138] and show the selectivity of the enzyme

itself.

The reactions that occur within the working electrode are shown in Equations 2.1, 2.2, and 2.3:

$$Lactate + LOX(FAD) \leftrightarrow Pyruvate + LOX(FADH_2) \tag{2.1}$$

$$LOX(FADH_2) + 2TTF^+ \leftrightarrow LOX(FAD) + 2TTF + 2H^+ \tag{2.2}$$

$$2TTF \leftrightarrow 2TTF^+ + 2e^- \tag{2.3}$$

where LOX refers to lactate oxidase enzyme, FAD refers to Flavin adenine dinucleotide of lactate oxidase, $FADH_2$ refers to the reduced version of FAD, and TTF refers to tetrathiafulvalene. Equations 2.1, 2.2, and 2.3 occur simultaneously once TTF is oxidized. Lactate reacts with LOX to produce pyruvate and reduce the FAD of LOX. The reduced version of LOX reacts with oxidized TTF to oxidize LOX and reduce TTF. TTF is oxidized to produce electrons, which are read out as current.

Electrode Printing

Gold electrodes were printed using commercially available Harima Nanopaste(Au) NPG-J gold ink in a Dimatix inkjet printer at ambient conditions. Dimatix inkjet printers employ a piezo inkjet cartridge. When a waveform is applied, ink droplets are deposited on the substrate below. The desired pattern is drawn in software such as AutoCAD and converted to a format compatible with Dimatix software for waveform application. Printed gold electrodes are sintered at 250 °C for 50 minutes. Ag/AgCl was printed using Engineered Materials Systems, Inc. CI-4001 ink in a screen printer. During screen printing, a silk screen with a predetermined pattern is flooded with ink. The ink then gets pressed through the pattern in the screen onto a substrate below using a squeegee. Printed Ag/AgCl electrodes are then baked at 110 °C in a vacuum oven for 2 hours. Electrodes were printed on PQA2 PEN 25 μm thick. Printed electrodes were encapsulated using laser-cut Teflon tape. Printed electrodes had circular active areas of 3 mm diameter, resulting in an active area of 0.07068 cm^2. This area was used to calculate sensitivity per area.

2.3 Mediating Layer Optimization

For sporting applications, sensors must achieve high sensitivity, with a linear range up to 30 mM lactate. Sensors with this linear range are best suited to sense the transition from aerobic to anaerobic metabolism. In order to achieve this, we optimized sensors based on sensitivity and linear range by changing the concentration of the TTF/CNT dispersion, as well as the amounts of chitosan, CNT, and enzyme in the enzyme layer. Each of these parameters was optimized independently.

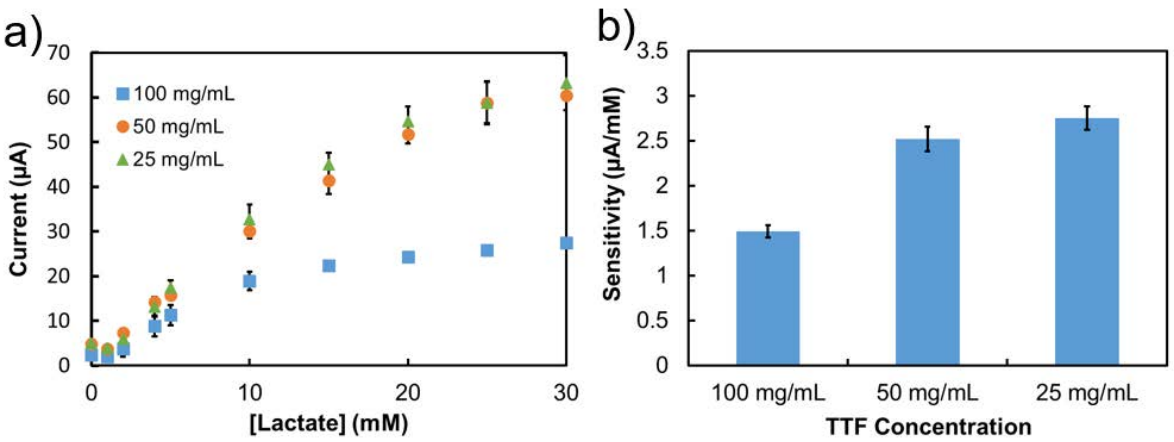

Figure 2.3: Characterization of mediating layer: a) showing current and linear range and b) showing sensitivity comparison for each concentration of TTF/CNT suspension. Error bars indicate standard deviation using at least 3 samples.

The mediating layer was optimized by changing the concentration of the TTF/CNT dispersion deposited on the working electrode surface. Because TTF is an organic semiconductor, conductive CNTs are employed to facilitate electron transfer. Since TTF is a small molecule, it crystallizes when deposited from solution. TTF forms smaller crystals when deposited from lower concentrations. With larger surface area to volume ratio, smaller crystals can contact the enzyme layer in more areas. 3 different concentrations of TTF/CNT dispersion were investigated, listed in Figure 2.3a and b by the TTF concentration as 100 mg/mL, 50 mg/mL, and 25 mg/mL. The other three parameters were held at 1% chitosan, 1% CNTs, and 12 units of enzyme. The concentrations of CNT in the dispersion changed corresponding to the concentration of TTF, such that for 100 mg/mL TTF the concentration of CNT was 5 mg/mL, and when the TTF concentration was diluted the CNT concentration was correspondingly diluted. Thus for 50 mg/mL TTF the CNT concentration was 2.5 mg/mL and for 25 mg/mL TTF, the CNT concentration was 1.25 mg/mL. For each of these concentrations of TTF, the volume of dispersion deposited was changed such that the same solid content was deposited for each concentration, from 3 μL for the highest concentration to 12 μL for the lowest. Figure 2.3 a,b shows the effect of TTF/CNT concentration on the linear range (2.3a) and sensitivity (2.3b) of the sensor. The linear range and sensitivity increase from up to 10 mM to up to 15 or 20 mM lactate and from 1.5 to 2.7 μA/mM respectively when TTF/CNT concentration decreases from 100 mg/mL to 25 mg/mL. This occurs because regardless of the concentration, the dispersion is deposited in 3 μL drops, one drop for the highest concentration to four drops for the lowest. Since these drops contain acetone and ethanol as solvents, which are both low boiling point and high vapor pressure,

the solvent evaporates before large crystals of TTF are allowed to form. However, for higher concentrations the crystals are larger and contain more impurities than a lower concentration of the same volume[133]. Thus the crystals of TTF formed from lower concentrations are smaller and cover a larger proportion of the sensor surface, facilitating closer contact between the TTF and the LOX molecules. 25 mg/mL TTF was determined to give sufficient sensor performance for sporting applications, so 25 mg/mL TTF was used in further optimization tests.

Methods

To make the mediating layer, carbon nanotubes were dispersed in ethanol in the specified concentration (1.25 mg/mL for optimized sensors) and sonified for 20 minutes at 40% amplitude using a Branson Digital Sonifier probe. TTF was dissolved in acetone at the corresponding concentration (25 mg/mL for optimized sensors). 400 μL of TTF solution was added to 2 mL CNT dispersion, and the resulting solution was sonified for 20 minutes at 40% amplitude. The TTF/CNT dispersion was then deposited on the working electrode surface (4 drops of 3 μL for optimized sensors).

Optimization results were measured using a commercial control setup involving printed WE, commercially available Ag/AgCl RE, and commercially available Pt wire CE. Reference electrodes were obtained from Koslow. All optimization was performed in Fisher pH 7.0 buffer containing potassium phosphate monobasic, sodium hydroxide, and water. Sodium-L-lactate was obtained from Sigma Aldrich.

2.4 Enzyme Layer Optimization

Chitosan Weight Percent

The enzyme layer was optimized in 3 steps: chitosan weight percent, CNT weight percent, and enzyme loading, shown in Figure 2.4a and b, Figure 2.5a and b, and Figure 2.6a and b. The amount of chitosan was optimized by varying the weight percent included in the enzyme layer. The other three parameters were held constant at 25 mg/mL TTF, 1% CNT, and 12 units of enzyme. Chitosan acts as an immobilizer and prevents efflux of enzyme into the surrounding environment, but chitosan is also a resistive polymer. This means that if too little chitosan is included in the layer formulation, the enzyme will not be properly immobilized. Improper immobilization results in lower linear range and sensitivity, as can be seen in Figures 2.4a and b, respectively, for 0.1% chitosan. When there is not enough chitosan to immobilize LOX, the linear range barely reaches 5 mM lactate. By comparison, when the enzyme is properly immobilized the linear range is up to 20 mM lactate. On the other hand, if too much chitosan is included, it can block the access between lactate and LOX and provide resistive losses. This results in lower currents and thus lower sensitivity, as can be seen in Figures 2.4a and b, respectively, for 1% chitosan. From Figures 2.4a and

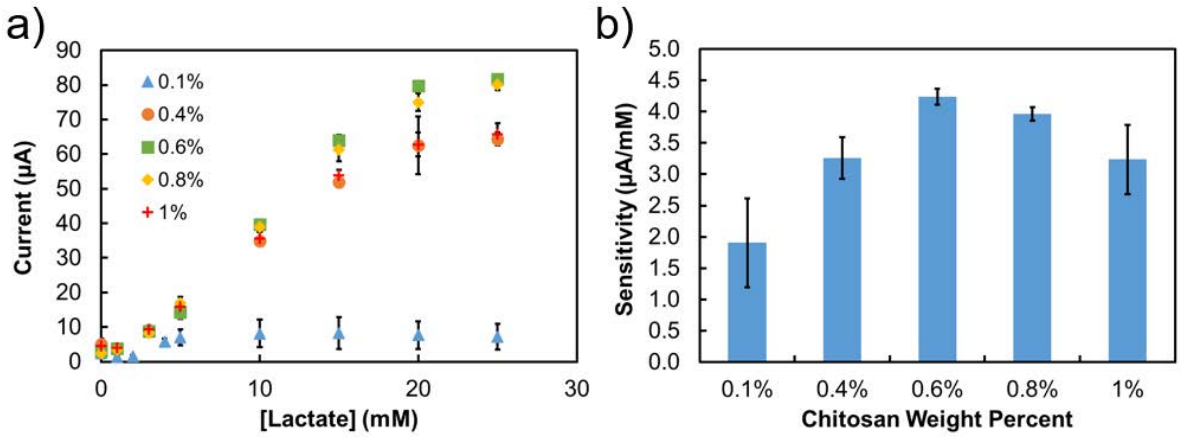

Figure 2.4: Characterization of chitosan content in enzyme layer: a) showing current and linear range and b) showing sensitivity comparison for each weight percent of chitosan. Error bars indicate standard deviation using at least 3 samples.

2.4b, the chitosan weight percent that gave the highest sensitivity and highest currents was 0.6%, which was used thereafter for optimizing the next steps of the enzyme layer.

CNT Weight Percent

The amount of CNT was optimized by varying the weight percent included in the enzyme layer. The other three parameters were held constant at 25 mg/mL TTF, 0.6% chitosan, and 12 units of enzyme. CNTs provide conductive pathways to aid in charge transfer efficiency between the enzyme and solution. If there are not enough CNTs in the sensor, charges will have more difficulty transferring between spatially separated ions. The result is lower currents and thus lower sensitivity, as can be seen in Figures 2.5a and b, respectively, for 0% and 0.25% CNTs. The linear range in both cases barely reaches 5 mM lactate, as it is visible in Figure 2.5a, indicating that not all of the enzyme included in the sensor is acting to its full reactivity. On the other hand, including too much CNT in the sensor can crowd LOX molecules, potentially blocking them from reacting with Lactate. Too much CNTs can result in lower current and thus lower sensitivity, as shown in Figures 2.5a and b, respectively, for 1.5% CNT. From Figures 2.5a and 2.5b, 1% CNT gave the highest sensitivity and highest currents.

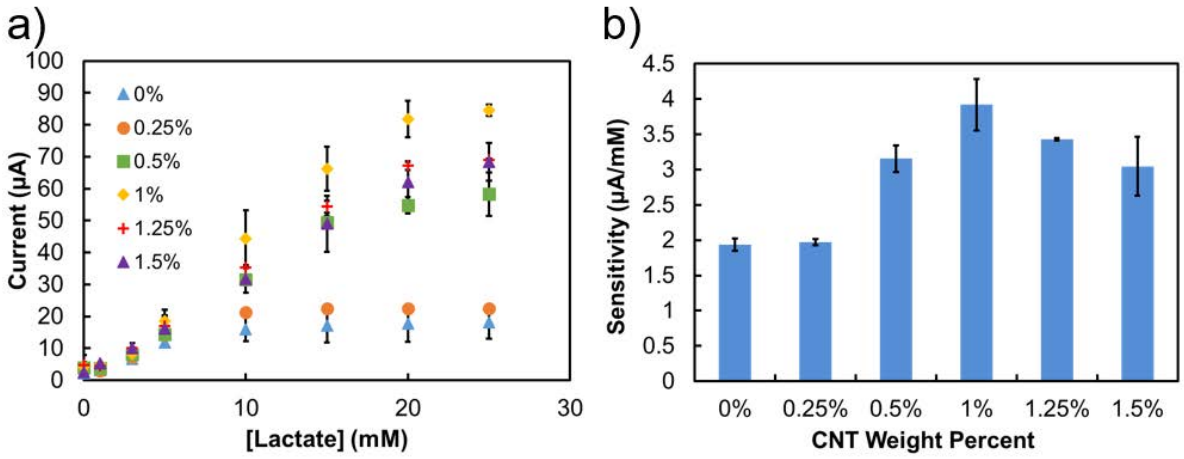

Figure 2.5: Characterization of CNT content in enzyme layer: a) showing current and linear range and b) showing sensitivity comparison for each weight percent of CNTs. Error bars indicate standard deviation using at least 3 samples.

Units of Enzyme

The enzyme loading was optimized by varying the units of enzyme included in the enzyme layer. The other three parameters were held constant at 25 mg/mL TTF, 0.6% chitosan, and 1% CNT. Lower enzyme loading results in resistive losses from too much chitosan, while higher enzyme loading can lead to efflux of enzyme into the surrounding environment. From Figures 2.6a and 2.6b, 7.5 units of enzyme gives the highest current and sensitivity. The resulting sensor has a linear range up to 20 mM lactate but is sensitive up to 25 mM lactate, as shown in Figure 2.6a, and has a high sensitivity as shown in Figure 2.6b.

Through optimization of the mediating and enzyme layers of a lactate sensor, the sensor performance was improved from 1.5 μA/mM or 21 μA*cm^{-2}/mM sensitivity with a linear range up to 10 mM lactate to a more physiologically relevant linear range up to 24 mM lactate with sensitivity of 4.8 μA/mM or 68 μA*cm^{-2}/mM. Device-to-device reproducibility in performance is shown in 2.7, wherein the calibration curves for 4 different sensors are overlaid on the same graph showing close agreement for corresponding concentrations of lactate. The resulting optimized sensors show sufficient performance for sporting applications of lactate sensing.

Methods

To make the enzyme layer, chitosan was dissolved in 1% acetic acid in water (0.6% chitosan by weight for optimized sensors), and CNTs were added (1% by weight for optimized sensors).

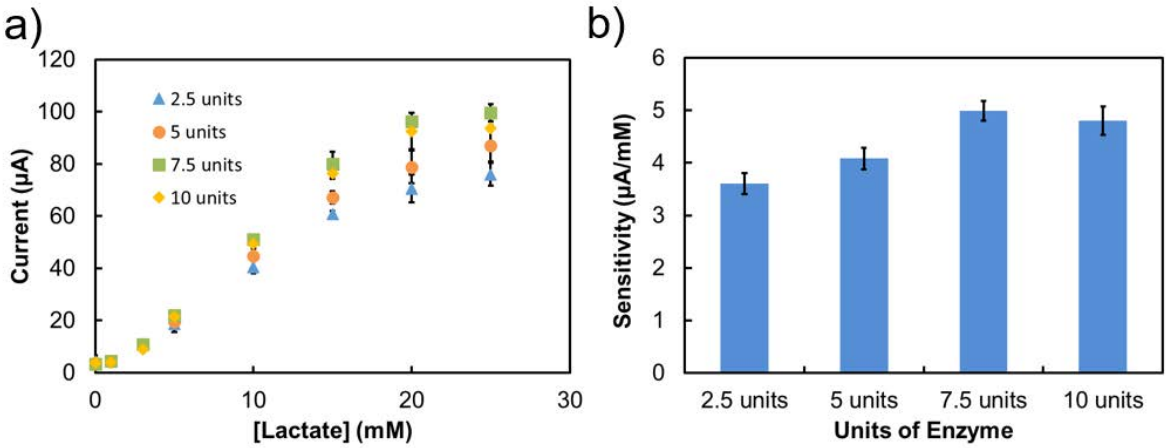

Figure 2.6: Characterization of enzyme content in enzyme layer: a) showing current and linear range and b) showing sensitivity comparison for each amount of units of enzyme. Error bars indicate standard deviation using at least 3 samples.

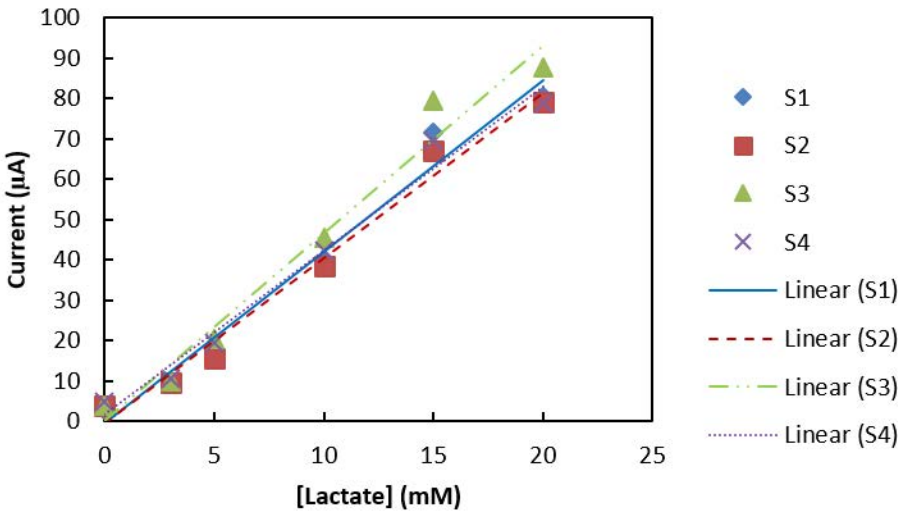

Figure 2.7: Four lactate sensor calibration curves (S1, S2, S3, and S4) overlaid to show sensor reproducibility.

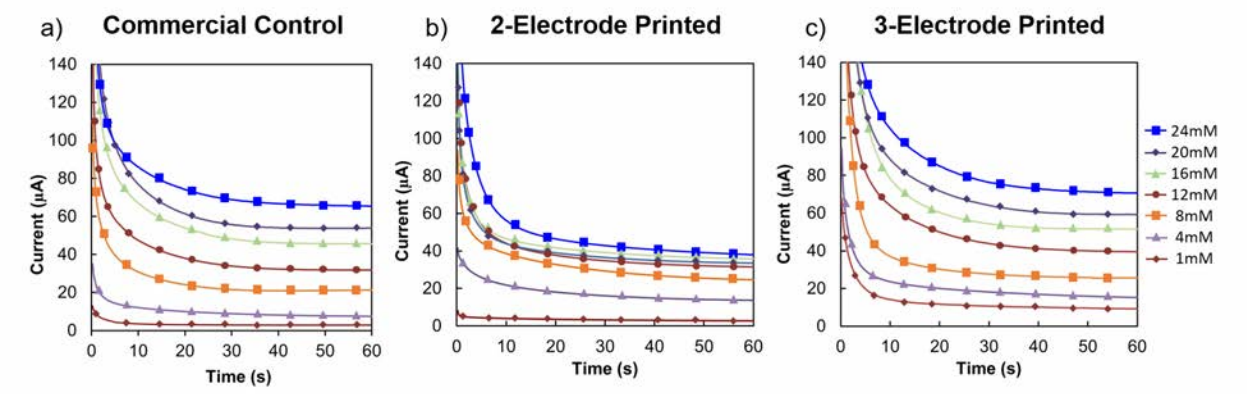

Figure 2.8: Chronoamperometry in three different configurations including a) commercial 3-electrode control configuration, b) 2-electrode printed configuration, and c) 3-electrode printed configuration.

This mixture was sonified for 20 minutes at 40% amplitude. In a separate vial, Lactate Oxidase was measured out and dissolved in Fisher pH 7.0 buffer (for optimized sensors, 1500 U/mL). The lactate oxidase mixture was mixed 1:1 with the chitosan and CNT mixture and deposited on top of the mediating layer (1 drop of 10 μL for optimized sensors). The sensors were then dried overnight in an environmental chamber at 35 °C.

2.5 Optimized Sensor Performance In Vitro

Printed working electrodes were optimized using a commercially available Ag/AgCl reference and a commercially available platinum counter electrode, referred to in Figure 2.8 as the Commercial Control. The resulting optimized sensor was characterized using chronoamperometry in 3 different sensor setups including the Commercial Control. The chronoamperometry in the Commercial Control configuration for concentrations of lactate of 1 mM, 4 mM, 8 mM, 12 mM, 16 mM, 20 mM, and 24 mM is shown in Figure 2.8a. These concentrations of lactate mimic physiological levels of lactate in sweat for sporting conditions. The printed working electrode was also tested using a printed reference electrode in a 2-electrode printed configuration with chronoamperometry shown in Figure 2.8b for the same lactate concentrations. Finally, the printed working electrode was tested with printed reference and counter electrodes in a 3-electrode printed configuration with chronoamperometry shown in Figure 2.8c with the same lactate concentrations. Figures 2.8a and 2.8c look very similar, indicating that the printed reference and counter electrodes work just as well as the commercially available reference and counter electrodes. However, the 2-electrode setup in Figure 2.8b exhibits clearly lower currents.

The effects of the 2-electrode setup are even clearer in Figure 2.9, the overlaid sensitivity

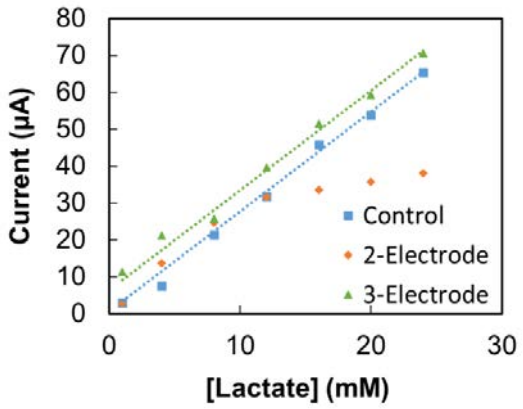

Figure 2.9: Sensitivity graph with steady state currents from 2.8 extracted onto the same graph

plots of each electrode configuration. The currents at 60s for Figures 2.8a, b, and c were plotted against lactate concentration to produce the sensitivity plot shown in Figure 2.9. While the commercial and printed 3-electrode configurations have the same sensitivity, offset by a small but constant current, the 2-electrode configuration does not have the same linear range as the other two. The 2-electrode configuration relies on the Ag/AgCl electrode to perform the function of both reference and counter electrodes. The reference electrode must maintain a stable potential in varying ionic environments, while the counter electrode works to counter the redox reactions that occur on the surface of the working electrode by allowing current to pass between the counter and working electrodes. It is challenging to maintain a constant potential while supplying current to the working electrode, thus 2-electrode configurations are expected to show lower currents and linear ranges than their 3-electrode counterparts[52]. This is demonstrated in Figure 2.8 and 2.9. The 3-electrode configurations, however, exhibit linear range and sensitivity sufficient for sporting applications.

Furthermore, when operated continuously for an hour in a single concentration of lactate as shown in Figure 2.10, the sensor exhibits 97% current retention, indicating this sensor could be useful for continuously monitoring an exercise session. The *in vitro* results in Figure 2.8, Figure 2.9, and Figure 2.10 indicate a promising sensor for determining the transition between aerobic and anaerobic metabolism. The current stability of the sensor is further studied by measuring a single sensor repeatedly over the course of 4 hours. The results of this study will be shown and further discussed in Chapter 3, though over the course of 4 hours the current in each concentration of lactate does not vary.

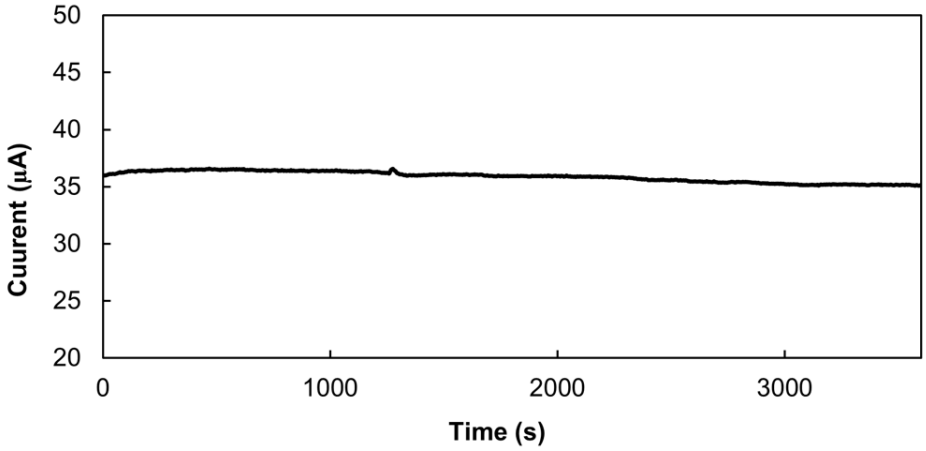

Figure 2.10: Sensor performance in one lactate concentration when operated continuously for one hour

2.6 Conclusion

In vitro testing of amperometric lactate sensors indicate that they have sufficient performance for on-body measurement of lactate for sporting applications. The results shown are promising for a future commercializable lactate sweat sensor. However, Chapter 3 will investigate the final figure of merit when assessing amperometric lactate sensors: selectivity.

In the transition between aerobic and anaerobic metabolism, a concentration change of about 10 mM lactate is anticipated in sweat. Based on the sensors optimized in this chapter, that would result in a current change of about 48 μA. While the exact numbers of lactate concentration vary from person to person based on their level of fitness and health and also based on measurement location on the body, the change in concentration is approximately the same from person to person. Accurate measurement of lactate in sweat can give an understanding of how efficiently the body is using oxygen during a workout.

An ideal, printed, flexible, wearable lactate sweat sensor holds many advantages over the current methods of measuring bodily lactate. Instead of monitoring blood, it non-invasively monitors sweat. It has the ability to monitor in real-time as opposed to collecting a sample for lab-scale spectroscopic testing. While the advantages of a wearable sensor are great, the accuracy of blood and spectroscopic sweat testing may not necessarily be met by these sensors, as will become clear in Chapter 3.

Chapter 3

Limitations of Enzymatic Sensors

3.1 Introduction

Salts are well-known to affect enzyme activity[47], though the effect of salt on enzymatic sensor performance is not yet well known. This work endeavored to characterize the effects of 5 different salts in ranges of physiologically relevant concentrations, though there are hundreds of constituents of sweat which have not yet been characterized for their effect on sensor performance[56]. This work incorporated salts and various solutions to mimic characteristics of sweat in a controlled lab environment. The ability to mimic *in vivo* characterization would allow us to produce a calibration curve that mimics sensor performance on the body in real sweat conditions. This is important to interpret lactate sensor data in real time if lactate sensors are ever to be used commercially. Ultimately, while sensors may perform well in a typical *in vitro* testing environment, this performance is not indicative of how sensors will perform in the presence of salts without a pH buffer present. This work investigates five chloride salts that are contained in sweat and considered primary electrolytes, though sweat has many more components which are not investigated in this work. Each salt affects sensor performance and enzyme activity differently. Until each component of sweat is investigated and accounted for alongside a lactate sensor, current lactate sensors can at best be labeled indicators of aerobic or anaerobic metabolism, but cannot give accurate lactate sweat concentrations.

3.2 Traditional Interfering Species

The last figure of merit to address is selectivity. Our sensor was characterized for selectivity in the traditional manner by continuously operating the sensor in 15 mM lactate and adding potentially interfering species one at a time, as shown in Figure 3.1. This work employed physiologically average concentrations of the standard interfering species for lactate: 0.084 mM creatinine, 0.17 mM glucose, 0.059 mM uric acid, and 0.01 mM ascorbic acid. Traditionally, creatinine, glucose, uric acid, and ascorbic acid are included in interference studies

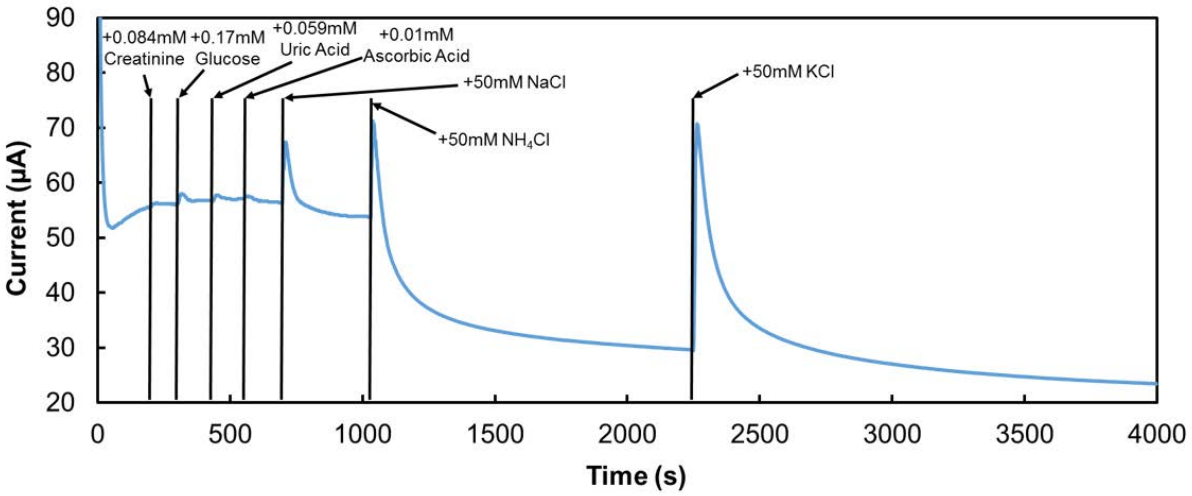

Figure 3.1: Sensor performance in traditional interference species plus salts

for lactate for two different reasons. Creatinine and glucose both undergo reactions with enzymes and are included to test the selectivity of the LOX enzyme for lactate[134, 138]. Uric acid and ascorbic acid both have low oxidation voltages and are included to test that the operation voltage of the sensor is low enough to prevent interference from oxidation[8, 58]. From Figure 3.1, these 4 species introduced minimal variation in sensor current, indicating no interference. In addition, this work acknowledges that salts are a major component of sweat[56], and included 3 extra salts which are major components of sweat: NaCl, NH_4Cl, and KCl. Sodium, ammonium, potassium, and chloride are all main components of sweat and thus provide a rigorous first step toward real sweat conditions. From Figure 3.1, each of these 3 chloride salts in 50 mM concentrations introduced major changes in current to the sensor, and thus interfere with sensor operation. For sodium, 50 mM is a physiologically relevant concentration, but for ammonium and potassium, physiologically relevant concentrations are much lower at 5 mM and 8 mM respectively. The interference observed in Figure 3.1 led to a deeper exploration of interference between enzymes and salts and an attempt to approximate real sweat *in vitro*.

3.3 In-depth Interference Study

Enzyme Activity

In order to fully understand the effects of interfering species on lactate sensors, it is imperative to perform enzyme activity measurements. Enzyme activity measurements indicate how quickly and effectively an enzyme can react in the presence of other materials. This

is important to understand because enzymes are the direct sensing mechanism and for accurate sensing that reliably follows a calibration curve, the enzymes need to react at the same rate in all measurement environments. If this is the case, we can accurately say that the sensitivity we obtain from sensors is fully a function of the concentration of lactate and not due to anything else present in solution interfering with the enzyme. This is described by Michaelis-Menten kinetics[7], which defines the current, I, in an amperometric sensor by Equation 3.1,

$$I = nFAv_a \tag{3.1}$$

Where n is the number of electrons transferred in the reaction, F is Faraday's constant, A is the area of the sensor, and v_a is the rate of reaction between the enzyme and its substrate. In this case, the enzyme is LOX and its substrate is Lactate. This rate of reaction is well-defined by Michaelis-Menten kinetics[30] by Equation 3.2,

$$v_a = [S_0]\frac{V_{max}}{K_m} \tag{3.2}$$

Where $[S_0]$ is the concentration of substrate, in this case lactate, K_m is the Michaelis constant for the given reaction, and V_{max} is the maximum rate of reaction the enzyme can achieve, given by the enzyme activity. By plugging Equation 3.2 into Equation 3.1 it becomes apparent that the current in a sensor is linearly dependent upon the concentration of lactate only when the enzyme activity is constant. However, if the concentration of lactate remains constant, the current in a sensor becomes linearly dependent upon enzyme activity. In unchanging conditions, this current is constant. However, in changing conditions, as on the body, current could change drastically. Thus, by measuring enzyme activity in the presence of varying solutions and varying metabolites found in sweat, we can gain a better understanding of how sensors will react to conditions on the body.

Enzyme activity is performed following the procedure reported by Toyobo[81, 132]. The procedure reported by Toyobo was followed exactly and used as the standard against which all other measurements were compared. Thus, when enzyme activity is reported as a percentage, it is compared to the exact procedure and materials used in the Toyobo documentation. The enzyme activity measurements achieved by following Toyobo's main procedure are counted as 100% enzyme activity for the purposes of this study. An example absorbance plot for a sample following Toyobo's main procedure is shown in Figure 3.2. The enzyme assay recipe developed by Toyobo involves the reactions in Equations 3.3 and 3.4,

$$\mathrm{L{-}lactate} + \mathrm{O_2} \xrightarrow{\mathrm{LOX}} \mathrm{Pyruvate} + \mathrm{H_2O_2} \tag{3.3}$$

$$2\,\mathrm{H_2O_2} + \text{4-Aminoantipyrine} + \mathrm{EHSPT} \xrightarrow{\text{peroxidase}} \mathrm{Quinoneimine\,dye} + 4\,\mathrm{H_2O} \tag{3.4}$$

Where EHSPT refers to N-ethy-N-(2-hydroxy-3-sulphopropyl)-m-toluidine and peroxidase refers to horseradish peroxidase. The quinoneimine dye produced from this reaction

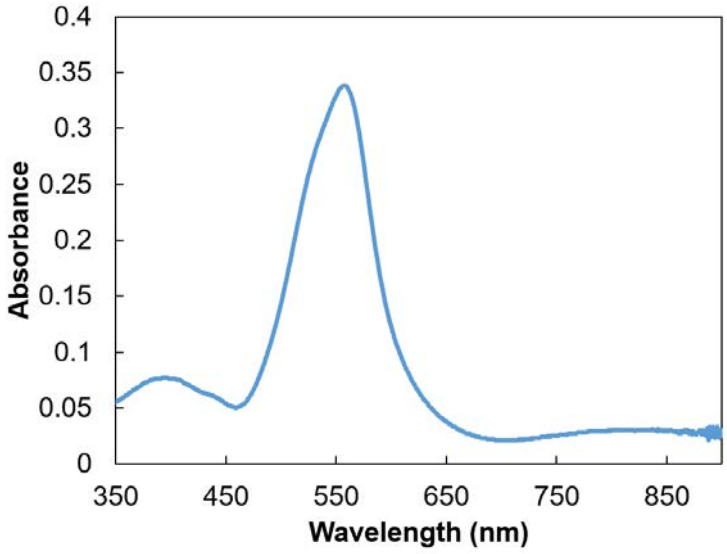

Figure 3.2: Full absorbance spectrum of an enzyme assay made using pH 7.5 potassium phosphate buffer as dictated by Toyobo, exhibiting a peak at 555 nm.

produces an absorbance peak at 555 nm, as is evident from the spectrum shown in Figure 3.2. Thus, enzyme activity is calculated using the absorbance at 555 nm wavelength using the equations dictated by Toyobo. When testing different solutions for their effect on enzyme activity, each solution specified was substituted in place of the standard pH 7.5 potassium phosphate buffer that Toyobo uses in the lactate solution portion of the enzyme assay, or solution (A) on the data sheet for lactate oxidase. When testing salts, two separate enzyme activity measurements were performed to attempt to ascertain the effect of the salt. To test the salt's effect on the enzyme itself, the salt in the specified concentration was incubated with the enzyme in solution for an hour at room temperature. To test the salt's effect on ionic interactions surrounding the enzyme, the salt in the specified concentration was mixed with the lactate solution.

Methods

Enzyme activity was performed using the procedure from Toyobo. Potassium phosphate buffer of pH 7.5 was made using potassium phosphate monobasic obtained from Sigma Aldrich, potassium phosphate dibasic obtained from Sigma Aldrich, and potassium hydroxide obtained from Sigma Aldrich. When comparing enzyme activity in various solutions, the potassium phosphate buffer of pH 7.5 in which the lactate was dissolved was exchanged for the various other solutions. Gibco Phosphate Buffered Saline was obtained from ThermoFisher Scientific. Enzyme was incubated with salt according to the procedure from Toy-

obo, salt was also mixed with the lactate solution prior to assay. Absorbance was measured using a Shimadzu UV-2600 UV-Vis Spectrometer. Activity was calculated using the method from Toyobo, then divided by calculated activity using the standard Toyobo procedure with no salt and no solvent substitutions to arrive at a percentage activity. Through this method, the reference activity is always 100%.

Salty Solution Investigation

To further approximate *in vivo* conditions in comparison with typical *in vitro* characterization, a variety of solutions were characterized *in vitro* including various buffers typically used to characterize sensors as well as non-pH-buffered solutions. Sensor performance, as well as enzyme activity are shown in Figure 3.3. Enzyme activity is shown in blue with activity reported as a percentage relative to the standard potassium phosphate buffer used for enzyme assay as reported by Toyobo[81, 132]. The scale for enzyme activity percentage is shown on the right of the graph. Sensitivity of corresponding sensors in solutions of lactate using each type of solution is shown in orange, with sensitivity scale shown on the left of the graph. The first solution listed is Potassium Phosphate Buffer, referring to the standard buffer used by Toyobo with a pH of 7.5, followed by Phosphate Buffered Saline from Gibco, a pH 7.4 buffer that includes sodium chloride in the formulation and is often used in sensor characterization. Yellow Buffer refers to Fisher's phosphate buffer with pH 7.0 which includes potassium hydroxide in the formulation. This is the solution which was used in this work for optimization and characterization of sensors. Water refers to deionized water. Sweat with no salts and Salty Sweat refer to house-made artificial sweat recipes using physiologically average amounts of the previously tested interference species. 84 μM creatinine, 0.17 mM glucose, 59 μM uric acid, and 10 μM ascorbic acid were dissolved in deionized water for Sweat (No Salts), while Salty Sweat includes these as well as 50 mM NaCl, 5 mM NH_4Cl, and 8 mM KCl. As indicated by the first 700 s of Figure 3.1, Sweat with no salts produces similar results in both sensitivity and enzyme activity as plain deionized water. The traditionally measured interfering species for lactate have very little effect on the sensor's performance.

3.4 Characterizing Effects of Individual Salts at Physiologically Average Levels

Five different chloride salts were investigated for their effects on enzyme activity and sensor performance: NaCl, NH_4Cl, KCl, $CaCl_2$, and $MgCl_2$, each of which is a constituent in sweat. The effect of nearly physiologically average concentrations of each of these salts on sensor current at 15 mM lactate is shown in Figure 3.4a. While some salts give lower currents at physiologically average concentrations (NaCl, $CaCl_2$, and $MgCl_2$), others give higher currents (NH_4Cl and KCl). To help explain why these salts affect sensor current, the same salt concentrations were used in Figure 3.4b when measuring enzyme activity. In

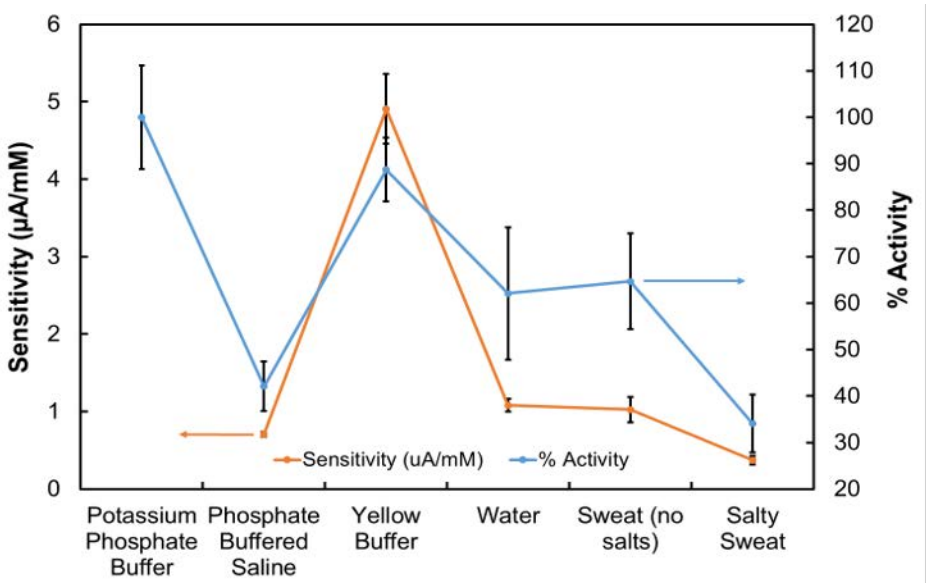

Figure 3.3: Sensor sensitivity and relative enzyme activity in varying solutions. Error bars indicate standard deviation using at least 3 samples.

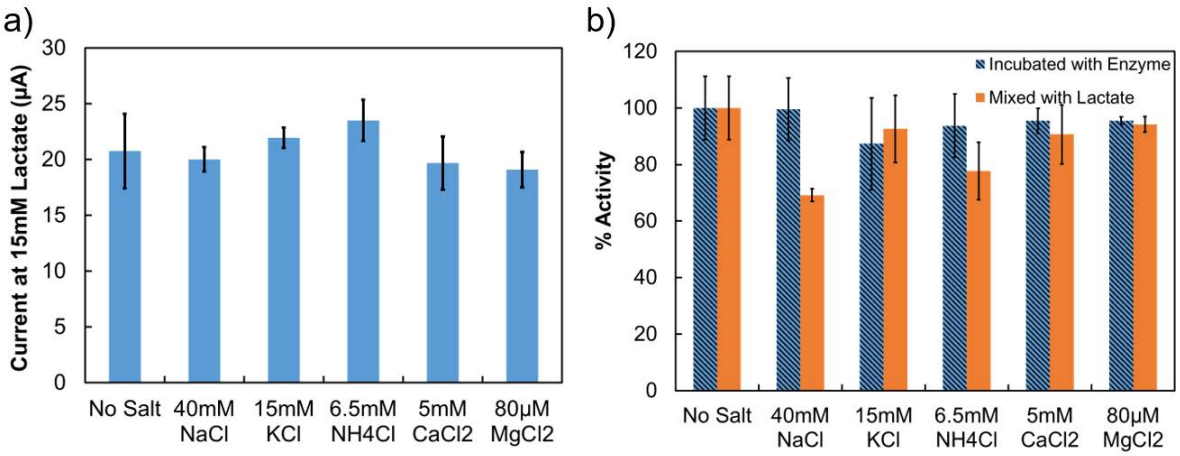

Figure 3.4: Performance in sweat-like conditions including: a) current in a lactate sensor at 15mM lactate with physiological concentrations of five different salts, and b) enzyme activity two ways in the presence of the same salts. Error bars indicate standard deviation using at least 3 samples.

Figure 3.4b, two different methods were employed for measuring enzyme activity in order to find one method which might predict sensor performance. The standard method for measuring enzyme activity in the presence of other species is shown in blue. This method involves incubating the enzyme with the determined concentration of salt for an hour prior to dilution for assay. In orange is a method from this work of mixing the salt with the lactate in the assay mixture, to mimic the changes that a salt may bring about to the redox reactions on a sensor. For some salts such as NaCl and NH_4Cl, incubation was a more accurate indicator of a salt's effect on sensor performance, indicating that salt affected the enzyme most within the sensor. Because the enzyme is the sensing mechanism, changes in enzyme activity will change a sensor's current output, even in the presence of the same concentration of lactate, as described by Equations 3.1 and 3.2. The sensor performance in the presence of the other salts, KCl, $CaCl_2$, and $MgCl_2$, was better indicated by mixing salt with the assay mixture, indicating that the salt affects ionic interactions surrounding a sensor more than the enzyme itself. This form of interference still affects sensor current because the ionic interactions prevent or facilitate lactate from reaching the enzyme to react and produce current in the sensor. The changes in sensor current corresponding from changes in enzyme activity are more clearly visible in the next subsection, in which sensors are investigated with a range of salt concentrations to determine their effects on sensitivity of a sensor as well as enzyme activity.

Even for a single salt, the effect on the sensor is highly dependent upon salt concentration, as seen in Figure 3.5, in which the current of a sensor in 15 mM lactate is plotted for 4 different concentrations of $CaCl_2$. The sensor response to increasing concentrations of $CaCl_2$ is nonlinear, indicating that sensor responses to metabolites in sweat warrant further study.

3.5 Characterizing the Effects of Individual Salts in a Range of Physiological Levels

We have further investigated NaCl, NH_4Cl, KCl, $CaCl_2$, and $MgCl_2$ for their effect on enzyme activity and sensor performance. To achieve this, each salt was investigated in a range of physiological levels of the cation while lactate was varied in a range of physiological levels. To obtain calibration graphs with sensitivities, sensors were measured in increasing concentrations of lactate in water, then allowed to rest in deionized water before measuring again in lactate in water with added salt. This procedure was repeated for each increasing concentration of salt. The sensors for these measurements were actively measured for over 4 hours with no major affects to current retention, as demonstrated in some of the salt discussions that have little to no effect on sensor performance such as $MgCl_2$. This means that the lactate sensors developed in this study have a lifetime much longer than the average workout time of one hour. It is notable that physiological levels of Cl^- ion can vary from 17 μM to 290 mM with average concentrations of about 23 mM[56]. It is important to note that the sensors in this study were measured in water, not pH buffer, thus their sensitivities

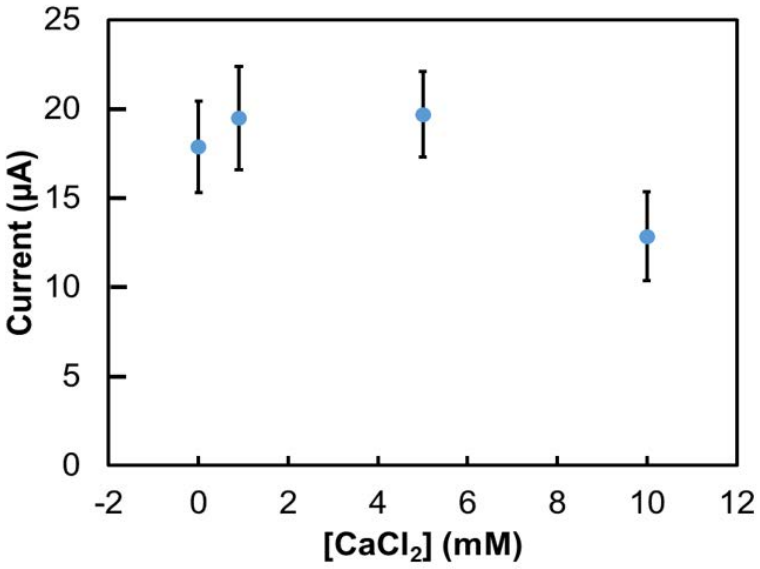

Figure 3.5: Sensor current at 15mM lactate for four different concentrations of one salt. Error bars indicate standard deviation using at least 3 samples.

are lower than the reported optimized sensor sensitivity.

NaCl

While 30-40 mM NaCl is considered physiologically average, Na^+ concentrations in sweat can range from 0.1 mM to 390 mM[56]. From this range, a small range of physiologically relevant concentrations of Na^+ concentrations were selected to study. Since the high and low extremes of concentrations typically occur in the case of clinical conditions, NaCl concentrations of 10 mM, 20 mM, 40 mM and 60 mM were chosen for investigating the effects of NaCl and particularly Na^+ concentration on lactate sensors and lactate oxidase. The results of this study are shown in Figure 3.6. For the purposes of NaCl, only the sensitivities of the sensor in 10 mM and 60 mM NaCl are provided on the graph to offer contrast. In 10mM NaCl, the sensitivity is 1.1 μA/mM lactate, while in 60 mM NaCl the sensitivity drops to 0.8 μA/mM lactate.

For comparison, enzyme activity was measured in each of the same concentrations of NaCl. Enzyme activity for salt incubated with the enzyme is shown in Table 3.1, while enzyme activity for salt mixed with the lactate solution is shown in Table 3.2. From Figure 3.6, it is clear that increasing the concentration of NaCl in sweat-like solutions will decrease sensor sensitivity. This follows the general trend of enzyme activity when NaCl is mixed in the lactate solution, shown in Table 3.2, in which enzyme activity reliably decreases as salt concentration increases. Enzyme activity when NaCl is incubated with the enzyme has

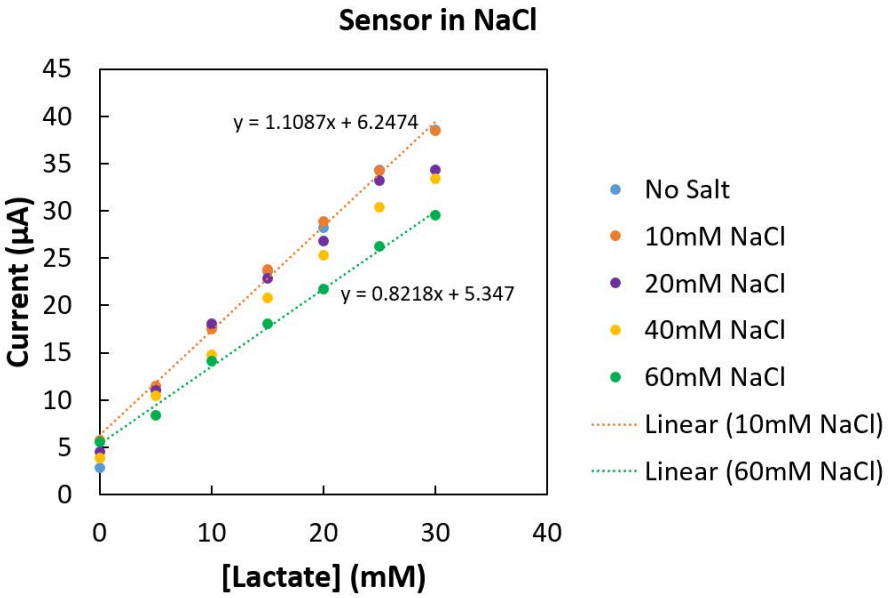

Figure 3.6: Calibration curves for a sensor in increasing concentrations of NaCl.

	% Activity	St. Dev. (%)
10mM	103.5	15.6
20mM	110.4	8.2
40mM	99.5	11.1
60mM	95.6	17.7

Table 3.1: Enzyme activity for varying concentrations of NaCl incubated with the enzyme. Standard deviation is calculated using at least 3 samples.

	% Activity	St. Dev. (%)
10mM	92.9	3.1
20mM	81.3	3.7
40mM	69.1	2.3
60mM	59.5	3.3

Table 3.2: Enzyme activity for varying concentrations of NaCl mixed with the lactate solution. Standard deviation is calculated using at least 3 samples.

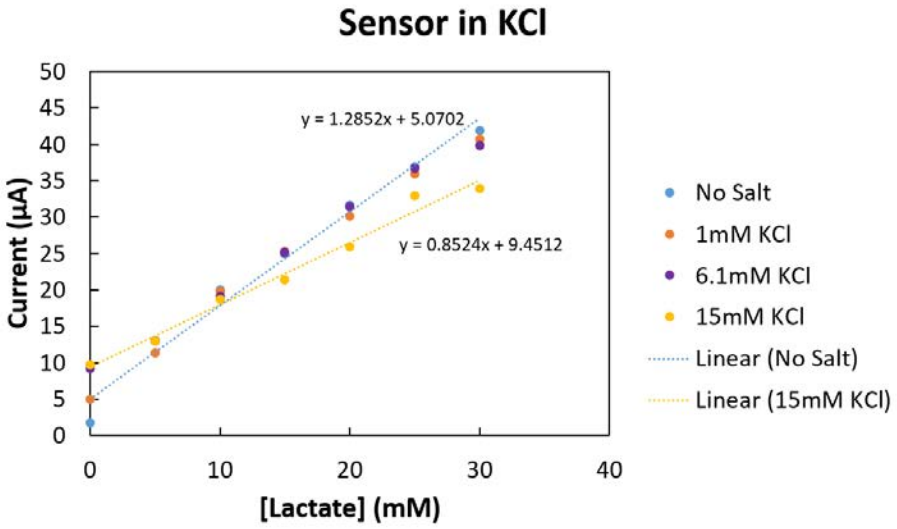

Figure 3.7: Calibration curves for a sensor in increasing concentrations of KCl.

	% Activity	St. Dev. (%)
1mM	116.6	2.1
6.1mM	95.0	3.1
15mM	87.4	16.2

Table 3.3: Enzyme activity for varying concentrations of KCl incubated with the enzyme. Standard deviation is calculated using at least 3 samples.

nonlinear behavior in that activity increases between 0 mM and 20 mM NaCl, but then decreases between 20 mM and 60 mM, as indicated in Table 3.1.

KCl

Physiologically average amounts of K^+ in sweat are between 6 and 8 mM. However, K^+ concentration in sweat can range from 6 μM to 38 mM. From this range, a smaller range of physiologically relevant concentrations were chosen as 1 mM, 6.1 mM, and 15 mM KCl for studying the effects of KCl and particularly K^+ on lactate sensors and lactate oxidase. The results of this study are shown in Figure 3.7. For the purposes of KCl, only the sensitivities of the sensor in no salt and 15 mM KCl are provided on the graph to offer contrast. In no salt, the sensitivity is 1.3 μA/mM lactate, while in 15 mM KCl the sensitivity drops to 0.85 μA/mM lactate.

For comparison, enzyme activity was measured in each of the same concentrations of

	% Activity	St. Dev. (%)
1mM	103.9	2.0
6.1mM	96.1	0.7
15mM	92.6	11.9

Table 3.4: Enzyme activity for varying concentrations of KCl mixed with the lactate solution. Standard deviation is calculated using at least 3 samples.

	% Activity	St. Dev. (%)
0.5mM	89.9	2.5
3.3mM	87.6	3.6
6.5mM	93.7	11.1
10mM	97.8	2.0

Table 3.5: Enzyme activity for varying concentrations of NH_4Cl incubated with the enzyme. Standard deviation is calculated using at least 3 samples.

KCl. Enzyme activity for salt incubated with the enzyme is shown in Table 3.3, while enzyme activity for salt mixed with the lactate solution is shown in Table 3.4. From Figure 3.7, it is clear that increasing the concentration of KCl in sweat-like solutions will decrease sensor sensitivity. This follows the general trend of enzyme activity when KCl is mixed in the lactate solution, shown in Table 3.4, as well as the general trend when KCl is incubated with the enzyme, shown in Table 3.3. For both methods, enzyme activity reliably decreases as concentration of salt increases. However, enzyme activity when 1 mM KCl is incubated with the enzyme goes far above enzyme activity with no salts (which is defined as 100% enzyme activity), indicating that enzyme activity with KCl mixed with the lactate mixture is a better indicator of the performance of sensors in the presence of KCl.

NH_4Cl

Physiologically, concentrations of NH_4^+ in sweat can vary from 0.47 mM to 27 mM, and physiologically average NH_4^+ is considered to be 5 mM[56]. From this range of physiologically possible concentrations of NH_4^+, a physiologically relevant range of NH_4Cl concentrations were chosen as 0.5 mM, 3.3 mM, 6.5 mM, and 10 mM. This spans most of the range of possible NH_4^+ concentrations that can be found in sweat since the range of concentrations is so small compared to other metabolites investigated here. The results of this study are shown in Figure 3.8. No sensitivity lines are provided on the graph for sensors in NH_4Cl to facilitate visualization of the overlap of data points. From Figure 3.8, there is no clear effect on sensors from changing NH_4Cl.

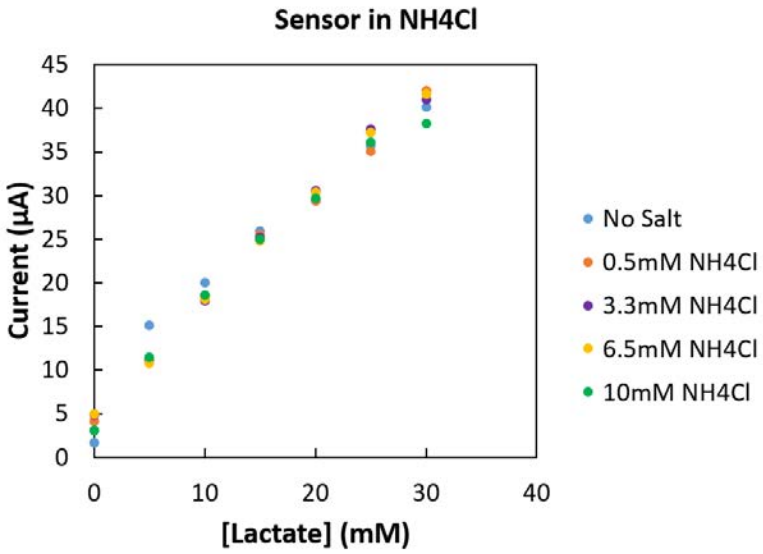

Figure 3.8: Calibration curves for a sensor in increasing concentrations of NH_4Cl.

	% Activity	St. Dev. (%)
0.5mM	105.6	6.3
3.3mM	82.7	5.2
6.5mM	77.6	10.2
10mM	89.2	5.0

Table 3.6: Enzyme activity for varying concentrations of NH_4Cl mixed with the lactate solution. Standard deviation is calculated using at least 3 samples.

For comparison, enzyme activity was measured in each of the same concentrations of NH_4Cl. Enzyme activity for salt incubated with the enzyme is shown in Table 3.5, while enzyme activity for salt mixed with the lactate solution is shown in Table 3.6. From Figure 3.8, there is no clear effect on sensors from increasing NH_4Cl concentration. This is also the case in both Table 3.5 and Table 3.6, where an overarching trend in enzyme activity does not emerge and all percentages are grouped around the same values.

$MgCl_2$

Physiologically, concentrations of Mg^{2+} in sweat can vary from 0.07 μM to 3.8 mM, and physiologically average Mg^{2+} is considered to be about 80 μM[56]. From this range of physiologically possible concentrations of Mg^{2+}, a smaller range of physiologically relevant

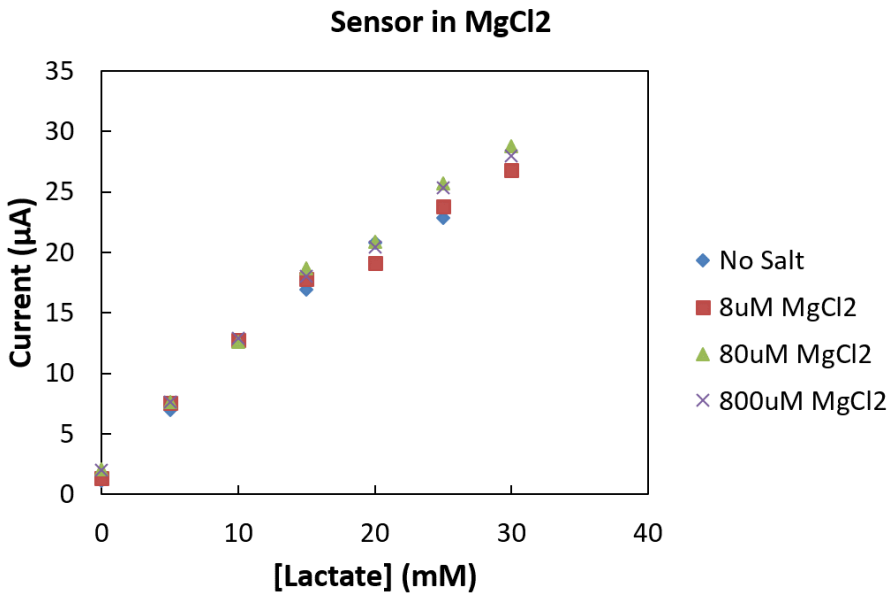

Figure 3.9: Calibration curves for a sensor in increasing concentrations of $MgCl_2$.

	% Activity	St. Dev. (%)
8μM	94.9	1.1
80μM	95.5	1.4
800μM	92.9	3.4

Table 3.7: Enzyme activity for varying concentrations of $MgCl_2$ incubated with the enzyme. Standard deviation is calculated using at least 3 samples.

$MgCl_2$ concentrations were chosen as 8 μM, 80 μM, and 800 μM. The results of this study are shown in Figure 3.9. No sensitivity lines are provided on the graph for sensors in $MgCl_2$ to facilitate visualization of the overlap of data points. From Figure 3.9, there is no clear effect on sensors from changing $MgCl_2$.

For comparison, enzyme activity was measured in each of the same concentrations of $MgCl_2$. Enzyme activity for salt incubated with the enzyme is shown in Table 3.7, while enzyme activity for salt mixed with the lactate solution is shown in Table 3.8. From Figure 3.9, there is no clear effect on sensors from increasing NH_4Cl concentration. This is also the case in both Table 3.7 and Table 3.8, where an overarching trend in enzyme activity does not emerge and all percentages are grouped around the same values.

	% Activity	St. Dev. (%)
8μM	94.1	5.4
80μM	94.2	2.7
800μM	98.4	1.4

Table 3.8: Enzyme activity for varying concentrations of $MgCl_2$ mixed with the lactate solution. Standard deviation is calculated using at least 3 samples.

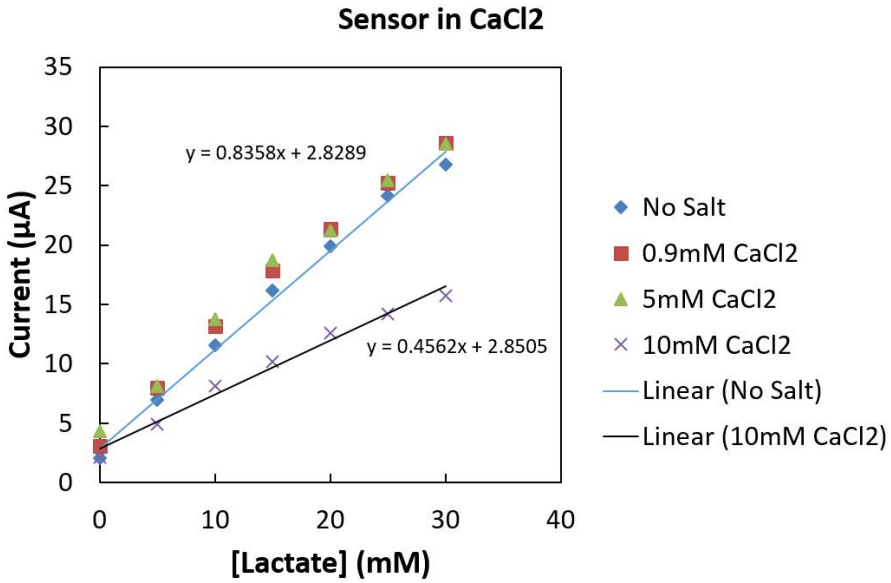

Figure 3.10: Calibration curves for a sensor in increasing concentrations of $CaCl_2$.

$CaCl_2$

Physiologically, concentrations of Ca^{2+} in sweat can vary from 4.7 μM to 15 mM, and physiologically average Ca^{2+} is considered to be about 5 mM[56]. From this range of physiologically possible concentrations of Ca^{2+}, a physiologically relevant range of $CaCl_2$ concentrations were chosen as 0.9 mM, 5 mM, and 10 mM. The results of this study are shown in Figure 3.10. For the purposes of $CaCl_2$, only the sensitivities of the sensor in no salt and 10 mM $CaCl_2$ are provided on the graph to offer contrast. In no salt, the sensitivity is 0.84 μA/mM lactate, while in 10 mM $CaCl_2$ the sensitivity drops to 0.46 μA/mM lactate.

For comparison, enzyme activity was measured in each of the same concentrations of $CaCl_2$. Enzyme activity for salt incubated with the enzyme is shown in Table 3.9, while enzyme activity for salt mixed with the lactate solution is shown in Table 3.10. From Figure 3.10, increasing $CaCl_2$ concentration has a nonlinear effect on sensor performance, increasing

	% Activity	St. Dev. (%)
0.9mM	104.5	1.0
5mM	95.5	4.4
10mM	95.6	3.2

Table 3.9: Enzyme activity for varying concentrations of $CaCl_2$ incubated with the enzyme. Standard deviation is calculated using at least 3 samples.

	% Activity	St. Dev. (%)
0.9mM	92.3	2.3
5mM	90.7	10.4
10mM	78.5	14.7

Table 3.10: Enzyme activity for varying concentrations of $CaCl_2$ mixed with the lactate solution. Standard deviation is calculated using at least 3 samples.

sensitivity between 0 mM and 0.9 mM $CaCl_2$ and decreasing sensitivity between 0.9 mM and 10 mM $CaCl_2$, which follows the trend for incubated enzyme activity when increasing and mixed enzyme activity when decreasing. In Table 3.9, the enzyme activity for the lowest concentration of $CaCl_2$ is above that of enzyme activity with no salt, while for 5 mM and 10 mM, enzyme activity has no discernable difference. In Table 3.10, enzyme activity consistently decreases as $CaCl_2$ concentration increases, with a major jump in activity between 5 mM and 10 mM, similar to the large change in sensor sensitivity between 5 mM $CaCl_2$ and 10 mM $CaCl_2$ seen in Figure 3.10.

The use of salts and non-buffered solutions was vital to determining more closely how sensors may perform *in vivo*, since sweat is a salty, non-buffered environment. Each salt affected sensor performance and enzyme activity differently, though the effect on enzyme activity indicates that salt is a major factor to take into consideration when developing enzymatic sensors.

3.6 Conclusion

The sensitivity of lactate sensors in Figure 3.3 very closely follows the trend for enzyme activity, which indicates that changing the lactate solution most affects the enzyme in an enzymatic sensor, not necessarily the other electrochemical reactions taking place in solution. Since the enzyme is the mode of sensing in enzymatic sensors, variations in activity are not ideal. To perform well, a sensor must react predictably to changing environments, ideally reacting selectively only to the constituent of interest.

While optimized sensors perform well in a pH-buffered *in vitro* environment, introduction

of any variables that bring conditions closer to those of *in vivo* measurements drastically affects sensor performance and render previously acquired sensitivity graphs inaccurate for comparing with on-body measurements. To better mimic on-body environments and get closer to accurate *in vivo* performance, artificial sweat should be used to characterize sensors. However, enzyme activity is known to be highly dependent upon temperature, pH, and salt[47, 81, 132], and while our study discusses five salts, there are hundreds of constituents of sweat[56]. In order to detect a transition between aerobic and anaerobic metabolism, a change in lactate in sweat of approximately 10 mM is expected. In our sensors, this change in lactate concentration corresponds to a change in current of approximately 10 μA. When we consider salt interference as shown in Figure 3.4a, the current in sensors at physiologically average concentrations of salt changes approximately 5 μA. The change in current due to salt interference is lower than the change in current required to detect the threshold between aerobic and anaerobic metabolism. Therefore, these sensors may still function well as indicators for the purposes of determining the transition between aerobic and anaerobic metabolism, even taking into account the interference of salts. However, it is unlikely that enzymatic lactate sensors will give accurate numerical readings for continuous health monitoring. The effects of each of the constituents in sweat on enzymatic sensors are not well known. In order to achieve an accurate measurement of lactate, a systematic study of each constituent in sweat would need to be performed for its effect on enzymatic sensors. Any constituents found to affect sensor performance would need to be included in a multiplexed sensor configuration where its effects are back-calculated to determine an accurate numerical value for lactate in sweat. From our studies, we conclude that at least sodium, potassium, and calcium must be included in such a multiplexed patch, in addition to pH and temperature before on-body studies are performed.

Chapter 4

Potentiometric Sensors for Sweat Sensing Applications

4.1 Introduction

Chapter 3 of this work endeavored to demonstrate that amperometric enzymatic sensors are as yet impractical for use in sweat sensing. In order to become practical, these sensors would need to be incorporated with many other sensors for any sweat components which may affect the activity of the enzyme. However, simple sweat sensors may still be realized in the form of potentiometric sensors.

Potentiometric sensors have a major advantage over amperometric sensors when concerned with sweat sensing. This advantage is selectivity. Potentiometric sensors measured with the same interfering species as the amperometric lactate sensor from Chapter 3 show little to no response[141]. This makes them an obvious choice for sweat sensing over amperometric sensors. Potentiometric sensors can be used to measure simple monovalent and divalent ions, thus making them incompatible with measuring lactate. Instead, this chapter will focus on ammonium (NH_4).

Ammonium in sweat can indicate low levels of carbohydrates, which are vital to performance while working out, and may also indicate metabolic condition[13, 49, 50, 92].

4.2 Potentiometric Sensor Operation

Potentiometric sensors operate using two electrodes as shown in Figure 4.1, a working electrode (WE) and a reference electrode (RE). Thus, these sensors are simpler than the amperometric sensors of Chapter 2 and 3. The RE is designed to maintain a consistent potential in varying ionic environments, while the WE utilizes an ionophore which reversibly binds with the ion of interest. The ion changes the potential at the surface of the electrode and potential is measured between the WE and RE. The ionophore for ammonium sensors is usually Nonactin[49]. The structure of Nonactin can be found in Figure 1.4.

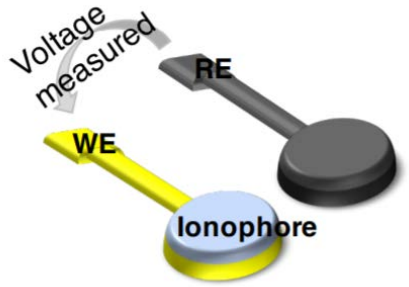

Figure 4.1: Depiction of the 2 electrodes used for potentiometric ammonium sensors.

The potential in a potentiometric ammonium sensor is proportional to the amount of ammonium present through the Nernst Equation 4.1.

$$E = E_0 + 2.3026\frac{RT}{zF}log_{10}(a_{ion}) \tag{4.1}$$

Where E is potential, E_0 is the standard potential, R is the ideal gas constant and T is the temperature, z is the ion charge, F is Faraday's constant, and a_{ion} is the ion activity. The ion activity is a function of the concentration of the ion and the ion activity coefficient. At sufficiently dilute concentrations, the ion activity coefficient is 1[20], thus the potential is considered to be a function primarily of the concentration of the ion in solution.

Since ammonium is a monovalent cation, the anticipated sensitivity of these sensors according to Equation 4.1 is 59.1 mV/decade, meaning that for every factor of ten increase in ammonium concentration, the potential of the sensor should increase by 59.1 mV.

Electrode Printing

Gold electrodes were printed using Harima Nanopaste(Au) NPG-J gold ink in a Dimatix inkjet printer at ambient conditions. Dimatix inkjet printers employ a piezo inkjet cartridge. When a waveform is applied, ink droplets are deposited on the substrate below. The desired pattern was generated in CAD software and converted to a format compatible with Dimatix software for waveform application. Printed gold electrodes were sintered at 250 °C for 50 minutes. Ag/AgCl was screen printed using Engineered Materials Systems, Inc. CI-4001 ink. During screen printing, a silkscreen with a predetermined pattern is flooded with ink. The ink then is pressed through the screen onto a substrate below. Printed Ag/AgCl electrodes were then baked at 120 °C in a vacuum oven for 2 hours. Electrodes were printed on PQA2 PEN 25 μm thick. Printed electrodes were encapsulated using laser-cut Teflon tape. Printed electrodes had circular active areas of 3 mm diameter, resulting in an active area of 0.07068 cm^2.

4.3 Sensor Performance in vitro

Methods

Working electrodes were made by mixing the components of the sensing membrane: 0.001 g ammonium ionophore I, 0.345 g 2-nitrophenyl octyl ether, and 0.159 g PVC in 5 mL of THF. The resulting solution was drop-casted on the printed working electrode sensor surface as 6 μL total in 3 separate 2 μL increments. The resulting working electrode was allowed to dry in a fume hood for 15 minutes.

The reference electrode employed a CNT transducer between the Ag/AgCl electrode and the membrane. This transducer was composed of 0.01 g of CNT and 0.05 g of F127 dissolved in 10 mL of THF, which were sonified for 1 hour in an ice bath using a Branson Digital Sonifier probe. The resulting mixture was deposited on the printed reference electrode surface as 4 μL total in 2 separate 2 μL increments.

The reference electrode further included a PVB and NaCl membrane, which was made by dissolving 1.58 g of PVB and 1.00 g of NaCl in 20 mL of methanol. This mixture was sonified for 30 minutes in an ice bath. The resulting mixture was deposited on top of the CNT transducer as 6 μ total in 3 separate 2 μL increments.

For sensitivity measurements, NH_4Cl was dissolved in deionized water, then diluted to various concentrations. A Keithley 2400 Series SourceMeter was used to measure potentials.

Results

Sodium and ammonium sensors have been previously reported by our research group[141]. For the purposes of reproducibility, this work endeavored to recreate fully printed ammonium sensors. The recipes for these sensors and reference electrodes were developed and tested by Zamarayeva et al[141] and were recreated as reported in this work.

The ammonium sensors were recreated for use in conjunction with other sensors developed within the group for a multi-sensor sweat patch. The ammonium sensor remained the responsibility of this work, while the remaining sensors, sodium and potassium, were developed and tested in conjunction by collaborators.

The results from ammonium sensors studies may be found in Figure 4.2. For potentiometric sensors, since no operation voltage needs to be determined, sensors may go directly from fabrication to measurement. Raw measurement data is shown on the left of Figure 4.2, where potential is measured over time in changing ammonium concentration.

The data on the right of Figure 4.2 is the same data for two sensors, S1 and S2, extrapolated onto a plot of potential as a function of concentration of ammonium in solution. The sensitivities of the two sensors match up very well and are near-Nernstian at 57.5 mV/decade $\pm$ 0.3 mV/decade. This promising data that matches well to what was found by Zamarayeva et al[141] was encouragement to pursue a multi-sensor patch.

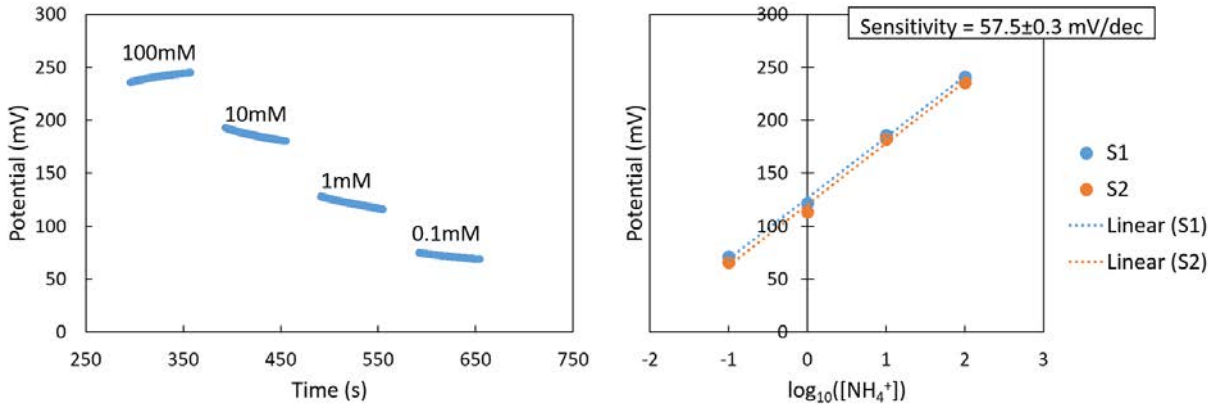

Figure 4.2: Left, response of ammonium sensor over time in changing ammonium concentration. Right, sensitivities of two sensors, S1 and S2, overlaid to show reproducibility.

4.4 Multiplexed Sensor Platform

Single metabolites in sweat can give very specific information. Chloride ion is the diagnostic standard for cystic fibrosis[54]. Sodium in sweat can indicate electrolyte imbalance and dehydration[17]. Lactate in sweat can indicate the transition from aerobic to anaerobic metabolism[37, 63, 109]. Alone, a single metabolite can give useful, though limited information. By putting multiple metabolites together, we can get a better overall view of a person's whole health, as each metabolite lends its information.

For this reason, a multiplexed, multi-sensor patch was proposed for sensing metabolites in sweat. A schematic of this patch is shown in Figure 4.3, which includes ammonium, sodium, and potassium. Ammonium in sweat indicates low levels of carbohydrates and can indicate metabolic conditions[13, 49, 50, 92]. Sodium in sweat can indicate electrolyte imbalance and dehydration[16, 17, 24, 117, 124]. Potassium in sweat can indicate hypokalemia in addition to how well the kidneys are functioning[16, 24, 57, 103, 117].

By combining all three of these sensors into a single patch, we can get more complete information into a person's workout and overall health. As depicted in Figure 4.3, the sensing patch would consist of 4 total electrodes: one working electrode for each ammonium, sodium, and potassium, and one shared reference electrode. This is possible because the reference electrode serves the same function for all three sensors and is made the same way.

4.5 Conclusion

While amperometric sensors are not yet fully ready for *in vivo* sweat sensing, potentiometric sensors offer a good alternative. They are relatively insensitive to other components of sweat and selective to the ion they are designed to measure[141]. Combining them allows us to

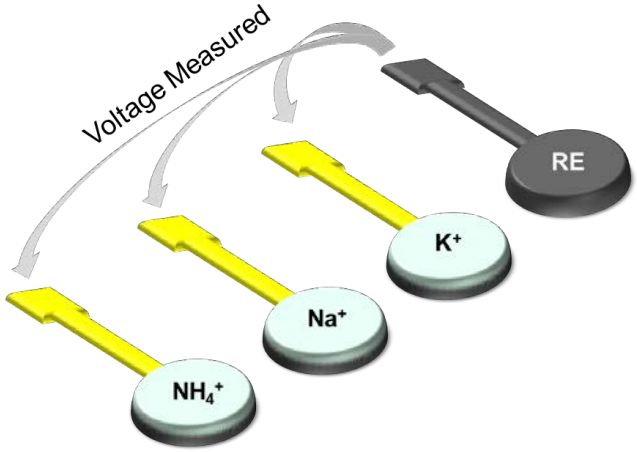

Figure 4.3: Depiction of the proposed multiplexed sweat sensing patch containing Ammonium, Sodium, and Potassium sensor working electrodes sharing the same reference electrode.

measure multiple metabolites at the same time, ensuring we get a more comprehensive view of a person's health. Such multi-sensor platforms can pave the way for incorporating multiple sensors with amperometric sensors to be able to measure lactate in sweat in the future.

Chapter 5

Potentiometric Nitrate Sensors for Soil Sensing Applications

5.1 Introduction

Crop yield is highly dependent upon application of enough fertilizer. One of the main components of agricultural fertilizer is nitrogen in the form of nitrate (NO_3-N)[137]. Yet nitrogen-rich fertilizer is one of the highest energy costs in agriculture and contributes to greenhouse gas emissions when used in excess[139]. Further, NO_3-N is highly mobile and readily leaches into its surroundings[26]. It has been shown that crop yield and fertilizer needs vary within a single field, not just field-to-field[26]. Using sensors to measure NO_3-N in many points across a field can inform precise application of fertilizer, conserve energy, and aid crop yield[75, 76]. Development of printed potentiometric nitrate sensors can assist in this endeavor.

Potentiometric sensors are composed of 2 electrodes: a working electrode (WE) and a reference electrode (RE). REs are typically composed of Ag/AgCl due to its ability to maintain a constant potential in varying ionic environments in addition to its ease of processing[40]. WE transducers are composed of an electrically conductive metal with a sensing membrane that is typically composed of an ionophore mixed with plasticizer and poly(vinyl chloride) (PVC)[9, 21, 24, 51, 93, 98, 117, 124, 136]. The ionophore reversibly binds with the ion of interest, changing the potential at the surface of the WE. This potential is measured with respect to the RE, and the magnitude of the potential is used to determine the concentration of ion present based on the Nernst Equation.

Many potentiometric nitrate sensors have been reported in literature for various purposes, including water monitoring[21, 36, 53, 123], bodily fluid testing[98], and soil monitoring[10, 21, 25, 53, 84]. There are also many nitrate sensors that have been developed using different sensing methods[3, 4, 11, 89, 100, 119]. State of the art nitrate tests involve taking a soil sample to a lab. There have been some attempts at in-field nitrate measurement[84], though these involve measuring nitrate at one point in the field. In-field sensors also tend not to be

scalable to measurement across a field, and are not degradable. While some printed nitrate sensors have been demonstrated[10, 25], the advantages of printing for soil sensing have not yet been realized to their full potential.

Printing addresses the needs of agricultural sensors in a unique way. Solution printing is an additive process which allows material to be deposited over large areas at high speeds and low temperatures[35, 79, 130]. Printing may be done with any solution-processable materials, which is something the area of printed electronics has long taken advantage of[16, 61, 63, 69, 70, 99, 107, 114, 118]. While often touted for the flexibility of using unconventional substrates with wearable form factors[69, 70], printing also allows the use of unconventional active materials[79, 108]. In particular, printing can be done using naturally degradable materials[59, 66, 83], which can be designed to degrade after a single crop cycle.

For an agricultural sensor to function properly, it must be insensitive to the many chemicals found in soil and fertilizer[128]. Additionally, the sensor's ability to detect an ion of interest should not be affected by fluctuating levels of these chemicals. Screening designs are an efficient way to identify significant interfering ions while minimizing the number of experiments required, and they are a first step to developing thorough models of a sensor in its intended environment [64].

In this work, we fabricate potentiometric nitrate sensors to measure NO_3-N and evaluate the sensor sensitivity and selectivity, as well as develop the formulation of a reference electrode for such sensors. We use printing methods to make the sensors with commercially available, non-degradable materials. Potentiometric nitrate working electrodes are first characterized with commercially available Ag/AgCl reference electrodes to determine reproducibility and sensitivity to nitrate in solution. Printed Ag/AgCl reference electrodes are characterized with commercially available Ag/AgCl reference electrodes in order to determine the relative insensitivity to nitrate in solution. Finally, selectivity of the nitrate working electrode is evaluated against several ions found in soil using the Definitive Screening Design. The resulting sensor has near-Nernstian response and insensitivity to chemicals commonly found in soil and fertilizers. These sensors act as a preliminary step toward fully degradable nitrate sensors which can be dispersed throughout a field to determine NO_3-N fertilizer needs. The conductors and insulators utilized in this study can be replaced with degradable conductors and insulators to realize degradable sensors in future studies.

5.2 Nitrate Sensor Operation

A potentiometric sensor is composed of two electrodes, as indicated in Figure 5.1 a): a working electrode (WE) and a reference electrode (RE). The RE is designed to maintain a consistent potential in varying ionic environments. The WE employs an ionophore which reversibly binds with the ion of interest, changing the local potential at the surface of the electrode. For this work, a nitrate ionophore was employed for nitrate selectivity. The potential in a potentiometric sensor is described by the Nernst equation:

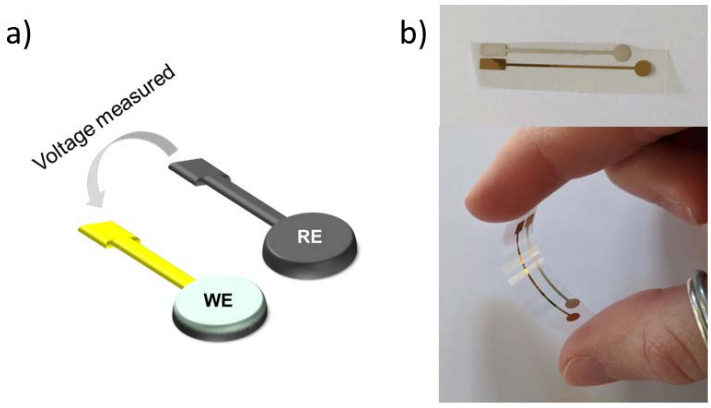

Figure 5.1: a) Schematic of the electrodes making up a potentiometric sensor. b) Image of printed potentiometric electrodes.

$$E = E_0 + 2.3026\frac{RT}{zF}log_{10}(a_{ion}) \tag{5.1}$$

Here, E is the potential measured from the sensor, E_0 is the standard potential, R is the ideal gas constant, T is the temperature, F is Faraday's constant, z is the number of electrons transferred in reaction, and a_{ion} is the ion activity. The ion activity is a function of the concentration of the ion in solution and the activity coefficient, which is 1 for sufficiently dilute solutions. Thus, a potentiometric sensor for a monovalent ion, such as nitrate, at room temperature is expected to exhibit a 59.1 mV change for every factor of ten change in concentration of the ion. For monovalent cations (z= +1), this is a positive relationship, where increasing concentration increases potential. However, for monovalent anions (z= -1), such as nitrate, this is a negative relationship where increasing concentration decreases potential.

Figure 5.1 b) shows printed working and reference electrodes on the same substrate. The WE is inkjet printed gold and the RE is screen printed Ag/AgCl. Membranes are drop-casted on top of the active areas.

The sensors in this work were developed to operate in a field, as shown in Figure 5.2. The vision of this project is to disperse nitrate and moisture sensors throughout a field which can then wirelessly communicate with readers attached to the irrigation system in a field. Since this irrigation system moves over the entirety of the field, each sensor in the field can eventually communicate. The sensors for this project would be designed to degrade after the crop is harvested, meaning they would not need to be recollected.

The sensor node to be dispersed is shown in Figure 5.3. Here, one of two sensors is chosen for each node: either nitrate or moisture. This sensor is mounted on a stake with an antenna

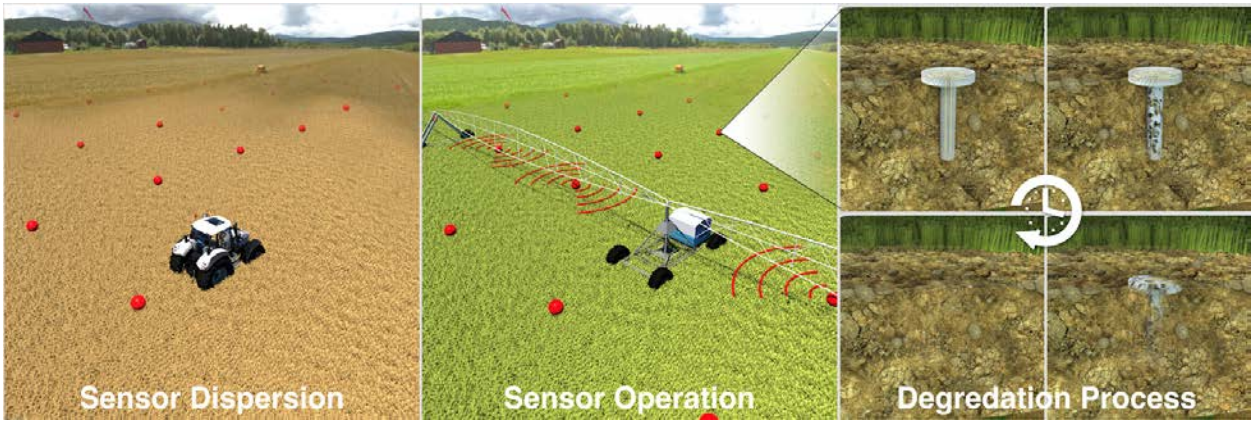

Figure 5.2: A schematic indicating the final goals of the Precision Agriculture using Networks of Degradable Analytical Sensors project. Sensors are dispersed throughout a field, where they can communicate wirelessly with readers mounted on a center-pivot irrigation arm. After the crop cycle, the sensor will degrade.

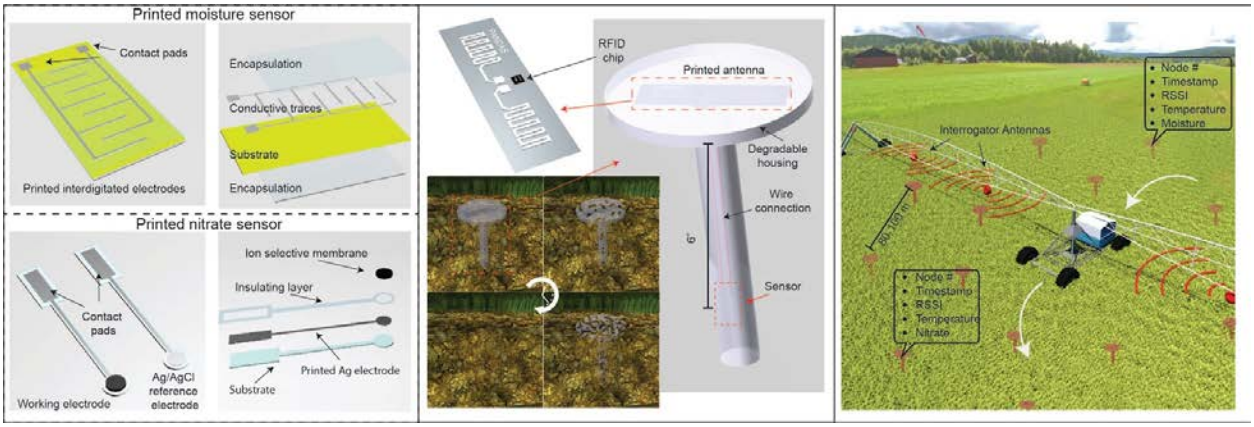

Figure 5.3: Schematic of the sensor node to be used in the Precision Agriculture using Networks of Degradable Analytical Sensors project. The node includes either a nitrate sensor or moisture sensor mounted on a stake with a chip and antenna which are used for wireless communication.

attached to a chip, which is used for wireless communication. The stake is designed so that the sensors will be positioned at about 6 inches below the soil surface.

The first step in achieving this vision, and focus of the work in this chapter, is on the development of the sensor itself. This work focuses on the nitrate sensor and ensuring meaningful measurements can be made in the presence of soil and fertilizer chemicals.

Electrode Printing

Gold electrodes were printed using Harima Nanopaste(Au) NPG-J gold ink in a Dimatix inkjet printer at ambient conditions. Dimatix inkjet printers employ a piezo inkjet cartridge. When a waveform is applied, ink droplets are deposited on the substrate below. The desired pattern was generated in CAD software and converted to a format compatible with Dimatix software for waveform application. Printed gold electrodes were sintered at 250 °C for 50 minutes. Ag/AgCl was screen printed using Engineered Materials Systems, Inc. CI-4001 ink. During screen printing, a silkscreen with a predetermined pattern is flooded with ink. The ink then is pressed through the screen onto a substrate below. Printed Ag/AgCl electrodes were then baked at 120 °C in a vacuum oven for 2 hours. Electrodes were printed on PQA2 PEN 25 μm thick. Printed electrodes were encapsulated using laser-cut Teflon tape. Printed electrodes had circular active areas of 3 mm diameter, resulting in an active area of 0.07068 cm^2.

5.3 Printed Working Electrode Development

Methods

Working electrodes were made by mixing Nitrate Ionophore VI 5.2 wt%, dibutyl phthalate 47.1 wt%, tetaroctylammonium chloride 0.6 wt%, and PVC 47.1 wt%. A total of 0.2 g of this mixture was dissolved in 1.3 mL of THF. The resulting solution was drop-casted on the printed working electrode sensor surface as 6 μL total in 3 separate 2 μL increments. The resulting working electrode was allowed to dry in a fume hood for 15 minutes.

For sensitivity measurements, $NaNO_3$ was dissolved in deionized water, then diluted to various concentrations. Commercial Ag/AgCl reference electrodes were obtained from Millipore Sigma (Z113107). A Keithley 2400 Series SourceMeter was used to measure potentials.

Results

Printed working electrodes were characterized with a commercially available Ag/AgCl reference electrode. Figure 5.4 a) indicates the performance of a nitrate sensor over time in decreasing concentrations of nitrate. This was chosen to indicate that the sensors have a fast reaction in both increasing and decreasing concentrations. Sensors showed no hysteresis, as denoted in Figure5.5. The range measured for the sensor in Figure5.4 a) is 0.05 mM nitrate to 20 mM nitrate, which corresponds to 3.2 to 1240 ppm. This range is more than sufficient to sense the amounts of nitrate-based nitrogen fertilizer in soil. In the Western United States, 40 ppm nitrate is considered barely excessive and most fertilizer recommendations are for applying 30 ppm[128].

Finally, the sensitivity graphs of 6 sensors are overlaid in Figure 5.4 b), showing close agreement from batch-to-batch. These sensors were measured in differing concentrations and ranges and overlaid on the same graph showing that despite changing experimental

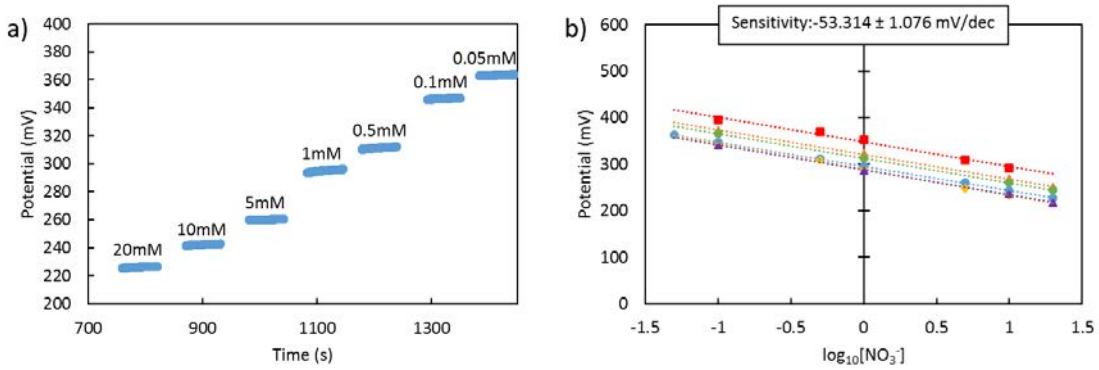

Figure 5.4: a) Potential over time of a printed nitrate sensor WE in changing concentrations of nitrate. WE is measured vs. a commercial Ag/AgCl RE. b) Sensitivity plot of 6 sensors overlaid, showing good repeatability and near-Nernstian response, even though some sensors were measured using differing concentrations or a subset of the range of concentrations.

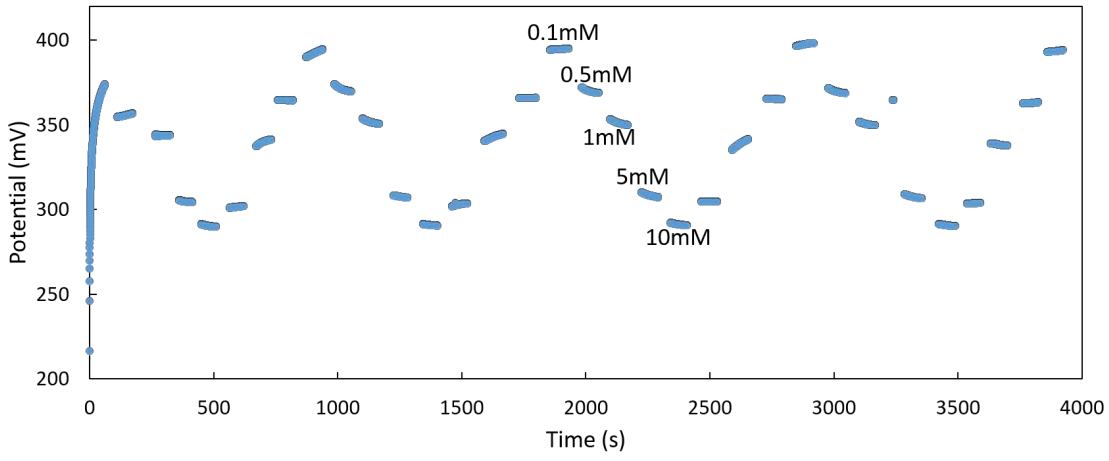

Figure 5.5: Graph of a single sensor, measuring potential over time in cycled increasing and decreasing concentrations of nitrate, showing no hysteresis.

conditions, sensors show good repeatability. These sensors have a near-Nernstian response of -53.3 mV/decade ± 1.1 mV/decade. For WE development and optimization purposes, printed WEs were measured against a commercial Ag/AgCl RE. Concurrently, printed REs which maintained consistent potential in changing nitrate environments were also developed.

5.4 Printed Reference Electrode Development

Methods

The printed Ag/AgCl reference electrodes with no membrane were used as-is after printing and encapsulating, hereafter referred to as the pristine Ag/AgCl reference electrodes.

The reference electrodes with membranes employed a CNT transducer between the Ag/AgCl electrode and the membrane. This transducer was composed of 0.01 g of CNT and 0.05 g of F127 dissolved in 10 mL of THF, which were sonified for 1 hour in an ice bath using a Branson Digital Sonifier probe. The resulting mixture was deposited on the printed reference electrode surface as 4 μL total in 2 separate 2 μL increments.

The reference electrode employing the PVB and NaCl membrane was made by dissolving 1.58 g of PVB and 1.00 g of NaCl in 20 mL of methanol. This mixture was sonified for 30 minutes in an ice bath. The resulting mixture was deposited on top of the CNT transducer as 6 μ total in 3 separate 2 μL increments.

The reference electrode employing the PVB, NaCl and $NaNO_3$ membrane was made by dissolving 1.58 g of PVB, 1.00 g of NaCl, and 1.00 g of $NaNO_3$ in 20 mL of methanol. This mixture was sonified for 30 minutes in an ice bath. The resulting mixture was deposited on top of the CNT transducer as 6 μ total in 3 separate 2 μL increments.

For sensitivity measurements, $NaNO_3$ was dissolved in deionized water, then diluted to various concentrations.

Results

While a printed nitrate WE was being developed, the printed RE was also optimized. This was done using a similar method as Zamarayeva, et al[141], where the printed RE was measured vs. a commercial Ag/AgCl RE to determine its response to changes in the ion of interest. The purpose of the RE is to maintain a constant potential in varying ionic environments. The magnitude of the potential of the RE matters less than the change in potential it exhibits in changing ion concentrations. If the RE is designed to maintain a constant potential in varying ionic environments, it is not ideal for it to exhibit large changes in potential when the ion of interest changes.

It has been shown that inclusion of the ion of interest in the membrane of a reference electrode reduces its sensitivity to that ion[20, 141]. Here, we aimed to confirm that point by optimizing the formulation of the RE. Pristine printed Ag/AgCl electrodes shown in Figure 5.6 a) were compared with printed Ag/AgCl electrodes with varying membrane combinations.

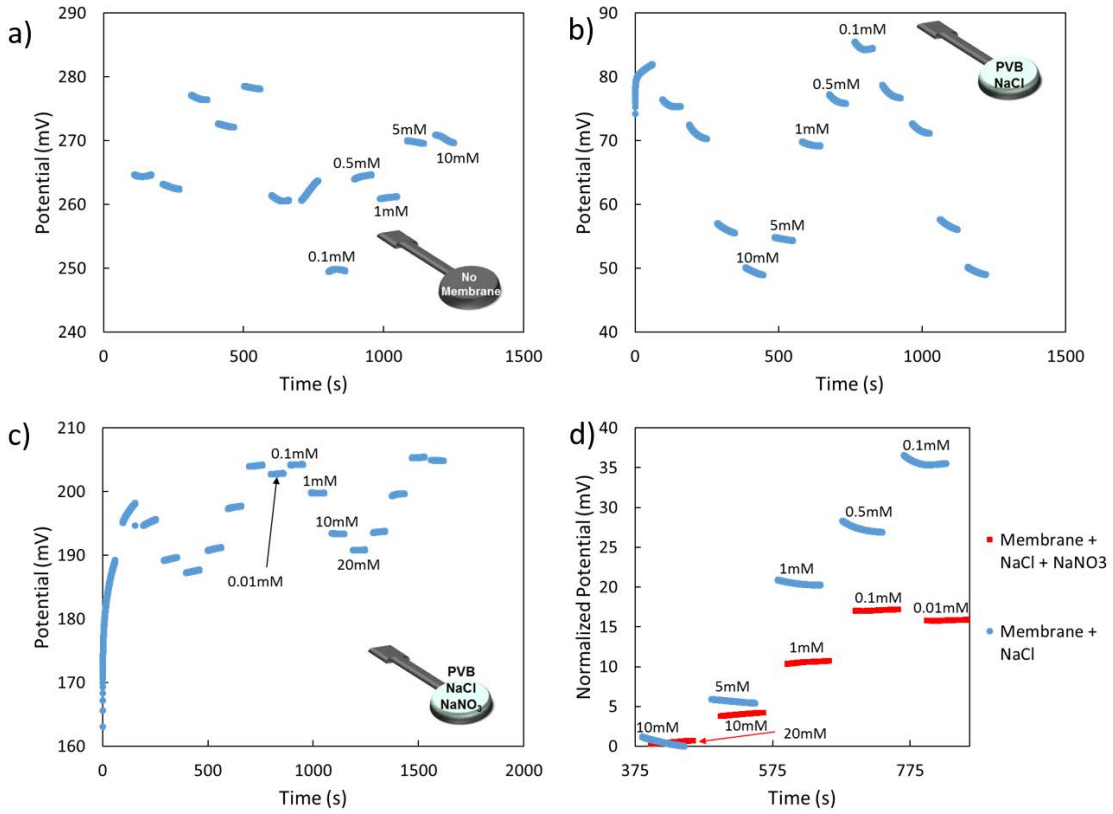

Figure 5.6: a) Potential over time in changing concentrations of nitrate of a printed Ag/AgCl electrode with no added membrane, measured vs. a commercial Ag/AgCl RE. b) Potential over time in changing concentrations of nitrate of a printed Ag/AgCl electrode with PVB membrane with NaCl added, measured vs. a commercial Ag/AgCl RE. c) Potential over time of a printed Ag/AgCl electrode with PVB membrane with NaCl and $NaNO_3$ added, measured vs. a commercial Ag/AgCl RE. d) Sections from b) and c) overlaid on a normalized potential plot over time to show the difference in potential change for changing concentrations of nitrate.

First, in Figure 5.6 b), the formulation demonstrated by Zamarayeva, et al[141] to work in chloride-rich environments was tested. This involved mixing NaCl with PVB to form a membrane. Second, in Figure 5.6 c), a new formulation was tested which involved mixing both NaCl and $NaNO_3$ with PVB to form a membrane.

Figure 5.6 d) shows normalized potentials from the RE with PVB and NaCl overlaid with the normalized potentials from the RE with PVB, NaCl, and $NaNO_3$. Normalized potentials were determined by subtracting the minimum absolute potential from all of the potentials of the RE. This allows for a direct comparison of the changes in potential for

each RE formulation, regardless of its absolute magnitude of potential. As shown in the vertical scales of Figures 5.6 a), b), and c), each electrode formulation results in a different magnitude potential, though each y-axis displays a 50 mV range at the relevant magnitude to better display the changes in potential for each electrode in a comparable manner.

For this WE, the formulation with a PVB, NaCl, and $NaNO_3$ membrane is ideal over the pristine Ag/AgCl and the RE with a PVB and NaCl membrane. The potential for the RE with a PVB, NaCl, and $NaNO_3$ membrane changes less than 20 mV over more than 4 orders of magnitude of changing nitrate concentration, while the RE with a PVB and NaCl membrane exhibits more than 35 mV difference over just 3 orders of magnitude of changing nitrate concentration. The pristine printed Ag/AgCl RE shows a difference of just over 20 mV for a 3 order of magnitude change in nitrate concentration. Of these three options, the RE with a PVB, NaCl, and $NaNO_3$ membrane changes the least even though the range of concentrations covered is higher, demonstrating that it is the most stable reference electrode of the three formulations we explored. Such a result is consistent with Cattrall's predictions[20].

While printed WEs were not measured with the printed REs for this particular work, the expected performance would be close to that achieved in Figure 5.4 d), with near-Nernstian behavior, possibly modified by approximately 5 mV/decade based on the potential changes of the RE. Testing each electrode separately was deemed sufficient since the focus of this study was to determine whether simple potentiometric nitrate sensors may be useful in soil. Future studies may choose to focus on the practical aspects of putting full sensors together and measuring directly in soil.

5.5 Definitive Screening of Sensor Selectivity

Methods

For cation selectivity analysis, 3 solutions were made: (1) 1 mM KNO_3 in deionized water, (2) 1 mM $NaNO_3$ in deionized water, and (3) 1 mM $NaNO_3$ with 1 mM NaCl in deionized water. Each solution contained the same amount of NO_3^- ion, though solution (1) contained 1 mM K^+, solution (2) contained 1 mM Na^+, and solution (3) contained 2 mM Na^+ and 1 mM Cl^- in addition to nitrate ion. A sensor was measured alternately in each of these solutions 11 times each to obtain 11 different sensor potentials for each solution.

Solutions for screening experiments were made as specified in Figure 5.8 a) and Figure 5.9 a) by dissolving solutes in deionized water. Experiment matrix generation and data analysis were performed using the design of experiments platform of the statistical software JMP 14 (SAS, Cary, USA).

For selectivity screening experiment 1, $NaNO_3$ was used as the source of NO_3^-, commercially available water-soluble Monopotassium Phosphate Fertilizer 0-52-34 from Greenway Biotech, Inc. containing P_2O_5 and K_2O was used as the source of P_2O_5, the same water-soluble fertilizer augmented with KCl was used as the source of K^+, $MgCl_2$ was used as the

source of Mg^{2+}, and Na_2SO_4 was used as the source of SO_4^{2-}. A single solution was made for each run outlined in Table 5.1 and is detailed in Figure 5.8 a), including concentration of each chemical for each run. Thus, 17 solutions were made for this experiment. The sensor potential was measured against a commercial Ag/AgCl RE in each solution to obtain the results in Figure 5.8 b) and Table 5.3.

For selectivity screening experiment 2, $NaNO_3$ was used as the source of NO_3^-, NaCl was used as the source of Cl^-, commercially available water-soluble Monopotassium Phosphate Fertilizer 0-52-34 from Greenway Biotech, Inc. containing P_2O_5 and K_2O was used as the source of P_2O_5, $NaNO_2$ was used as the source of NO_2^-, and Na_2SO_4 was used as the source of SO_4^{2-}. A single solution was made for each run outlined in Figure 5.9 a). The sensor potential was measured in each solution to obtain the results in Figure 5.9 b) and Table 5.6.

Results

A potentiometric chemical sensor should change potential only in the presence of the analyte of interest. To test selectivity of the printed nitrate sensor, WEs were measured against a commercial Ag/AgCl RE in solutions of potentially interfering ions common to soils.

An initial experiment tested sodium and potassium cations for interference with the nitrate sensor, since these ions are most prevalent in agricultural fertilizers. The box plots in Figure 5.7 show the distributions of measured potential of a single sensor in three salt solutions, with 11 observations per group. The box plot on the left in Figure 5.7 shows measurements taken in 1 mM KNO_3, the middle shows measurements taken in 1 mM $NaNO_3$, and the right shows measurements taken in 1 mM $NaNO_3$ with 1 mM NaCl. For this experiment, 1 mM was chosen because it lies in the middle of the known measurement range of the sensor and is near the upper limit of what is found in soil[128]. The comparative similarity between the three plots suggests that the nitrate sensor is insensitive to both the cation associated with the NO_3^- ion and a changing cation concentration, as well as chloride. Even though drift in sensor potential over time tended to increase the range of measurements, none of the ions in this experiment were shown to affect the nitrate sensor.

Screening experiments are an economical way to identify important factors in a system when a large number of potential variables may affect the response. The Definitive Screening Design is a three level experiment that can identify active factors using a number of runs that is at minimum one more than twice the number of factors for an even number of factors and three more than twice the number of factors for an odd number of factors [64]. This is far fewer runs than a full factorial experiment testing every possible combination of factor levels. We demonstrate the use of this design for selectivity testing of the printed WE against several ions common to soils. Table 5.1 shows the design structure of the experiment. Here, we use 5 factors (or chemicals). We add 4 extra runs to increase the power of the experiment, resulting in 17 runs.

The levels used in the first experiment are detailed in Table 5.2, and graphical results are presented in Figure 5.8. The upper limits (+1 value) represent a maximum of what is

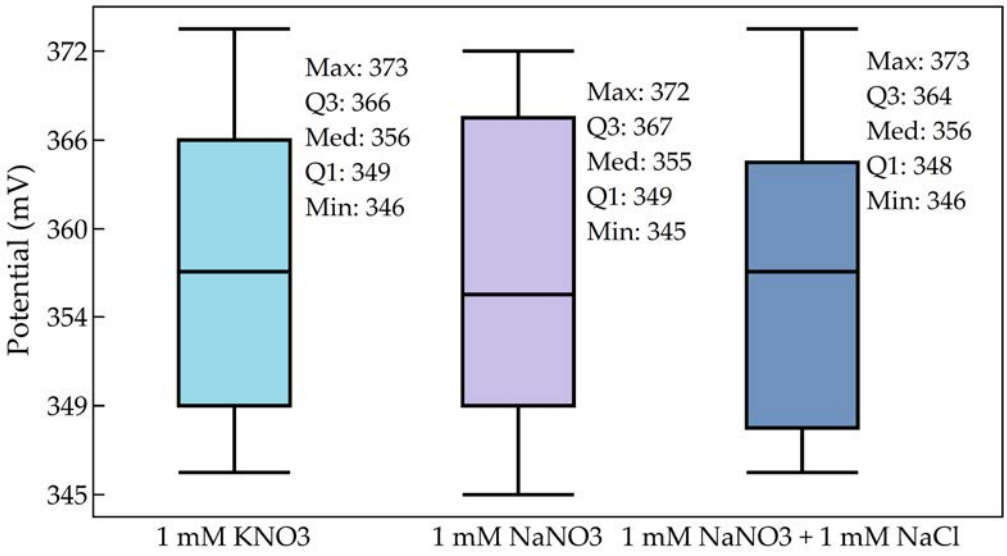

Figure 5.7: Distributions of nitrate sensor potential in three different salt solutions of 1 mM NO_3^- measured against a commercial RE. Sample means (left to right): 357.4 mV, 357.6 mV, 357.3 mV; 11 observations per group. Since the means and ranges for each solution are so similar, none of the ions show effects on the nitrate sensor.

considered barely excessive in soil in the western United States[128]. The details for the source of each chemical in this experiment can be found in the Methods section.

In Figure 5.8 a), the coded values in the design structure of Table 5.1 are substituted for their factor levels from Table 5.2, and then the rows are randomized giving the chemical amounts in each run. In Figure 5.8 b), the experimental data is ordered by factor, and the slope of each line indicates the sensitivity of the nitrate sensor to the respective ion. Thus, a horizontal line suggests little interference. Statistical analysis showed only nitrate to have a significant effect on the nitrate sensor, which is visible in the nitrate graphs as a steeper best-fit line compared to those of the other ions. The raw data graphed in Figure 5.8 b) is shown in Table 5.3 and the model developed by JMP 14 is outlined in Table 5.4.

A second definitive screening experiment was executed with the lower limits of each potential interfering ion set to 0 and upper limits set to twice what is considered excessive in soil in the western United States[97, 128]. The chemicals tested here are not expected to be present in soil at their upper factor limits. The factor list has changed to eliminate codependence between factors, since the range of chemical concentrations was more than doubled. The units for nitrate in this experiment have also changed to reflect what should give a linear response. This treatment of nitrate units is what should be used in any future experiments which aim to create a model for nitrate sensor behavior from definitive screening experiments, since the result will be linear behavior. The details for the source of each

Entry	X1	X2	X3	X4	X5
1	0	+1	+1	+1	+1
2	0	-1	-1	-1	-1
3	+1	0	+1	+1	-1
4	-1	0	-1	-1	+1
5	+1	-1	0	+1	+1
6	-1	+1	0	-1	-1
7	+1	-1	-1	0	+1
8	-1	+1	+1	0	-1
9	+1	+1	-1	-1	0
10	-1	-1	+1	+1	0
11	+1	-1	+1	-1	-1
12	-1	+1	-1	+1	+1
13	+1	+1	-1	+1	-1
14	-1	-1	+1	-1	+1
15	+1	+1	+1	-1	+1
16	-1	-1	-1	+1	-1
17	0	0	0	0	0

Table 5.1: Five factor Definitive Screening Design with four extra runs, generated with JMP 14. Factor levels are given as their coded values. Run order was randomized for the experiments.

Factor with Levels	-1	0	+1	Units
NO_3^-	10	25	40	ppm
P_2O_5	20	60	100	ppm
K^+	150	475	800	ppm
Mg^{2+}	60	180	300	ppm
SO_4^{2-}	2	11	20	ppm

Table 5.2: Factor table for first definitive screening of potential interfering species for nitrate sensors.

a)

Run	NO_3^- (ppm)	P_2O_5 (ppm)	K^+ (ppm)	Mg^{2+} (ppm)	SO_4^{2-} (ppm)
1	25	60	475	180	11
2	10	60	150	60	20
3	10	20	800	300	11
4	25	100	800	300	20
5	10	20	150	300	2
6	10	100	150	300	20
7	10	100	475	60	2
8	40	20	800	60	2
9	40	100	150	60	11
10	25	20	150	60	2
11	10	100	800	180	2
12	40	20	150	180	20
13	40	20	475	300	20
14	40	60	800	300	2
15	10	20	800	60	20
16	40	100	150	300	2
17	40	100	800	60	20

b)

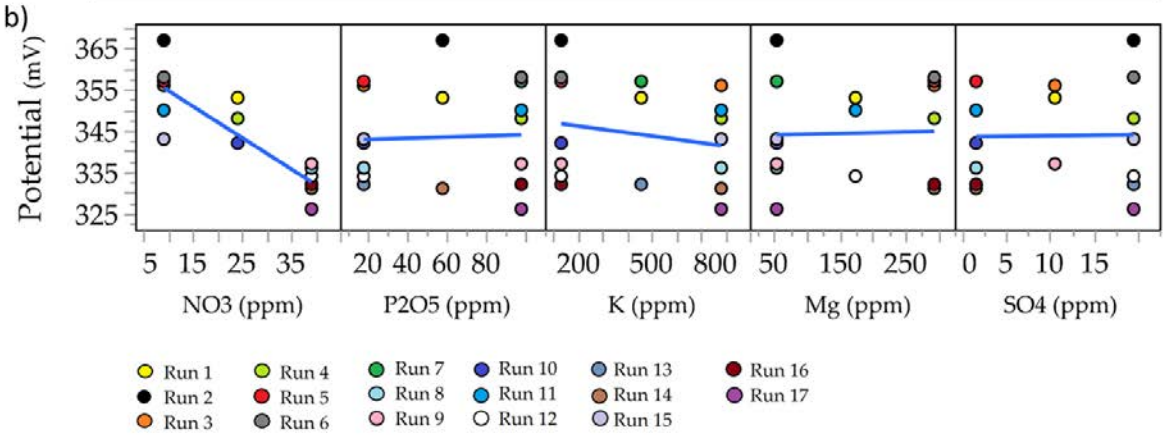

Figure 5.8: a) Table of runs for first definitive screening experiment with assigned values for each factor for each run, with b) effects plots from definitive screening experiment using upper limits of what is considered barely excessive in soil. Each data point on each graph in b) corresponds to the results from a single run which is a row in a).

Run	Average Potential, Trial 1 (V)	Average Potential, Trial 2 (V)
1	0.298	0.353
2	0.299	0.367
3	0.291	0.356
4	0.284	0.348
5	0.297	0.357
6	0.300	0.358
7	0.304	0.357
8	0.283	0.336
9	0.290	0.337
10	0.293	0.342
11	0.299	0.350
12	0.284	0.334
13	0.282	0.332
14	0.282	0.331
15	0.302	0.343
16	0.284	0.332
17	0.285	0.326

Table 5.3: Table of data acquired from the first definitive screening test. These are the voltage values used in the plots in Figure 5.8

Term	Estimate	Standard Error	t-Value	p-Value
Intercept	344.65	1.4049	245.32	¡0.0001
NO_3 (ppm)	-11.43	1.5481	-7.382	¡0.0001

Table 5.4: Model coefficients, standard errors, t-values, and p-values. P-values ¡ 0.05 indicate a significant sensitivity to the ion or compound. Root-mean-square error (RMSE) = 5.793; Correlation coefficient (R^2) = 0.78.

Factor with Levels	-1	0	1	Units
$\log_{10}([NO_3^-])$	-0.7924	-0.4914	-0.1903	$\log_{10}$(mM)
Cl^-	0	50	100	ppm
P_2O_5	0	100	200	ppm
NO_2^-	0	50	100	ppm
SO_4^{2-}	0	20	40	ppm

Table 5.5: Factor table for second definitive screening test of potential interfering species for nitrate sensors.

Run	Average Potential, Trial 1 (V)	Average Potential, Trial 2 (V)
1	0.371	0.318
2	0.360	0.308
3	0.362	0.313
4	0.368	0.319
5	0.362	0.318
6	0.354	0.310
7	0.370	0.324
8	0.387	0.338
9	0.348	0.309
10	0.372	0.330
11	0.375	0.337
12	0.359	0.322
13	0.347	0.313
14	0.348	0.324
15	0.369	0.330
16	0.359	0.325
17	0.357	0.324

Table 5.6: Table of data acquired from the second definitive screening test. These are the voltage values used in the plots in Figure 5.9

chemical in this experiment can be found in the Methods section. The factor table for this experiment is shown in Table 5.5, and graphical results are shown in Figure 5.9, with the data in Table 5.6.

The experimental data showed NO_3^-, P_2O_5, and NO_2^- to significantly affect sensor signal, though nitrate had the greatest effect, as visible in Figure 5.9.

Slight drift in measured potential over time is typically minimized in the nitrate sensor with extended conditioning. We disregard the effects of time-dependent drift for the screening experiments, since the aim of this work is to determine the efficacy of nitrate sensors and

a)

Run	$\log_{10}([NO_3^-])$	Cl^- (ppm)	P_2O_5 (ppm)	NO_2^- (ppm)	SO_4^{2-} (ppm)
1	-0.4914	0	0	0	0
2	-0.1903	50	200	100	0
3	-0.1903	100	200	0	40
4	-0.7924	0	0	100	0
5	-0.1903	0	200	0	0
6	-0.1903	0	100	100	40
7	-0.7924	0	200	100	20
8	-0.7924	0	200	0	40
9	-0.1903	100	0	100	0
10	-0.7924	100	200	50	0
11	-0.7924	100	100	0	0
12	-0.4914	100	200	100	40
13	-0.1903	0	0	50	40
14	-0.1903	100	0	0	20
15	-0.7924	50	0	0	40
16	-0.4914	50	100	50	20
17	-0.7924	100	0	100	40

b)

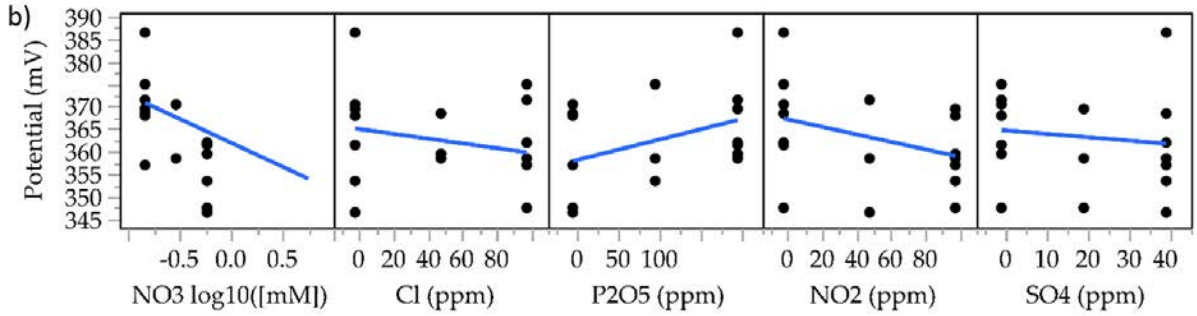

Figure 5.9: a) Table of runs for second definitive screening experiment with assigned values for each factor for each run, with b) effects plots from definitive screening experiment using upper limits of twice what is considered barely excessive in soil. The data points on each graph in b) correspond to the results from a run in a).

Term	Estimate	Standard Error	t-Value	p-Value
Intercept	362.44	1.2202	297.02	¡0.0001
NO_3 log10([mM])	-8.429	1.3446	-6.268	¡0.0001
P_2O_5 (ppm)	4.5357	1.3446	3.3732	0.005
$NaNO_2$ (ppm)	-4.143	1.3446	-3.081	0.0088

Table 5.7: Model coefficients, standard errors, t-values, and p-values. RMSE = 5.031; R^2 = 0.82.

Component	Weight (g)	Weight %
Nitrate Ionophore VI	0.0104	5.2
Dibutyl Phthalate	0.0942	47.1
Tetraoctylammonium Chloride	0.0012	0.6
PVC	0.0942	47.1
Total	0.2	100

Table 5.8: Composition of WE sensing membrane. The 0.2 g of dry components was dissolved in 1.3 mL of THF.

identify potentially interfering ions. An exact model for nitrate sensor behavior may include a term to account for potential drift. Follow-up experimentation is necessary to arrive at an accurate model for the effects of P_2O_5 and $NaNO_2$ at these excessive ranges.

5.6 Investigation of Degradable Polymers in Sensing Membrane

Since the nitrate sensors developed for the purposes of this work are intended for use as degradable soil sensors, this work endeavored to determine if degradable polymers could be used in lieu of PVC in the WE sensing membrane. The WE sensing membrane composition used throughout this chapter is given in Table 5.8. This is the membrane composition which gave the results reported in previous sections of this chapter. In this section, the PVC portion of the composition outlined in Table 5.8 was traded for poly(lactic acid) (PLA) and poly(caprolactone) (PCL) in the same weight percent as PVC, keeping all other components the same.

To ensure the only variable tested was the use of degradable polymers, sensors employing PVC (labeled PVCNitrate) were made and measured the same day as sensors made with PCL (labeled PCLNitrate) and sensors made with PLA (labeled PLANitrate). The results from these sensors are shown in Figure 5.10, which agrees closely with the results of sensors throughout the chapter. Sensors show near-Nernstian response in a wide range of concentrations of nitrate. Two sensors are shown in Figure 5.10, with results from the first shown in Figure 5.10 a) and b) and the results from the second shown in Figure 5.10 c) and d).

From these graphs, we can see that the fabrication procedure followed the day of making these sensors was consistent with that of previously fabricated sensors. The sensitivities of the tested sensors were -53.4 mV/decade and -49.9 mV/decade. These are near-Nernstian. However, it is possible and fully expected that the composition of the membrane using PVC may not be the optimal composition of the membrane using another polymer. This acknowledged, if the polymer is able to properly form a matrix to hold the ionophore, the response should be close to Nernstian.

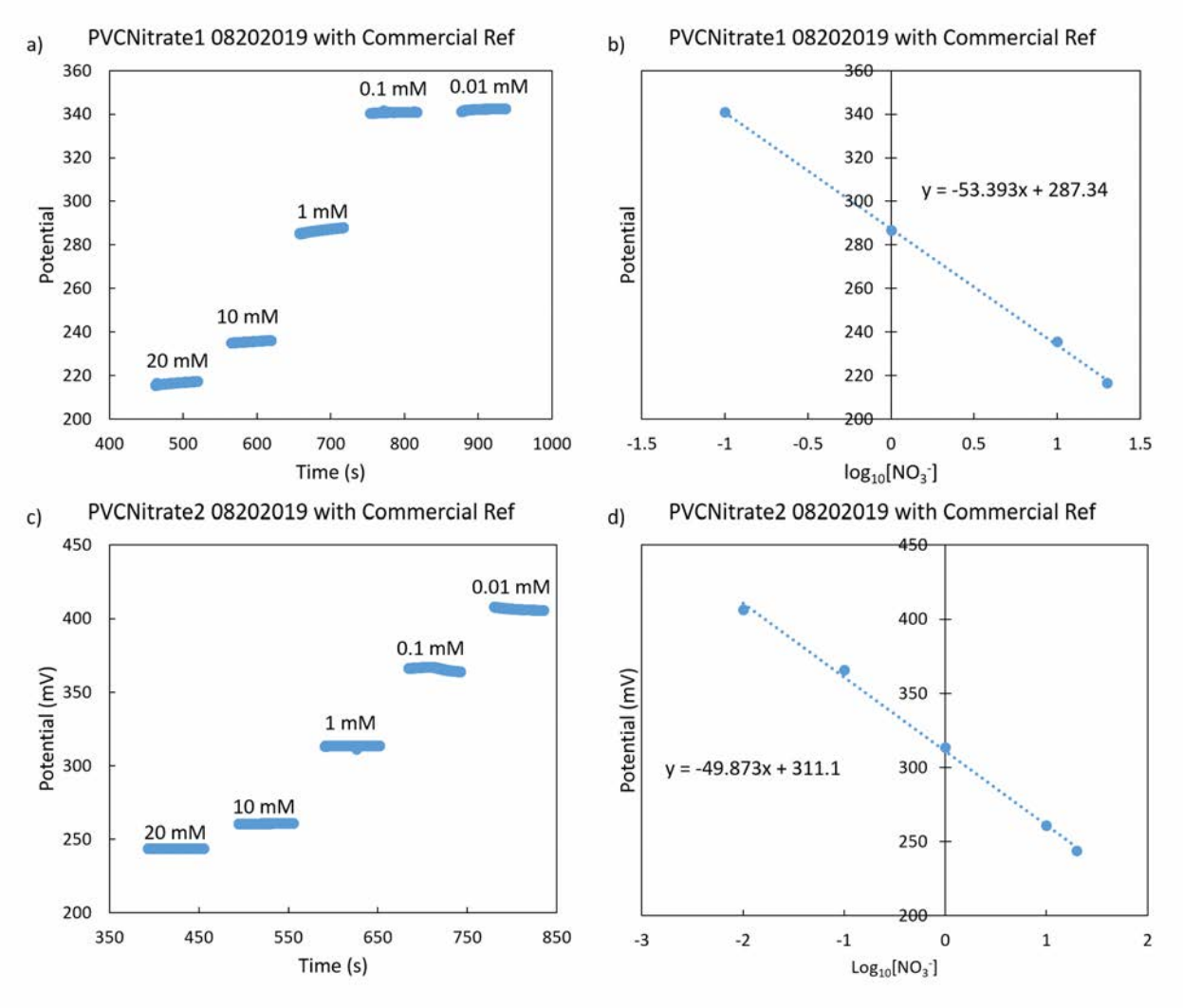

Figure 5.10: Response of two different WEs made with PVC made the same day as electrodes made with degradable polymers for reference. a) The response of PVCNitrate1 in nitrate over time with b) the points plotted for sensitivity. c) The response of PVCNitrate2 in nitrate over time with d) the point plotted for sensitivity. Printed WEs were measured vs. a commercial RE.

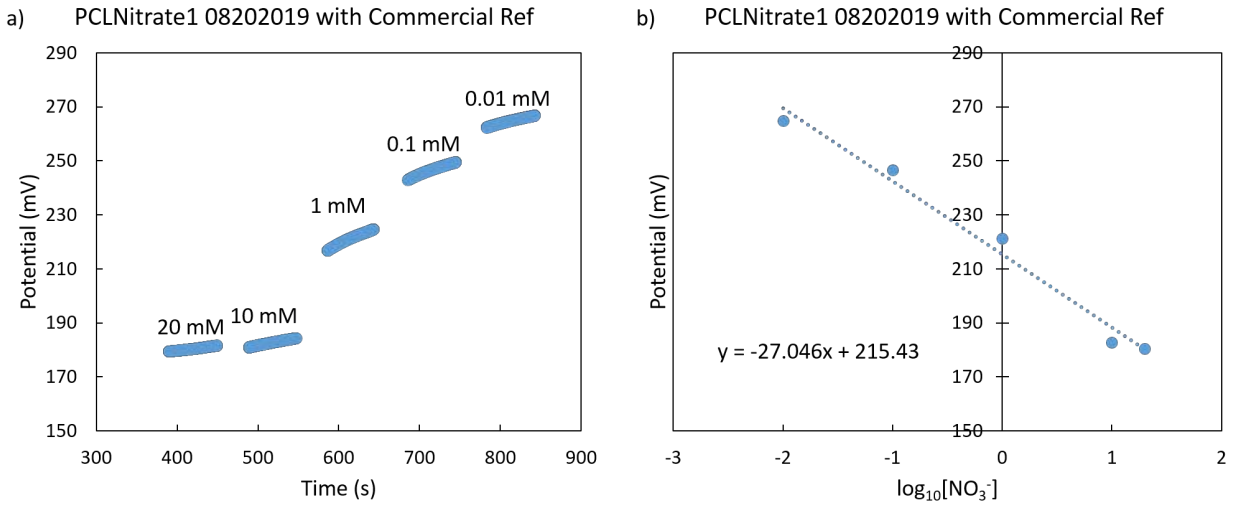

Figure 5.11: a) The response of a working electrode employing PCL instead of PVC in changing concentrations of nitrate over time. b) The potentials plotted to extract sensitivity. Printed WEs were measured vs. a commercial RE.

The results from a sensor using PCL instead of PVC are shown in Figure 5.11, where the response of the sensor in changing concentrations of nitrate over time is shown in Figure 5.11 a) and the sensitivity is shown in Figure 5.11 b). The sensitivity of this sensor is -27.0 mV/decade. This is nearly half the expected Nernstian response, indicating that PCL is not properly forming a matrix to hold the ionophore in place.

The results from a sensor using PLA instead of PVC are shown in Figure 5.12, where the response of the sensor in changing concentrations of nitrate over time is shown in Figure 5.12 a) and the sensitivity is shown in Figure 5.12 b). The sensitivity of this sensor is -27.7 mV/decade. This is also nearly half the expected Nernstian response, indicating the PLA is also not properly forming a matrix to hold the ionophore in place.

Both PCL and PLA showed nearly half the expected Nernstian sensitivity, indicating they may both have something in common, whether in structure or other properties, which prevent both from performing as a proper ionophore matrix. Since both polymers showed similar response, the properties of PVC, PCL and PLA were all investigated in further depth. The purpose of this was to attempt to understand why PVC is used with such prevalence in potentiometric sensors[9, 21, 24, 51, 93, 98, 117, 124, 136].

First, glass transition temperature and crystalline nature were investigated to see if the behavior of PCL and PLA were simple to explain using basic polymer characteristics. The glass transition temperatures and crystallinity of PVC, PCL, and PLA are listed in Table 5.9. Here, it is clear that if glass transition temperature alone were the factor that dictated polymer behavior in potentiometric sensors, PLA would perform much closer to PVC. This

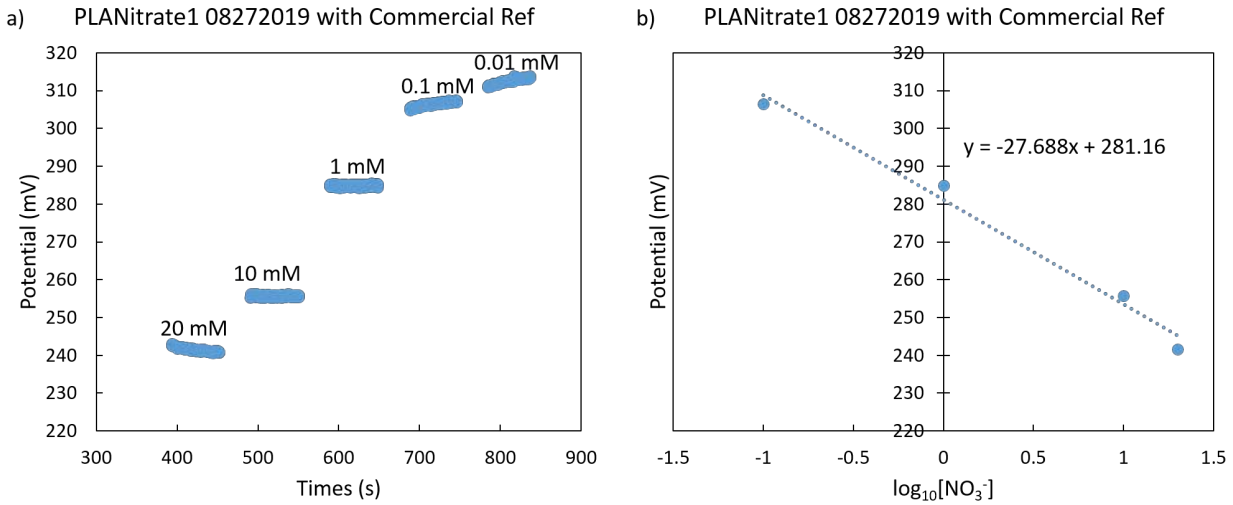

Figure 5.12: a) The response of a working electrode employing PLA instead of PVC in changing concentrations of nitrate over time. b) The potentials plotted to extract sensitivity. Printed WEs were measured vs. a commercial RE.

Polymer	Glass Transition (°C)	Crystallinity
PVC	82	Amorphous
PCL	-60	Semi-crystalline
PLA	60-65	Can be Amorphous or Semi-crystalline

Table 5.9: Enzyme activity for varying concentrations of $MgCl_2$ incubated with the enzyme. Standard deviation is calculated using at least 3 samples.

table also makes it clear why plasticizers such as dibutyl phthalate are incorporated in PVC membranes. The plasticizer functions to lower the glass transition temperature of PVC, producing flexible polymer films which are soft and mechanically stable. In fact, PCL with its -60 °C glass transition temperature could be used as a plasticizer itself. In fact, it has been shown that using a polymeric plasticizer can extend the lifetime of a PVC membrane in comparison to those employing a non-polymeric plasticizer[140].

Further, if crystallinity alone dictated a polymer's performance when used in a potentiometric sensing membrane, PLA would show performance somewhere between PVC and PCL. It is clear that glass transition temperature and crystallinity alone cannot dictate how well a polymer performs in a potentiometric sensing membrane.

Instead, we turn to the polymer chemical structures to illuminate why PCL and PLA show similar performances. The chemical structures of each polymer are shown in Figure 5.13, with PVC shown on the left, PCL in the middle, and PLA on the right. Here, the

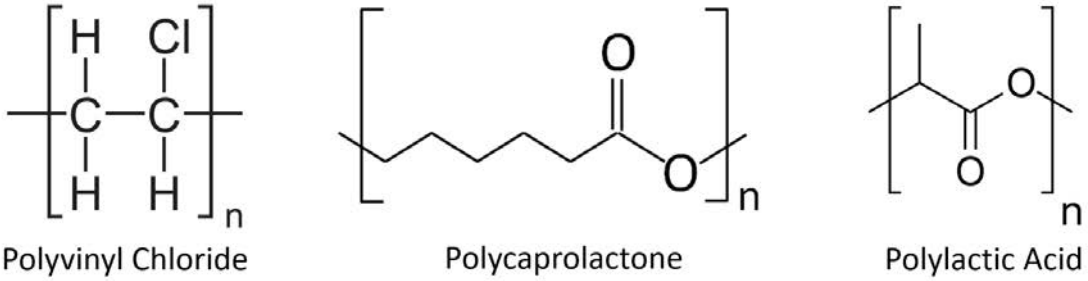

Figure 5.13: The chemical structures for PVC (left), PCL (center) and PLA (right).

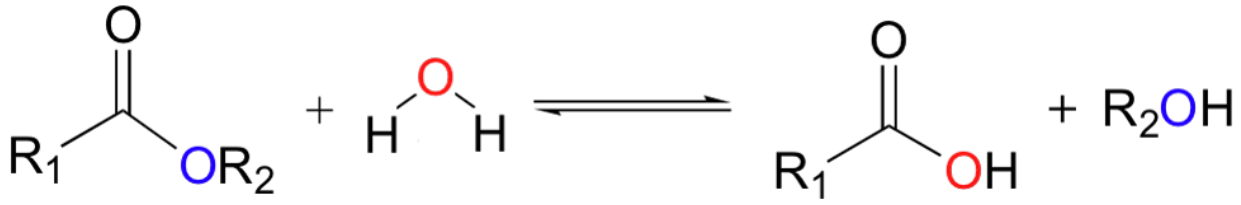

Figure 5.14: A schematic of the process of hydrolysis, where the ester group of a polymer reacts with water to break off a side chain leaving a carboxylic acid group instead.

difference becomes glaringly obvious. PCL and PLA both have an ester group where PVC has none. Further investigation into the degradation mechanisms of these polymers shows that they both degrade by the same mechanism: hydrolysis. This means that in the presence of water, the ester group between monomers will break down into a carboxylic acid group, separating monomers, as shown in Figure 5.14.

This breakdown mechanism is particularly sinister when combined with sensors which are characterized in solutions of nitrate dissolved in deionized water and are destined for use in fields of moist soil to be in the presence of water for its foreseeable lifetime. This unique structure incorporating an ester group, combined with the breakdown mechanism of hydrolysis, ensures that these sensors are doomed for failure. This explains why both PCL and PLA had similar, non-Nernstian performance when integrated into potentiometric sensing membranes.

From this study, it was determined that while a fully degradable sensor may be ideal, the poor sensor performance determined that degradable polymers were not worth using to replace PVC. The working electrode membrane is approximately 0.5 mg, where the conductor, substrate, and insulator are larger by approximately an order of magnitude, and the total sensing node is larger by up to 5 orders of magnitude. Thus, for the purposes of this work,

a PVC-based sensing membrane was deemed acceptable for use.

5.7 Conclusion

Printed potentiometric nitrate sensors with near-Nernstian sensitivity of -53.3 mV/dec ± 1.1 mV/dec were demonstrated. These sensors were shown to be insensitive to common chemicals found in soil at average soil levels. However, these sensors experience interference at highly excessive concentrations of P_2O_5 and NO_2^-, which should be considered when applying these sensors in a region with high levels of specific chemicals. It is possible that at low concentration ranges, the effect on the sensor was too small to be identified, resulting in a false negative. However, in this case the effect on the sensor due to these normal chemical concentration ranges would likely also be too small to cause interference in the field. A printed reference with relatively low sensitivity to nitrate was developed using a membrane composed of PVB with NaCl and $NaNO_3$. Since these sensors are printed, the materials employed in this study can be substituted for degradable materials to realize a naturally degradable sensor.

It should be noted that the PVC in the working electrode sensing membrane cannot be substituted for a degradable polymer if the degradable polymer breaks down by hydrolysis. When choosing degradable material replacements, the effects on sensor performance should be weighed carefully, noting both the relative weight of the portion of the sensor in question and the degradation in sensor performance it may produce. The conductor, for instance, makes up a large portion of the sensor. Theoretically, if the conductor is conductive enough, changing the conductor will not affect the sensor's sensitivity. Thus, replacing the conductor with a degradable material is high priority when transitioning to degradable sensors. The sensing membrane, on the other hand, makes up a small portion of the sensor and is vital to maintaining the sensor's sensitivity. Thus, the sensing membrane must be handled with care, and the use of non-degradable materials is most appropriate here.

Chapter 6

Conclusions and Future Work

6.1 Conclusions

The work in this thesis represents significant progress toward sensors for many applications. The use of printing facilitates customization and is ideal for the applications presented in this work. Two types of electrochemical sensors are investigated: amperometric and potentiometric. Two applications are also invested: sweat sensing and soil sensing. Print-based fabrication techniques are ideal for sweat sensing because they enable the use of substrates with flexible form factors, which match those of skin much more closely than devices fabricated using lithographic processes can. Conformation with skin is important in continuous sweat monitoring to ensure that sweat is measured as it is produced. Print-based fabrication techniques are ideal for soil sensing because solution processing allows for fabrication using innovative materials such as naturally degradable materials, thus enabling the development of what can in future become a fully printed, fully degradable sensing node.

Chapter 1 served as an assessment of literature to date on printed electrochemical sensors. Most printed amperometric sensors have been developed for sweat sensing purposes, though some have been shown useful for food, blood, saliva, and milk sensing. Most printed potentiometric sensors have also been developed for sweat sensing purposes, though some have been shown useful for water testing, soil monitoring, and corrosion monitoring.

The development of lactate sensors in Chapter 2 was also done with the intention of sweat monitoring. The lactate sensors combined inkjet printed gold working and counter electrodes with screen printed Ag/AgCl reference electrodes on 25 μm thin PEN to allow for highly conformal sensors. The printed sensors were optimized for maximum linear range and sensitivity, resulting in sensors which had the best performance yet reported in literature. These sensors had sensitivity of 4.8 μA/mM and a linear range up to 24 mM lactate, which made them useful for detection of lactate in sweat during workouts, when an increase in lactate indicates the transition from aerobic metabolism to anaerobic metabolism. Sensors were able to be operated continuously for more than an hour with 97% current retention.

The sensors resulting from Chapter 2 were rigorously tested for selectivity in Chapter 3.

One of the most desirable qualities of a sensor is that it sense only what it is designed to sense. This is not the case for enzymatic sweat sensors. Even though the chemical reaction between an enzyme and its substrate is highly selective, the activity of the enzyme, or how well it reacts with its environment, is highly affected by the presence of salt. This is not ideal for a sensor designed to be used in sweat, which is inarguably salty. The presence of these salts renders the calibration curves obtained in pH buffered, non-salty environments completely inaccurate. Until the components of sweat can be fully characterized for their effect on enzymatic sensor performance and accounted for in a multi-sensor patch, enzymatic sensors cannot be used in sweat.

Chapter 4 endeavored to show that sweat sensing could still be done using potentiometric sensors, which rely on ionophores as the sensing method instead of enzymes. It has been shown that this type of sensor is insensitive to the salts present in sweat[141], which is a marked improvement upon the enzymatic sweat sensor. Results for ammonium sensors were shown, along with a proposal for a multi-sensor patch incorporating ammonium, sodium, and potassium. The multi-sensor patch would be made using inkjet printed gold working electrodes and a single screen printed Ag/AgCl reference electrode. By including multiple metabolites in one sensing patch, we would be able to gain more information about one person's health. This also serves as a step toward incorporating multiple sweat metabolite sensors to compensate for their effect on enzymatic sensors.

A potentiometric sensor was also utilized in Chapter 5, wherein a nitrate sensor for soil was developed. This nitrate sensor was fabricated using an inkjet printed gold working electrode and a screen printed Ag/AgCl reference electrode. The printed electrodes were developed separately. The working electrode showed near-Nernstian response to nitrate in solution, while the reference electrode showed minimal response to nitrate in solution. Further, the working electrode showed relative insensitivity to chemicals commonly found in soil at normal soil levels, though at excessive levels, P_2O_5 and $NaNO_2$ presented interference with the sensor. Finally, the composition of the working electrode was investigated for the possibility of using a degradable polymer in lieu of the typical PVC. It was determined that the performance of the sensor degraded too much to make integration of a degradable polymer worth the time it would take to optimize. The polymers investigated, PCL and PLA, both degrade through hydrolysis which is not ideal for a sensor which will be in the presence of water for its entire working life. Based on the relative weight of the membrane to that of the entire sensing node, up to 5 orders of magnitude difference, the use of non-degradable PVC in the sensing membrane was deemed acceptable.

6.2 Suggestions for Future Work

Though the work in this dissertation indicates steps toward various commercializable electrochemical sensors, much more must be done before achieving true commercializability. Avenues for further study have been identified throughout this thesis and are summarized here. Here, suggestions for future work are outlined by type of sensor and applications. The

wonder of these sensors is that they are not limited to the applications outlined in this thesis, though. One of the opportunities for future work is adapting enzymatic lactate sensors for use in food sensing. Food also gives off ammonia when it spoils. Both of these specific sensors can be adapted into food sensors. Furthermore, nitrate in soil leaches into groundwater, making that water less safe for human consumption. Nitrate sensors can be used for water sensing as well as soil sensing. The applications mentioned in this thesis are by no means the only applications for sensors, much less the only applications for sensing the specific ions mentioned. The applications in this thesis merely offer a starting point for developing the sensors in question.

Enzymatic Sweat Sensors

The lactate sensors developed in this work were shown to have too much interference from salts to be used as sensors as yet. However, a sweat lactate indicator could still be employed. This indicator would essentially act as a traffic light, indicating whether a person is working out aerobically or anaerobically by just monitoring changes in lactate, without trying to determine the specific amount of lactate present.

If enzymatic sensors were to ever be used as sensors for the specific amount of anything present in sweat, they would first need to be rigorously evaluated for the effect of each constituent in sweat on enzyme activity and sensor performance, as was done in Chapter 3 for NaCl, KCl, NH_4Cl, $MgCl_2$, and $CaCl_2$. This could be prohibitive due to the sheer number of constituents in sweat[56], though over time it may be done. Then, the enzymatic sensor in question, must be incorporated with sensors for each constituent in sweat known to affect enzyme activity and sensor performance. Thus, by measuring the amount of each constituent present and using the current measured from the enzymatic sensor, the amount of substrate may be calculated knowing the effect of each amount of constituent on sensor performance. Alternatively, a membrane may be employed which only allows lactate diffusion to the sensor surface. Such a membrane would need to be extensively studied for its effect on sensor performance and reproducibility.

Potentiometric Sweat Sensors

Potentiometric ammonium sensors were reported in this work, and potentiometric sodium sensors have been previously reported[141]. Potentiometric potassium sensors have been developed in conjunction with this work, and a multi-sensor measurement system has been developed for reading multi-metabolite sensing patches. The final step in this work is to put each of the individual pieces together. First, the three sensors must be fabricated on the same substrate. While this may be difficult, there is precedence showing it can be done[141]. Second, these sensors must be measured using the multi-sensor measurement system *in vitro* to ensure the system and sensors are all working properly together. This measurement can be repeated with a Keithley 2400 Series SourceMeter to ensure accuracy.

There are several steps to *in vivo* measurements. Being able to measure these sensors on the body is important to their function as sweat sensors. Proper encapsulation must be designed for the board used for this multi-sensor patch. Sweat is ubiquitous on the body and is conductive, meaning it has the potential to short pathways on the board which would otherwise not be shorted. This is a very important step in *in vivo* measurements which cannot be ignored. Obtaining IRB approval for *in vivo* measurements is also vital. Finally, these sensors will most likely perform best if integrated with a microfluidic channel designed to flow sweat over then away from the electrode surface as it is produced[96, 124]. A microfluidic channel would benefit the multi-sensor patch greatly.

Ultimately, sweat sensors should be incorporated with a thermistor, to ensure the calibration of the sensors, since temperature is one of the factors which affects sensitivity of potentiometric sensors according to the Nernst equation. Sensors should also be tested for the effects of pH, and a pH sensor should be included if any effects are observed.

Finally, more sensors may be developed for integration with those listed in this thesis. Ionophores have been developed for many ions which can be incorporated with the existing ion sensors. On this point, only the availability of materials is the limit!

Nitrate Soil Sensors

The opportunities for continued work on potentiometric sensors for determination of nitrate in soil are rich with possibilities. First and foremost being the integration of the printed working electrode with the printed reference electrode presented in this work. The combination of printed electrodes is expected to give similar performance to that of the printed working electrode measured with the commercial reference, ± 5 mV/decade. This is the most pressing of the future work.

It will also be important to test the lifetime of the sensors and any potential drift they may have. This will affect their field performance. While the lifetime of a sensor printed with non-degradable materials is expected to be much longer than that of a sensor printed with degradable materials, both lifetimes are valuable information to have.

Testing the sensor physically in soil will also be vital to being able to predict how it performs in a field. To this end, multiple soil types should be gathered - sand, topsoil, and potting soil. Each soil has a unique moisture holding capacity and will have its own challenges for measuring nitrate. In each of these soils, known amounts of nitrate fertilizer may be added and measured in a demonstration of the sensor working in soils.

Finally, as degradable inks are developed, they can be integrated into the fabrication of the sensor. Each degradable material should be incorporated one-by-one and tested to ensure proper functioning of the sensor, and to see if any single factor prevents the sensor from performing similarly to one made with non-degradable materials.

This sensor was developed to be integrated with a full sensing node. The vision for this project, as outlined in Chapter 5,is to develop sensors which can be deployed throughout a field and wirelessly addressed to give real-time information about the state of a field. The final steps of this project are to integrate the sensor with the rest of the sensing node - the

stake, antenna, chip, etc. - and deploy the node(s) in a field with RFID readers attached to the field's center pivot irrigation system. In this way, a wirelessly addressable sensing node may be realized.

Bibliography

[1] A. Abellán-Llobregat et al. "A stretchable and screen-printed electrochemical sensor for glucose determination in human perspiration". In: *Biosensors and Bioelectronics* 91 (May 2017), pp. 885–891. ISSN: 18734235. DOI: 10.1016/j.bios.2017.01.058.

[2] N. Abramova et al. "Application of an ion-selective field effect transistor with a photocured polymer membrane in nephrology for determination of potassium ions in dialysis solutions and in blood plasma". In: *Talanta* (2000). ISSN: 00399140. DOI: 10.1016/S0039-9140(00)00408-2.

[3] M. E.E. Alahi et al. "Practical nitrate sensor based on electrochemical impedance measurement". In: *Conference Record - IEEE Instrumentation and Measurement Technology Conference*. Vol. 2016-July. Institute of Electrical and Electronics Engineers Inc., July 2016. ISBN: 9781467392204. DOI: 10.1109/I2MTC.2016.7520554.

[4] Md Eshrat E. Alahi et al. "A Temperature Compensated Smart Nitrate-Sensor for Agricultural Industry". In: *IEEE Transactions on Industrial Electronics* 64.9 (Sept. 2017), pp. 7333–7341. ISSN: 02780046. DOI: 10.1109/TIE.2017.2696508.

[5] Sagir Alva, Lee Yook Heng, and Musa Ahmad. "Screen-Printed Potassium Ion Sensor Fabricated From Photocurable and Self- Plasticized Acrylic Film". In: *Journal of Physical Therapy Science* 17.2 (2006), pp. 141–150. DOI: 10.1002/anie.200605068.

[6] I. Alvear-Ordenes et al. "Sweat lactate, ammonia, and urea in rugby players". In: *International Journal of Sports Medicine* (2005). ISSN: 01724622. DOI: 10.1055/s-2004-830380.

[7] *Amperometric biosensors*. URL: http://www1.lsbu.ac.uk/water/enztech/amperometric.html.

[8] M. Mazloum Ardakani et al. "Electrocatalytic characteristics of uric acid oxidation at graphite–zeolite-modified electrode doped with iron (III)". In: *Journal of Electroanalytical Chemistry* 586.1 (Jan. 2006), pp. 31–38. ISSN: 1572-6657. DOI: 10.1016/J.JELECHEM.2005.09.015. URL: https://www.sciencedirect.com/science/article/pii/S0022072805004687.

[9] R. D. Armstrong and G. Horvai. *Properties of PVC based membranes used in ion-selective electrodes*. Jan. 1990. DOI: 10.1016/0013-4686(90)85028-L.

[10] J. Artigas et al. "Application of ion sensitive field effect transistor based sensors to soil analysis". In: *Computers and Electronics in Agriculture* (2001). ISSN: 01681699. DOI: 10.1016/S0168-1699(00)00187-3.

[11] Micaela Badea et al. *New electrochemical sensors for detection of nitrites and nitrates*. Tech. rep. 2001, pp. 66–72. URL: www.elsevier.com/locate/jelechem.

[12] Barbara Ballarin et al. "An amperometric glucose biosensor prototype fabricated by thermal inkjet printing". In: *Biosensors and Bioelectronics* 20 (2005), pp. 2019–2026. DOI: 10.1016/j.bios.2004.09.022. URL: https://www.researchgate.net/publication/7992987.

[13] Amay J. Bandodkar and Joseph Wang. *Non-invasive wearable electrochemical sensors: A review*. July 2014. DOI: 10.1016/j.tibtech.2014.04.005.

[14] Amay J. Bandodkar et al. "Epidermal tattoo potentiometric sodium sensors with wireless signal transduction for continuous non-invasive sweat monitoring". In: *Biosensors and Bioelectronics* (2014). ISSN: 18734235. DOI: 10.1016/j.bios.2013.11.039.

[15] Mallika Bariya, Hnin Yin Yin Nyein, and Ali Javey. *Wearable sweat sensors*. 2018. DOI: 10.1038/s41928-018-0043-y.

[16] Mallika Bariya et al. "Roll-to-Roll Gravure Printed Electrochemical Sensors for Wearable and Medical Devices". In: *ACS Nano* 12.7 (July 2018), pp. 6978–6987. ISSN: 1936086X. DOI: 10.1021/acsnano.8b02505.

[17] M. F. Bergeron. *Heat cramps: Fluid and electrolyte challenges during tennis in the heat*. Mar. 2003. DOI: 10.1016/S1440-2440(03)80005-1.

[18] Jan Bijman and Paul M. Quinton. "Lactate and bicarbonate uptake in the sweat duct of cystic fibrosis and normal subjects". In: *Pediatric Research* (1987). ISSN: 15300447. DOI: 10.1203/00006450-198701000-00017.

[19] Michael J. Buono, N. V L Lee, and Paul W. Miller. "The relationship between exercise intensity and the sweat lactate excretion rate". In: *Journal of Physiological Sciences* (2010). ISSN: 18806546. DOI: 10.1007/s12576-009-0073-3.

[20] Robert W. Cattrall. *Chemical sensors*. Oxford University Press, 1997, p. 74. ISBN: 9780198500902.

[21] Jittima Choosang et al. "Simultaneous Detection of Ammonium and Nitrate in Environmental Samples Using on Ion-Selective Electrode and Comparison with Portable Colorimetric Assays". In: *Sensors* 18.10 (Oct. 2018), p. 3555. ISSN: 1424-8220. DOI: 10.3390/s18103555. URL: http://www.mdpi.com/1424-8220/18/10/3555.

[22] A. Cranny et al. "Screen-printed potentiometric Ag/AgCl chloride sensors: Lifetime performance and their use in soil salt measurements". In: *Sensors and Actuators, A: Physical*. Vol. 169. 2. Elsevier, Oct. 2011, pp. 288–294. DOI: 10.1016/j.sna.2011.01.016.

[23] Eric Crouch et al. "A novel, disposable, screen-printed amperometric biosensor for glucose in serum fabricated using a water-based carbon ink". In: *Biosensors and Bioelectronics* 21.5 (Nov. 2005), pp. 712–718. ISSN: 09565663. DOI: 10.1016/j.bios.2005.01.003.

[24] V. A.T. Dam, M. A.G. Zevenbergen, and R. Van Schaijk. "Flexible Ion Sensors for Bodily Fluids". In: *Procedia Engineering*. 2016. DOI: 10.1016/j.proeng.2016.11.155.

[25] Van Anh T. Dam and Marcel A.G. G. Zevenbergen. "Low Cost Nitrate Sensor for Agricultural Applications". In: *2019 20th International Conference on Solid-State Sensors, Actuators and Microsystems and Eurosensors XXXIII, TRANSDUCERS 2019 and EUROSENSORS XXXIII*. Institute of Electrical and Electronics Engineers Inc., June 2019, pp. 1285–1288. ISBN: 9781728120072. DOI: 10.1109/TRANSDUCERS.2019.8808327. URL: https://ieeexplore.ieee.org/document/8808327/.

[26] J.A. Delgado et al. "Nitrogen fertilizer management based on site-specific management zones reduces potential for nitrate leaching". In: *Journal of Soil and Water Conservation* 60.6 (2005).

[27] Mary J. Donahue et al. "High-Performance Vertical Organic Electrochemical Transistors". In: *Advanced Materials* (2018). ISSN: 15214095. DOI: 10.1002/adma.201705031.

[28] Ievgen Duboriz and Alexander Pud. "Polyaniline/poly(ethylene terephthalate) film as a new optical sensing material". In: *Sensors and Actuators, B: Chemical* (2014). ISSN: 09254005. DOI: 10.1016/j.snb.2013.09.005.

[29] L Henry Edmunds et al. *Reinnervation of the reimplanted canine lung*. Tech. rep. 5. 1971. URL: www.physiology.org/journal/jappl.

[30] *Effects of solute diffusion on the kinetics of immobilised enzymes*. URL: http://www1.lsbu.ac.uk/water/enztech/diffusion.html.

[31] H M Emrich et al. "Sweat Composition in Relation to Rate of Sweating in Patients with Cystic Fibrosis of the Pancreas". In: *Pediatric Research* 2.6 (Nov. 1968), pp. 464–478. ISSN: 0031-3998. DOI: 10.1203/00006450-196811000-00004. URL: http://www.nature.com/doifinder/10.1203/00006450-196811000-00004.

[32] B Falk et al. "Sweat lactate in exercising children and adolescents of varying physical maturity". In: *Journal of applied physiology (Bethesda, Md. : 1985)* (1991). ISSN: 8750-7587.

[33] Mohammad H. Faridnia et al. "Amperometric biosensor for determination of lactate in sweat". In: *Analytica Chimica Acta* (1993). ISSN: 00032670. DOI: 10.1016/0003-2670(93)80082-V.

[34] N Fellmann, G Grizard, and J Coudert. "Human frontal sweat rate and lactate concentration during heat exposure and exercise". In: *Journal of applied physiology: respiratory, environmental and exercise physiology* (1983). ISSN: 0161-7567.

[35] Abhinav M Gaikwad, Ana Claudia Arias, and Daniel A Steingart. "Recent Progress on Printed Flexible Batteries: Mechanical Challenges, Printing Technologies, and Future Prospects". In: (). DOI: 10.1002/ente.201402182.

[36] Jordi Gallardo, Salvador Alegert, and Manuel Del Valle. "A flow-injection electronic tongue based on potentiometric sensors for the determination of nitrate in the presence of chloride". In: *Sensors and Actuators, B: Chemical* 101.1-2 (June 2004), pp. 72–80. ISSN: 09254005. DOI: 10.1016/j.snb.2004.02.027.

[37] Wei Gao et al. "Fully integrated wearable sensor arrays for multiplexed in situ perspiration analysis". In: *Nature* (2016). ISSN: 14764687. DOI: 10.1038/nature16521.

[38] R. Garjonyte et al. "Prussian Blue- and lactate oxidase-based amperometric biosensor for lactic acid". In: *Sensors and Actuators, B: Chemical* (2001). ISSN: 09254005. DOI: 10.1016/S0925-4005(01)00845-0.

[39] Jennifer Y. Gerasimov et al. "An Evolvable Organic Electrochemical Transistor for Neuromorphic Applications". In: *Advanced Science* (2019). ISSN: 21983844. DOI: 10.1002/advs.201801339.

[40] P T Gilbert. *THE USE OF SILVER-SILVER CHLORIDE REFERENCE ELECTRODES IN DILUTE SOLUTIONS*. Tech. rep. 1947. URL: http://pubs.rsc.org/en/content/articlepdf/1947/df/df9470100320.

[41] Katelyn P. Goetz et al. "Charge-transfer complexes: new perspectives on an old class of compounds". In: *Journal of Materials Chemistry C* 2.17 (Apr. 2014), p. 3065. ISSN: 2050-7526. DOI: 10.1039/c3tc32062f. URL: http://pubs.rsc.org/en/content/articlehtml/2014/tc/c3tc32062f%20http://xlink.rsc.org/?DOI=C3TC32062F.

[42] J M Green et al. "Gender differences in sweat lactate." In: *European journal of applied physiology* (2000). ISSN: 14396319. DOI: 10.1007/s004210050676.

[43] J. M. Green et al. "Effects of high and low blood lactate concentrations on sweat lactate response". In: *International Journal of Sports Medicine* (2000). ISSN: 01724622. DOI: 10.1055/s-2000-8483.

[44] J. M. Green et al. "Lactate-sweat relationships in younger and middle-aged men". In: *Journal of Aging and Physical Activity* (2001). ISSN: 10638652. DOI: 10.1123/japa.9.1.67.

[45] J. Matt Green et al. "Sweat lactate response between males with high and low aerobic fitness". In: *European Journal of Applied Physiology* (2004). ISSN: 14396319. DOI: 10.1007/s00421-003-0968-2.

[46] Matt J. Green et al. "Sweat lactate response during cycling at 30°C and 18°C WBGT". In: *Journal of Sports Sciences* (2004). ISSN: 02640414. DOI: 10.1080/02640410310001641575.

[47] H Greenway and C B Osmond. *Salt Responses of Enzymes from Species Differing in Salt Tolerance*. Tech. rep. 1972, pp. 256–259.

[48] I. Gualandi et al. "Textile Organic Electrochemical Transistors as a Platform for Wearable Biosensors". In: *Scientific Reports* (2016). ISSN: 20452322. DOI: 10.1038/srep33637.

[49] Tomàs Guinovart et al. "A potentiometric tattoo sensor for monitoring ammonium in sweat". In: *The Analyst* 138.22 (Nov. 2013), p. 7031. ISSN: 0003-2654. DOI: 10.1039/c3an01672b. URL: http://xlink.rsc.org/?DOI=c3an01672b.

[50] Tomàs Guinovart et al. "Potentiometric sensors using cotton yarns, carbon nanotubes and polymeric membranes". In: *Analyst* 138.18 (Sept. 2013), pp. 5208–5215. ISSN: 13645528. DOI: 10.1039/c3an00710c.

[51] Manuel Gutiérrez et al. "Electronic tongue for the determination of alkaline ions using a screen-printed potentiometric sensor array". In: *Microchimica Acta* 163.1-2 (Sept. 2008), pp. 81–88. ISSN: 00263672. DOI: 10.1007/s00604-007-0894-9.

[52] Owen J. Guy and Kelly-Ann D. Walker. "Graphene Functionalization for Biosensor Applications". In: *Silicon Carbide Biotechnology* (Jan. 2016), pp. 85–141. DOI: 10.1016/B978-0-12-802993-0.00004-6. URL: https://www.sciencedirect.com/science/article/pii/B9780128029930000046#s0080%20https://www.sciencedirect.com/science/article/pii/B9780128029930000046.

[53] E. H. Hansen, Animesh K. Ghose, and J. Růžička. "Flow injection analysis of environmental samples for nitrate using an ion-selective electrode". In: *The Analyst* 102.1219 (Jan. 1977), pp. 705–713. ISSN: 00032654. DOI: 10.1039/an9770200705.

[54] Leland Hansen et al. "Sweat Chloride Analysis by Chloride Ion-Specific Electrode Method Using Heat Stimulation". In: *American Journal of Clinical Pathology* 49.6 (June 1968), pp. 834–841. ISSN: 0002-9173. DOI: 10.1093/ajcp/49.6.834.

[55] J. P. Hart et al. "Studies towards a disposable screen-printed amperometric biosensor for progesterone". In: *Biosensors and Bioelectronics* 12.11 (Dec. 1997), pp. 1113–1121. ISSN: 09565663. DOI: 10.1016/S0956-5663(97)00033-X.

[56] Christopher J. Harvey, Ryan F. LeBouf, and Aleksandr B. Stefaniak. "Formulation and stability of a novel artificial human sweat under conditions of storage and use". In: *Toxicology in Vitro* (2010). ISSN: 08872333. DOI: 10.1016/j.tiv.2010.06.016.

[57] Qing He et al. "Enabling Inkjet Printed Graphene for Ion Selective Electrodes with Postprint Thermal Annealing". In: *ACS Applied Materials and Interfaces* (2017). ISSN: 19448252. DOI: 10.1021/acsami.7b00092.

[58] Jianshe Huang et al. "Simultaneous electrochemical determination of dopamine, uric acid and ascorbic acid using palladium nanoparticle-loaded carbon nanofibers modified electrode". In: *Biosensors and Bioelectronics* 24.4 (Dec. 2008), pp. 632–637. ISSN: 0956-5663. DOI: 10.1016/J.BIOS.2008.06.011. URL: https://www.sciencedirect.com/science/article/pii/S0956566308002704.

[59] Kun-Che Hung, Ching-Shiow Tseng, and Shan-hui Hsu. "Synthesis and 3D Printing of Biodegradable Polyurethane Elastomer by a Water-Based Process for Cartilage Tissue Engineering Applications". In: *Advanced Healthcare Materials* 3.10 (Oct. 2014), pp. 1578–1587. ISSN: 21922640. DOI: 10.1002/adhm.201400018. URL: http://doi.wiley.com/10.1002/adhm.201400018.

[60] Robert M Iannlello and Alexander M Yacynych. "Immobilized Enzyme Chemically Modified Electrode as an Amperometric Sensor". In: *Analytical Chemistry* 53.13 (1981), pp. 2090–2095. URL: https://pubs.acs.org/sharingguidelines.

[61] Somayeh Imani et al. "A wearable chemical-electrophysiological hybrid biosensing system for real-time health and fitness monitoring". In: *Nature Communications* 7.1 (Sept. 2016), p. 11650. DOI: 10.1038/ncomms11650. URL: http://www.nature.com/articles/ncomms11650.

[62] Emmanuel I. Iwuoha, Armin Rock, and Malcolm R. Smyth. "Amperometric L-Lactate Biosensors: 1. Lactic Acid Sensing Electrode Containing Lactate Oxidase in a Composite Poly-L-lysine Matrix". In: *Electroanalysis* (1999). ISSN: 10400397. DOI: 10.1002/(SICI)1521-4109(199905)11:5<367::AID-ELAN367>3.0.CO;2-0.

[63] Wenzhao Jia et al. "Electrochemcial tattoo biosensors for real-time noninvasive lactate monitoring in human perspiration". In: *Anal. Chem* 85 (2013). ISSN: 00032700. DOI: 10.1021/ac401573r. URL: https://pubs.acs.org/sharingguidelines.

[64] Bradley Jones and Christopher J. Nachtsheim. "A class of three-level designs for definitive screening in the presence of second-order effects". In: *Journal of Quality Technology* 43.1 (2011), pp. 1–15. ISSN: 00224065. DOI: 10.1080/00224065.2011.11917841.

[65] Milica Jović et al. "Large-scale layer-by-layer inkjet printing of flexible iridium-oxide based pH sensors". In: *Journal of Electroanalytical Chemistry* (2018). ISSN: 15726657. DOI: 10.1016/j.jelechem.2017.11.032.

[66] Mohammad Nazmul Karim et al. "Towards UV-curable inkjet printing of biodegradable poly (lactic acid) fabrics". In: *Journal of Materials Science* 50.13 (July 2015), pp. 4576–4585. ISSN: 15734803. DOI: 10.1007/s10853-015-9006-0.

[67] Vassiliki Katseli, Anastasios Economou, and Christos Kokkinos. "Single-step fabrication of an integrated 3D-printed device for electrochemical sensing applications". In: *Electrochemistry Communications* 103 (June 2019), pp. 100–103. ISSN: 13882481. DOI: 10.1016/j.elecom.2019.05.008.

[68] Gregg Kenausis, Qiang Chen, and Adam Heller. "Electrochemical Glucose and Lactate Sensors Based on "Wired" Thermostable Soybean Peroxidase Operating Continuously and Stably at 37 °C". In: *Analytical Chemistry* (1997). ISSN: 0003-2700. DOI: 10.1021/ac961083y.

[69] Yasser Khan et al. "Flexible Hybrid Electronics: Direct Interfacing of Soft and Hard Electronics for Wearable Health Monitoring". In: *Advanced Functional Materials* (2016). ISSN: 16163028. DOI: 10.1002/adfm.201603763.

[70] Yasser Khan et al. "Monitoring of Vital Signs with Flexible and Wearable Medical Devices". In: *Advanced Materials* (2016). ISSN: 15214095. DOI: 10.1002/adma.201504366. URL: www.advmat.de.

[71] Dion Khodagholy et al. "Organic electrochemical transistor incorporating an ionogel as a solid state electrolyte for lactate sensing". In: *Journal of Materials Chemistry* 22.10 (Feb. 2012), p. 4440. ISSN: 0959-9428. DOI: 10.1039/c2jm15716k. URL: http://xlink.rsc.org/?DOI=c2jm15716k.

[72] Jayoung Kim et al. "Noninvasive Alcohol Monitoring Using a Wearable Tattoo-Based Iontophoretic-Biosensing System". In: *ACS Sensors* 1.8 (Aug. 2016), pp. 1011–1019. ISSN: 23793694. DOI: 10.1021/acssensors.6b00356.

[73] J. Kimura, Y. Kawana, and T. Kuriyama. "An immobilized enzyme membrane fabrication method using an ink jet nozzle". In: *Biosensors* 4.1 (Jan. 1989), pp. 41–52. ISSN: 0265-928X. DOI: 10.1016/0265-928X(89)80033-1. URL: https://www.sciencedirect.com/science/article/pii/0265928X89800331.

[74] T. J. Kistenmacher, T. E. Phillips, and D. O. Cowan. "The crystal structure of the 1:1 radical cation–radical anion salt of 2,2'-bis-l,3-dithiole (TTF) and 7,7,8,8-tetracyanoquinodimethane (TCNQ)". In: *Acta Crystallographica Section B Structural Crystallography and Crystal Chemistry* (1974). ISSN: 0567-7408. DOI: 10.1107/S0567740874003669.

[75] B. Koch et al. "Economic Feasibility of Variable-Rate Nitrogen Application Utilizing Site-Specific Management Zones". In: *Agronomy Journal* 96.6 (Nov. 2004), pp. 1572–1580. ISSN: 00021962. DOI: 10.2134/agronj2004.1572. URL: http://doi.wiley.com/10.2134/agronj2004.1572.

[76] Bradley Koch and Rajiv Khosla. *The Role of Precision Agriculture in Cropping Systems*. 2003. DOI: 10.1300/J144v09n01{_}02.

[77] Yasunori Kondoh, Michi Kawase, and Shinji Ohmori. "D-Lactate concentrations in blood, urine and sweat before and after exercise". In: *European Journal of Applied Physiology and Occupational Physiology* (1992). ISSN: 03015548. DOI: 10.1007/BF01466280.

[78] Barbara Kowalewska and Pawel J. Kulesza. "Application of tetrathiafulvalene-modified carbon nanotubes to preparation of integrated mediating system for bioelectrocatalytic oxidation of glucose". In: *Electroanalysis* (2009). ISSN: 10400397. DOI: 10.1002/elan.200804396.

[79] Frederik C Krebs. "Fabrication and processing of polymer solar cells: A review of printing and coating techniques". In: (2008). DOI: 10.1016/j.solmat.2008.10.004. URL: www.elsevier.com/locate/solmat.

[80] Peter Kukumberg et al. "Sweat: A potential marker of clinical activity in panic disorder". In: *Neuroendocrinology Letters* (2009). ISSN: 0172780X.

[81] *LCO-301 LACTATE OXIDASE from Microorganism L-Lactate: oxygen oxidoreductase (EC 1.1.3.2)*. Tech. rep. URL: http://www.toyobo-global.com/seihin/xr/enzyme/pdf_files/2010_189_192_LCO_301.pdf.

[82] Y. S. Lee and D. D. Lee. "Visible Optical Sensing of Ammonia Based Polyaniline Film". In: *Proceedings of IEEE Sensors*. 2002. DOI: 10.1109/icsens.2002.1036989.

[83] Rongfeng Li et al. *Recent progress on biodegradable materials and transient electronics*. Sept. 2018. DOI: 10.1016/j.bioactmat.2017.12.001.

[84] Yanhua Li et al. "An ISE-based On-Site Soil Nitrate Nitrogen Detection System". In: *Sensors* 19.21 (Oct. 2019), p. 4669. ISSN: 1424-8220. DOI: 10.3390/s19214669. URL: https://www.mdpi.com/1424-8220/19/21/4669.

[85] Yuqing Lin et al. "A facile electrochemical method for simultaneous and on-line measurements of glucose and lactate in brain microdialysate with prussian blue as the electrocatalyst for reduction of hydrogen peroxide". In: *Analytical Chemistry* (2007). ISSN: 00032700. DOI: 10.1021/ac070966u.

[86] Haiying Liu and Jiaqi Deng. "An amperometric lactate sensor employing tetrathiafulvalene in Nafion film as electron shuttle". In: *Electrochimica Acta* (1995). ISSN: 00134686. DOI: 10.1016/0013-4686(95)00099-Z.

[87] Claire M. Lochner et al. "All-organic optoelectronic sensors for pulse oximetry". In: *Nature Communications* (2014). DOI: 10.1038/ncomms6745. URL: www.nature.com/naturecommunications.

[88] Heike S. Mader and Otto S. Wolfbeis. "Optical ammonia sensor based on upconverting luminescent nanoparticles". In: *Analytical Chemistry* (2010). ISSN: 00032700. DOI: 10.1021/ac1007283.

[89] M R Mahmoudian et al. "A sensitive electrochemical nitrate sensor based on polypyrrole coated palladium nanoclusters". In: (2015). DOI: 10.1016/j.jelechem.2015.05.026. URL: http://dx.doi.org/10.1016/j.jelechem.2015.05.026.

[90] F. Meyer et al. "Effect of age and gender on sweat lactate and ammonia concentrations during exercise in the heat". In: *Brazilian Journal of Medical and Biological Research* (2007). ISSN: 0100879X. DOI: 10.1590/S0100-879X2007000100017.

[91] Olaf Mickelsen and Ancel Keys. *THE COMPOSITION OF SWEAT, WITH SPECIAL REFERENCE TO THE VITAMINS* Downloaded from*. Tech. rep. URL: http://www.jbc.org/.

[92] Kohji Mitsubayashi et al. "Analysis of metabolites in sweat as a measure of physical condition". In: *Analytica Chimica Acta* (1994). ISSN: 00032670. DOI: 10.1016/0003-2670(94)80004-9.

[93] G. J. Moody, R. B. Oke, and J. D.R. Thomas. "A calcium-sensitive electrode based on a liquid ion exchanger in a poly(vinyl chloride) matrix". In: *The Analyst* (1970). ISSN: 00032654. DOI: 10.1039/an9709500910.

[94] ASHOK MULCHANDANI, AMARJEET S. BASSI, and ANDREW NGUYEN. "Tetrathiafulvalene-mediated Biosensor for L-lactate in Dairy Products". In: *Journal of Food Science* (1995). ISSN: 17503841. DOI: 10.1111/j.1365-2621.1995.tb05610.x.

[95] Miloslav Nič et al., eds. *IUPAC Compendium of Chemical Terminology*. Research Triagle Park, NC: IUPAC, June 2009. ISBN: 0-9678550-9-8. DOI: 10.1351/goldbook. URL: http://goldbook.iupac.org.

[96] Hnin Yin Yin Nyein et al. "A Wearable Electrochemical Platform for Noninvasive Simultaneous Monitoring of Ca ¡sup¿2+¡/sup¿ and pH". In: *ACS Nano* 10.7 (July 2016), pp. 7216–7224. ISSN: 1936-0851. DOI: 10.1021/acsnano.6b04005.

[97] O. L. Oke. *Nitrite toxicity to plants [38]*. 1966. DOI: 10.1038/212528a0.

[98] Shuto Osaki et al. "Investigation of Polyurethane Matrix Membranes for Salivary Nitrate ISFETs to Prevent the Drift". In: *Sensors* 19.12 (June 2019), p. 2713. ISSN: 1424-8220. DOI: 10.3390/s19122713. URL: https://www.mdpi.com/1424-8220/19/12/2713.

[99] Aminy E. Ostfeld et al. "Screen printed passive components for flexible power electronics". In: *Scientific Reports* 5.1 (Oct. 2015), pp. 1–11. ISSN: 20452322. DOI: 10.1038/srep15959.

[100] Gunjan Pandey, Ratnesh Kumar, and Robert J Weber. "Real Time Detection of Soil Moisture and Nitrates Using On-Board In-Situ Impedance Spectroscopy". In: (2013). DOI: 10.1109/SMC.2013.188. URL: https://www.researchgate.net/publication/269326946.

[101] Alexandros Pantelopoulos and Nikolaos G. Bourbakis. *A survey on wearable sensor-based systems for health monitoring and prognosis*. 2010. DOI: 10.1109/TSMCC.2009.2032660.

[102] Hong Jun Park et al. "Potentiometric performance of flexible pH sensor based on polyaniline nanofiber arrays". In: *Nano Convergence* (2019). ISSN: 21965404. DOI: 10.1186/s40580-019-0179-0.

[103] Marc Parrilla et al. "A Textile-Based Stretchable Multi-Ion Potentiometric Sensor". In: *Advanced Healthcare Materials* 5.9 (May 2016), pp. 996–1001. ISSN: 21922640. DOI: 10.1002/adhm.201600092. URL: http://doi.wiley.com/10.1002/adhm.201600092.

[104] Marc Parrilla et al. "A Wearable Paper-Based Sweat Sensor for Human Perspiration Monitoring". In: *Advanced Healthcare Materials* (2019). ISSN: 21922659. DOI: 10.1002/adhm.201900342.

[105] M. J. Patterson, S. D.R. Galloway, and M. A. Nimmo. "Effect of induced metabolic alkalosis on sweat composition in men". In: *Acta Physiologica Scandinavica* (2002). ISSN: 00016772. DOI: 10.1046/j.1365-201x.2002.00927.x.

[106] Mark J. Patterson, Stuart D.R. Galloway, and Myra A. Nimmo. "Variations in regional sweat composition in normal human males". In: *Experimental Physiology* (2000). ISSN: 09580670. DOI: 10.1111/j.1469-445X.2000.02058.x.

[107] Margaret E Payne et al. "Printed, Flexible Lactate Sensors: Design considerations Before performing on-Body Measurements". In: *Scientific Reports* 9 (2019). DOI: 10.1038/s41598-019-49689-7. URL: https://doi.org/10.1038/s41598-019-49689-7.

[108] Adrien Pierre et al. "All-Printed Flexible Organic Transistors Enabled by Surface Tension-Guided Blade Coating". In: *Advanced Materials* 26.32 (Aug. 2014), pp. 5722–5727. ISSN: 09359648. DOI: 10.1002/adma.201401520. URL: http://doi.wiley.com/10.1002/adma.201401520.

[109] P. Pilardeau et al. "Secretion of eccrine sweat glands during exercise." In: *British journal of sports medicine* (1979). ISSN: 03063674. DOI: 10.1136/bjsm.13.3.118.

[110] Jianfeng Ping, Jian Wu, and Yibin Ying. "Screen-printed potentiometric strip for calcium ion determination in water and milk". In: *American Society of Agricultural and Biological Engineers Annual International Meeting 2012, ASABE 2012*. 2012. ISBN: 9781622762088. DOI: 10.13031/2013.42656.

[111] Adrian Polliack, Richard Taylor, and Dan Bader. *Analysis of sweat during soft tissue breakdown following pressure ischemia*. Tech. rep. 2. 1993, pp. 250–259.

[112] Yiheng Qin et al. "Inkjet-printed bifunctional carbon nanotubes for pH sensing". In: *Materials Letters* (2016). ISSN: 18734979. DOI: 10.1016/j.matlet.2016.04.048.

[113] Kavita Rathee et al. "Biosensors based on electrochemical lactate detection: A comprehensive review". In: *Biochemistry and Biophysics Reports* 5 (Mar. 2016), pp. 35–54. ISSN: 2405-5808. DOI: 10.1016/J.BBREP.2015.11.010. URL: https://www.sciencedirect.com/science/article/pii/S2405580815001302.

[114] Brent A. Ridley, Babak Nivi, and Joseph M. Jacobson. "All-inorganic field effect transistors fabricated by printing". In: *Science* 286 (1999), pp. 746–749. URL: www.sciencemag.org.

[115] B J Rosenstein and G R Cutting. "The diagnosis of cystic fibrosis: a consensus statement. Cystic Fibrosis Foundation Consensus Panel." In: *The Journal of pediatrics* 132.4 (Apr. 1998), pp. 589–95. ISSN: 0022-3476. DOI: 10.1016/S0022-3476(98)70344-0. URL: http://www.ncbi.nlm.nih.gov/pubmed/9580754.

[116] James W. Ross. "Calcium-selective electrode with liquid ion exchanger". In: *Science* (1967). ISSN: 00368075. DOI: 10.1126/science.156.3780.1378.

[117] Nipapan Ruecha et al. "Fully Inkjet-Printed Paper-Based Potentiometric Ion-Sensing Devices". In: *Analytical Chemistry* 89.19 (Oct. 2017), pp. 10608–10616. ISSN: 15206882. DOI: 10.1021/acs.analchem.7b03177.

[118] Mahsa Sadeghi et al. "Printed Flexible Organic Transistors with Tunable Aspect Ratios". In: *Advanced Electronic Materials* 6.2 (Feb. 2020), p. 1901207. ISSN: 2199-160X. DOI: 10.1002/aelm.201901207. URL: https://onlinelibrary.wiley.com/doi/abs/10.1002/aelm.201901207.

[119] R. Joshi Sanket et al. "Development of a low cost nitrate detection soil sensor". In: *Proceedings of the 2017 International Conference on Wireless Communications, Signal Processing and Networking, WiSPNET 2017*. Vol. 2018-January. Institute of Electrical and Electronics Engineers Inc., Feb. 2018, pp. 1272–1275. ISBN: 9781509044412. DOI: 10.1109/WiSPNET.2017.8299968.

[120] Priyabrata Sarkar et al. "Screen-printed amperometric biosensors for the rapid measurement of L- and D-amino acids". In: *Analyst* 124.6 (Jan. 1999), pp. 865–870. ISSN: 00032654. DOI: 10.1039/a901404g.

[121] F. Sato, M. Burgers, and K. Sato. "Some characteristics of adrenergic human eccrine sweating". In: *Experientia* (1974). ISSN: 00144754. DOI: 10.1007/BF01921584.

[122] Michael Schäferling. *The art of fluorescence imaging with chemical sensors*. 2012. DOI: 10.1002/anie.201105459.

[123] Benjamin Schazmann et al. "A wearable electrochemical sensor for the real-time measurement of sweat sodium concentration". en. In: *Analytical Methods* 2.4 (Apr. 2010), p. 342. ISSN: 17599660. DOI: 10.1039/b9ay00184k.

[124] Juliane R. Sempionatto et al. "Skin-worn Soft Microfluidic Potentiometric Detection System". In: *Electroanalysis* (2019). ISSN: 15214109. DOI: 10.1002/elan.201800414.

[125] Rei Shiwaku et al. "A printed organic amplification system for wearable potentiometric electrochemical sensors". In: *Scientific Reports* (2018). ISSN: 20452322. DOI: 10.1038/s41598-018-22265-1.

[126] Amy Smart et al. "An Electrocatalytic Screen-Printed Amperometric Sensor for the Selective Measurement of Thiamine (Vitamin B1) in Food Supplements". In: *Biosensors* 9.3 (Aug. 2019), p. 98. ISSN: 2079-6374. DOI: 10.3390/bios9030098. URL: https://www.mdpi.com/2079-6374/9/3/98.

[127] *Sodium ionophore X Selectophore®,functiontested — 97600-39-0 — C60H80O12 — Sigma-Aldrich*. URL: https://www.sigmaaldrich.com/catalog/product/sial/71747?lang=en&region=US.

[128] *Soil Test Interpretation Guide — OSU Extension Catalog — Oregon State University*. URL: https://catalog.extension.oregonstate.edu/ec1478.

[129] Xenofon Strakosas, Manuelle Bongo, and Roisín M. Owens. *The organic electrochemical transistor for biological applications*. 2015. DOI: 10.1002/app.41735.

[130] R. A. Street et al. "From printed transistors to printed smart systems". In: *Proceedings of the IEEE* 103.4 (Apr. 2015), pp. 607–618. ISSN: 15582256. DOI: 10.1109/JPROC.2015.2408552.

[131] R P Taylor, A A Polliack, and D L Bader. "The analysis of metabolites in human sweat: Analytical methods and potential application to investigation of pressure ischaemia of soft tissues". In: *Annals of Clinical Biochemistry* (1994). ISSN: 0004-5632. DOI: 10.1177/000456329403100103.

[132] Atsusi Toda and Yoshiaki Nishiya. "Gene cloning, purification, and characterization of a lactate oxidase from Lactococcus lactis subsp. cremoris IFO3427". In: *Journal of Fermentation and Bioengineering* 85.5 (Jan. 1998), pp. 507–510. ISSN: 0922-338X. DOI: 10.1016/S0922-338X(98)80070-6. URL: https://www.sciencedirect.com/science/article/pii/S0922338X98800706.

[133] Peter G Vekilov. "Nucleation." In: *Crystal growth & design* 10.12 (Nov. 2010), pp. 5007–5019. ISSN: 1528-7483. DOI: 10.1021/cg1011633. URL: http://www.ncbi.nlm.nih.gov/pubmed/21132117%20http://www.pubmedcentral.nih.gov/articlerender.fcgi?artid=PMC2995260.

[134] August Wilhelm Wahlefeld and Günter Holz. "Creatinine". In: *Methods of Enzymatic Analysis* (Jan. 1974), pp. 1786–1790. DOI: 10.1016/B978-0-12-091304-6.50029-X. URL: https://www.sciencedirect.com/science/article/pii/B978012091304650029X.

[135] Joseph Wang et al. "Screen-printed amperometric biosensors for glucose and alcohols based on ruthenium-dispersed carbon inks". In: *Analytica Chimica Acta* 300.1-3 (Jan. 1995), pp. 111–116. ISSN: 00032670. DOI: 10.1016/0003-2670(94)00357-R.

[136] You Wang et al. "All-solid-state blood calcium sensors based on screen-printed poly(3,4-ethylenedioxythiophene) as the solid contact". In: *Sensors and Actuators, B: Chemical* (2012). ISSN: 09254005. DOI: 10.1016/j.snb.2012.07.064.

[137] Zhao Hui Wang, Yan fang Miao, and Sheng Xiu Li. "Wheat responses to ammonium and nitrate N applied at different sown and input times". In: *Field Crops Research* 199 (Dec. 2016), pp. 10–20. ISSN: 03784290. DOI: 10.1016/j.fcr.2016.09.002.

[138] Mary E Washko and Eugene W Rice. *Determination of Glucose by an Improved Enzymatic Procedure*. Tech. rep. URL: http://clinchem.aaccjnls.org/content/clinchem/7/5/542.full.pdf.

[139] Jeremy Woods et al. "Energy and the food system". In: *Philosophical Transactions of the Royal Society B: Biological Sciences* 365.1554 (Sept. 2010), pp. 2991–3006. ISSN: 0962-8436. DOI: 10.1098/rstb.2010.0172. URL: https://royalsocietypublishing.org/doi/10.1098/rstb.2010.0172.

[140] Elsayed M. Zahran et al. "Polymeric plasticizer extends the lifetime of PVC-membrane ion-selective electrodes". In: *Analyst* 139.4 (Jan. 2014), pp. 757–763. ISSN: 13645528. DOI: 10.1039/c3an01963b.

[141] Alla M. Zamarayeva et al. "Optimization of the printed flexible sensors for continuous monitoring of sodium ammonium and lactate in sweat". In: (2020), to be submitted for publication.

[142] Erica Zeglio and Olle Inganäs. *Active Materials for Organic Electrochemical Transistors*. 2018. DOI: 10.1002/adma.201800941.